

UNIVERSITY OF SÃO PAULO

Faculty of Pharmaceutical Sciences

Graduate Program Drug and Medicinal Products

Department of Pharmacy

Concentration Area: Pharmaceutical Production and Control

**Nanostructured lipid carrier containing hydroxymethylnitrofurazone:
preparation, characterization and *in vitro* and *in vivo* evaluation of
leishmanicidal activity**

ALINE DE SOUZA

Thesis to obtain the title of DOCTOR

Supervisor: Prof. Dr. Nádia Araci Bou Chacra

São Paulo

2021

UNIVERSITY OF SÃO PAULO

Faculty of Pharmaceutical Sciences

Graduate Program Drug and Medicinal Products

Department of Pharmacy

Concentration Area: Pharmaceutical Production and Control

**Nanostructured lipid carrier containing hydroxymethylnitrofurazone:
preparation, characterization and *in vitro* and *in vivo* evaluation of
leishmanicidal activity**

ALINE DE SOUZA

Original Version

Thesis to obtain the title of DOCTOR

Supervisor: Prof. Dr. Nádia Araci Bou Chacra

São Paulo

2021

Aline de Souza

Title: Nanostructured lipid carrier containing hydroxymethylnitrofurazone: preparation, characterization and *in vitro* and *in vivo* evaluation of leishmanicidal activity

Examination Board
Of
Thesis to obtain the title of DOCTOR

Prof. Dr.
Supervisor/President

1st examiner

2nd examiner

3rd examiner

4th examiner

São Paulo, _____ de _____ 2021.

Ficha catalográfica

Ficha Catalográfica elaborada eletronicamente pelo autor, utilizando o programa desenvolvido pela Seção Técnica de Informática do ICMC/USP e adaptado para a Divisão de Biblioteca e Documentação do Conjunto das Químicas da USP

Bibliotecária responsável pela orientação de catalogação da publicação:
Marlene Aparecida Vieira - CRB - 8/5562

d719n de Souza, Aline
Nanostructured lipid carrier containing
hydroxymethylnitrofurazone: preparation,
characterization and in vitro and in vivo
evaluation of leishmanicidal activity / Aline de
Souza. - São Paulo, 2021.
126 p.

Tese (doutorado) - Faculdade de Ciências
Farmacêuticas da Universidade de São Paulo.
Departamento de Farmácia - Programa de Pós-Graduação
em Fármaco e Medicamentos.
Orientador: Bou-Chacra, Nádia Araci

1. leishmaniasis. 2. nanostructured lipid
carrier. 3. lymphatic system . 4.
hydroxymethylnitrofural. 5. oral administration. I.
T. II. Bou-Chacra, Nádia Araci, orientador.

Blessed is the man who finds wisdom, and the man who gains understanding. Proverbs 3.13

Dedication

To God who has helped me so far.

To my parents for all support and love.

To my sibling for their love and affection.

To my friends for the laughs and friendship.

Acknowledgements

To God for guiding me and helping me to overcome obstacles. To my parents for always supporting my dreams. To my siblings, Gabi and Vitor, for all their love, affection and encouragement. To my friends Pâmela, Priscila, Polianna and Raquel for their encouragement.

To Prof. Dr. Nádia A. Bou Chacra for her guidance, teachings and constant encouragement to carry out this work. To Doctors Gabriel Lima de Barros Araújo, Leandro Augusto Calixto, Paulo Cotrim, Ana Cristina Breithaupt Faloppa and Cristiano Jesus Correia and the laboratory technician Edite Kanashiro for their help, interaction and contribution to my work.

To the current and former colleagues in the laboratory: Megumi, Mirla, Débora, Eduardo, Maria Christina, Lis, Osvaldo, Isabela, Jéssica, Iván thank you for your friendship, company and help.

To the Department of Pharmacy, Faculty of Pharmaceutical Sciences, University of São Paulo, for the opportunity and accomplishment of this work.

To CAPES (Coordenação de Aperfeiçoamento de Pessoal do Nível Superior), for providing the scholarship for all the years of my Doctorated Degree under Faculty of Pharmacy and Pharmaceutical Sciences of University of São Paulo.

To all my friends and family, thank you so much. To all the people who were part of my life and somehow contributed for me to get here, my eternal thanks.

RESUMO

De Souza, A. Carreador lipídico nanoestruturado contendo hidroximetilnitrofural: preparação, caracterização físico-química e avaliação *in vitro* e *in vivo* da atividade leishmanicida. 2021. 126 pags. Tese (Doutorado) – Faculdade de Ciências Farmacêuticas, Universidade de São Paulo, São Paulo.

A leishmaniose, uma doença tropical negligenciada (DTN), é um conjunto de doenças causadas por protozoários parasitas obrigatórios do gênero *Leishmania*. E tem como formas principais a leishmaniose cutânea e visceral. O tratamento inclui antimoniais pentavalentes. Esses fármacos apresentam várias desvantagens, como necessidade de administração parenteral, uso de altas dosagens, longa duração do tratamento, toxicidade grave, resistência e eficácia variável. O candidato ao fármaco hidroximetilnitrofural (NFOH), um pró-fármaco derivado do nitrofural, apresentou alta atividade em culturas de células infectadas pelo *Trypanosoma cruzi* e menor toxicidade quando comparado ao nitrofural. Devido à sua baixa solubilidade em água e biodisponibilidade reduzida, o NFOH falhou nos testes de eficácia *in vivo*. Os sistemas nanoestruturados de liberação de fármacos têm potencial para superar esses desafios devido às suas vantagens evidentes: maior eficácia terapêutica, menor toxicidade, liberação modificada do fármaco e aumento da absorção gastrointestinal de fármacos com baixa solubilidade em água. O objetivo deste projeto será a preparação e avaliação das características físico-químicas de um carreador lipídico nanoestruturado contendo hidroximetilnitrofural (NLC-NFOH). O NFOH apresentou a maior solubilidade no Miglyol® 840 entre os lipídios líquidos testados. Para lipídios sólidos, Gelucire® 50/13 e Precirol® ATO5 se mostraram mais adequados para a solubilização de NFOH. O NLC-NFOH otimizado consistiu desses três lipídios. Esses lipídios foram selecionados usando Technobis Crystal 16™, microscopia e DSC. Diferentes ferramentas de seleção de lipídios forneceram conhecimento científico relevante para o desenvolvimento de NLC. O NLC-NFOH teve z-average de $198,6 \pm 5,4$ nm, PDI de $0,11 \pm 0,01$ e potencial zeta de $-13,7 \pm 0,7$ mV. Este estudo permitiu o desenvolvimento por abordagem de *Design Space* do primeiro NLC-NFOH com potencial para tratar a leishmaniose por via oral. O desenvolvimento de um

método bioanalítico sensível utilizando HPLC e a avaliação de algumas figuras analíticas de mérito para a validação permitiram a quantificação de NFOH e NF em soro. O método bioanalítico para análise de NFOH e NF usou coluna de HPLC Zorbax SB-C18, 5 μm , (4,6 x 250 mm). A fase móvel foi constituída por acetonitrila: água (20:80 v / v) com vazão de 1,2 ml / min, com detecção no UV de 370 nm. A linearidade de NFOH e NF foi encontrada na faixa de 0,025–3,0 μg / ml com um coeficiente de correlação de $r > 0,98$. A precisão foi de 2,44 a 13,77% para NFOH e 2,61 a 18,42%; a precisão foi de 2,66 a 14,28% para NFOH e 2,09 a 19,06% para NF. O método mostrou-se adequado para avaliação efetiva do NFOH no soro. NLC-NFOH (2,8 mg / kg) foi administrado aos animais por gavagem, e o modelo de bloqueio do fluxo de quilomícrons foi realizado com injeção intraperitoneal de cicloheximida. A presença de NFOH no soro foi avaliada com e sem cicloheximida. O ensaio de citotoxicidade de NLC-NFOH e branco-NLC mostrou mais de 90% de células viáveis na concentração máxima utilizada (2560 μM). NFOH e NF foram detectados 1h após a gavagem de DMSO-NFOH ou NLC-NFOH, sem o pré-tratamento com cicloheximida. As concentrações encontradas para DMSO-NFOH e NLC-NFOH foram 0,0316 e 0,0291 μg / mL, respectivamente. O NLC apresentou a absorção do NFOH pelo sistema linfático, demonstrada pelo bloqueio do fluxo dos quilomícrons.

Palavras-Chave: leishmanioses, carreador lipídico nanoestruturado, sistema linfático, hidroximetilnitrofural, administração oral

ABSTRACT

De Souza, A. Nanostructured lipid carrier containing hydroxymethylnitrofurazone: preparation, characterization and *in vitro* and *in vivo* evaluation of leishmanicidal activity. 2021. 126p. Tese (Doutorado) – Faculdade de Ciências Farmacêuticas, Universidade de São Paulo, São Paulo.

Leishmaniasis, a neglected tropical disease (NTD), is a set of diseases caused by obligatory parasitic protozoa of the genus *Leishmania*. And it has cutaneous and visceral leishmaniasis as its main forms. Treatment includes pentavalent antimonials. These drugs have several disadvantages, such as the need for parenteral administration, use of high dosages, long duration of treatment, severe toxicity, resistance and variable efficacy. The candidate for hydroxymethylnitrofurazone drug (NFOH), a prodrug derived from nitrofurazone, showed high activity in cell cultures infected with *Trypanosoma cruzi* and less toxicity when compared to nitrofurazone. Due to its low solubility in water and reduced bioavailability, NFOH has failed the *in vivo* efficacy tests. Nanostructured drug delivery systems have the potential to overcome these challenges due to their evident advantages: greater therapeutic efficacy, less toxicity, modified drug release and increased gastrointestinal absorption of drugs with low water solubility. The objective of this project will be the preparation and evaluation of the physicochemical characteristics of a nanostructured lipid carrier containing hydroxymethylnitrofurazone (NLC-NFOH). The NFOH showed the highest solubility in Miglyol® 840 among the tested liquid lipids. For solid lipids, Gelucire® 50/13 and Precirol® ATO5 proved to be more suitable for the solubilization of NFOH. The optimized NLC-NFOH consisted of these three lipids. These lipids were selected using a quick Technobis Crystal 16™ methodology, microscopy and DSC. Different lipid selection tools provided scientific knowledge relevant to the development of NLC. The NLC-NFOH had an average z of 198.6 ± 5.4 nm, a PDI of 0.11 ± 0.01 and a zeta potential of -13.7 ± 0.7 mV. This study allowed a design space development approach of the first NLC-NFOH with the potential to treat leishmaniasis orally. The development of a sensitive bioanalytical method using HPLC and evaluation of some analytical figures of merit for the validation allowed the quantification of NFOH and NF. The bioanalytical method for analysis of NFOH and NF use Zorbax SB-C18,

5 μ m, (4.6x250mm) HPLC column. The mobile phase was consisted of acetonitrile:water (20:80 v/v) with flow rate of 1.2 ml/min, at UV detection of 370 nm. The linearity of NFOH and NF was found in the range 0.025–3.0 μ g/ml with a correlation coefficient of $r > 0.98$. The precision was 2.44 to 13.77% for NFOH and 2.61 to 18.42%; the accuracy was 2.66 to 14.28% for NFOH and 2.09 to 19.06% for NF. The method showed to be suitable for effectively evaluation of NFOH in serum. NLC-NFOH (2.8 mg/kg) was administered to animals by gavage, and the blocking flow of the chylomicrons model was performed with an intraperitoneal injection of cycloheximide. The presence of NFOH in serum was evaluated with and without cycloheximide. The cytotoxicity assay of NLC-NFOH and blank-NLC showed more than 90% viable cells at the maximum concentration used (2560 μ M). NFOH and NF were detected at 1h after the gavage of DMSO-NFOH or NLC-NFOH, without the pretreatment with cycloheximide. The concentration found for DMSO-NFOH and NLC-NFOH were 0.0316 and 0.0291 μ g/mL, respectively. The NLC presented the NFOH absorption by the lymphatic system, demonstrated by blocking chylomicrons flow.

Keywords: leishmaniasis, nanostructured lipid carrier, lymphatic system, hydroxymethylnitrofural, oral administration

PREFACE

This thesis is an original work by Aline de Souza completed under the supervision of Prof. Dr. Nádia Araci Bou-Chacra at the Faculty of Pharmaceutical Sciences - University of São Paulo. Most parts of the work were performed at the Dr. Bou-Chacra lab facilities. Some experiments were also carried out at different lab facilities at the University of São Paulo, as Dr. Ana Cristina Breithaupt Faloppab lab at Medical School, Heart Institute (InCor), LIM 11 and Dr. Paulo Cesar Cotrim Seroepidemiology, Cellular and Molecular Immunology Laboratory of the Institute of Tropical Medicine at USP. The bioanalytical analysis was performed at the Federal University of São Paulo with Dr. Leandro Calixto.

Chapter 1 of this thesis focuses on the current review of promising nanotherapies for treating leishmaniasis. The chapter compiles the findings of recent studies while underscoring the importance of nanotechnology for treating leishmaniasis. The chapter emphasizes the different formulations, as nanometallic, liposomes, nanolipids, nonpolymeric, and nanocrystals, to treat the different forms of leishmaniasis. It was published as Aline de Souza, Débora Soares Souza Marins, Samir Leite Mathias, Lis Marie Monteiro, Megumi Nishitani Yukuyama, Cauê Benito Scarim, Raimar Löbenberg, Nádia Araci Bou-Chacra, with the title of Promising nanotherapy in treating leishmaniasis **in International Journal of Pharmaceutics**, 2018, 547, 421-431.

Chapter 2 focuses on developing a novel NFOH-loaded nanostructured lipid carrier (NLC) for oral administration to treat leishmaniasis, using a design space approach. Hydroxymethylnitrofurazone (NFOH) is a nitrofurazone derivative and has potential use in treating this disease. Using an NLC formulation, we expect to overcome NFOH limitations as low water solubility and bioavailability by improving pharmacokinetics and modifying drug delivery. Two solid lipids were used to develop an NLC-NFOH that presented a z-average of 198.6 ± 5.4 nm, PDI of 0.11 ± 0.01 , and zeta potential of -13.7 ± 0.7 mV. A preliminary *in vivo* assay was performed by oral administration of NLC-NFOH. It was published as Aline de Souza, Megumi Nishitani Yukuyama, Eduardo José Barbosa, Lis Marie Monteiro, Ana Cristina Breithaupt Faloppa, Leandro Augusto Calixto, Gabriel Lima de Barros Araújo, Nikoletta Fotaki, Raimar Löbenberg, Nádia Araci Bou-Chacra. With the title of A new medium-

throughput screening design approach for developing hydroxymethylnitrofurazone (NFOH) nanostructured lipid carrier for treating leishmaniasis in **Colloids and Surfaces B: Biointerfaces**, 2020, 193, 111097.

Chapter 3 of this thesis aimed to develop and evaluate some analytical figures of merit of a bioanalytical method using HPLC to quantify NFOH and NF in serum. The developed method was linear ($r > 0.98$) for both substances at the range of 0.025 to 3.0 $\mu\text{g/mL}$. The precision (RSD) was 2.44 to 13.77% for NFOH and 2.61 to 18.42% for NF; the accuracy was 2.66 to 14.28% for NFOH and 2.09 to 19.06% for NF. The method presented suitable for the evaluation of NFOH and NF in serum.

Chapter 4 focuses on analyzing the absorption of NFOH by the lymphatic system using cycloheximide chylomicrons blocking the flow. This evaluation was done comparing the NLC-NFOH formulation developed during this project and a DMSO-NFOH solution. Both were administered orally to healthy Wistar rats with or without the use of cycloheximide. NLC presented NFOH absorption by the lymphatic system, showing a potential to be used for treating leishmaniasis.

List of figures

Figure 1-1. Cycle of life of Leishmaniasis parasite	6
Figure 2-1. Chemical structure of hydroxymethylnitrofurazone (A) and nitrofurazone (B).	45
Figure 2-2. Optical micrographs (x10) of (A) NFOH; (B) Gelucire® 50/13; (C) Gelucire® 50/13 and NFOH (2.0mg/g) and (D) Gelucire® 50/13 and NFOH (10mg/g).	53
Figure 2-3. DSC curves of hydroxymethylnitrofurazone (NFOH), Gelucire® 50/13, and NFOH and Gelucire® 50/13 – physical mixture (PM) obtained at $\beta = 10^{\circ}\text{C}/\text{min}$. ..	54
Figure 2-4. Contour plots of the NLC-NFOH mathematical model for z-average, containing the following variables: Gelucire® 50/13, Precirol® ATO 5, Miglyol® 840, Poloxamer® 188, and Water	58
Figure 2-5. Distribution of the particle size for NLC-NFOH (F2) by the liquid diffraction dispersion laser method.	59
Figure 2-6. Chromatogram of hydroxymethylnitrofurazone (NFOH) in rat plasma after oral administration of NLC-NFOH.....	60
Figure 3-1. Chemical structure of hydroxymethylnitrofurazone (A) and nitrofurazone (B)	74
Figure 3-2. Maximum NFOH (5.0 $\mu\text{g}/\text{mL}$) absorbance in the range of 190-600 nm... ..	77
Figure 3-3. Chromatogram of hydroxymethylnitrofurazone (NFOH) and nitrofurazone (NF) standards solution (5.0 $\mu\text{g}/\text{mL}$) and blank serum matrix. Chromatographic conditions: Mobile Phase - acetonitrile:water (20:80); wavelength= 370nm; volume of injection= 20 μL	79
Figure 3-4. Linear regression for the curve calibration of hydroxymethylnitrofurazone (NFOH) and nitrofurazone (NF) in rat serum.	81

Figure 3-5. Chromatogram of rat serum after oral administration of nanostructured lipid carrier with NFOH. Chromatographic conditions: Mobile Phase - acetonitrile:water (20:80); wavelength= 370nm; volume of injection= 20 μ L.83

Figure 4-1. Chromatogram of rat serum for quantification of NFOH after oral administration of NLC-NFOH and DMSO-NFOH. Chromatographic conditions: Mobile Phase - acetonitrile:water (20:80); wavelength= 370nm; volume of injection= 20 μ L. 93

List of tables

Table 1-1. <i>Metallic and metal oxide nanoparticle delivery systems for treating leishmaniasis.</i>	12
Table 1-2 - <i>Lipid matrix nanoparticle delivery systems for treating leishmaniasis.</i>	20
Table 1-3 - <i>Polymeric nanoparticle delivery systems for treating leishmaniasis.</i>	25
Table 2-1. <i>Variables and level of extreme vertex experiment in developing NLC-NFOH.</i>	51
Table 2-2. <i>Enthalpy of fusion (kJ/mg) and crystallinity index to determine NFOH solubility in solid lipids by differential scanning calorimetry.</i>	54
Table 2-3. <i>Experimental matrix of extreme vertex experiment, with five-factor, grade 3, two-level D-Optimal mixture statistical design and values of z-average and PDI of NLC-NFOH.</i>	55
Table 2-4. <i>Analysis of variance for z-average</i>	57
Table 2-6. <i>Observed and predicted z-average, polydispersity index (PDI) and zeta potential (ZP) results from NLC-NFOH for F1 and F2.</i>	58
Table 2-7. <i>Stability of NLC-NFOH, F2 formulation:</i>	62
Table 3-1. <i>Linear regression for the curve calibration of hydroxymethylnitrofurazone (NFOH) and nitrofurazone (NF) in rat serum.</i>	80
Table 3-2. <i>Analysis of variance for NFOH analysis.</i>	81
Table 3-3. <i>Analysis of variance for NF analysis.</i>	82
Table 3-4. <i>Precision and Accuracy of NFOH and NF at serum.</i>	82
Table 4-1. <i>The evaluation of NFOH and NF concentration in serum after the one-hour oral administration.</i>	93

List of Equations

Equation 2-149

Equation 2-2.....50

Equation 2-3.....50

Equation 2-4.....57

Equation 3-176

Equation 3-2.....77

Equation 3-3.....77

Summary

DEDICATION.....	III
ACKNOWLEDGEMENTS.....	V
RESUMO.....	VII
ABSTRACT.....	IX
PREFACE	XI
LIST OF FIGURES.....	XIII
LIST OF TABLES	XV
LIST OF EQUATIONS	XVI
CHAPTER 1 : PROMISING NANOTHERAPY IN TREATING LEISHMANIASIS	1
1.1. INTRODUCTION.....	3
1.2. LEISHMANIASIS INFECTION	5
1.3. OVERVIEW OF CURRENT CHEMOTHERAPY	7
1.4. RECENT ADVANCES IN TREATING LEISHMANIASIS: IMPACT OF NANOTECHNOLOGY	7
1.4.1. <i>The role of metallic and metal oxide nanoparticle</i>	<i>8</i>
1.4.2. <i>Liposome: challenges and opportunities</i>	<i>13</i>
1.4.3. <i>The scope of lipid nanoparticle.....</i>	<i>15</i>
1.4.4. <i>Polymeric nanoparticle: synthetic and natural matrices.....</i>	<i>22</i>
1.4.5. <i>Nanocrystal, an encapsulating-carrier free nanoparticle</i>	<i>26</i>
1.5. FINAL CONSIDERATIONS AND FUTURE TRENDS	27
1.6. REFERENCES.....	28
CHAPTER 2 : A NEW MEDIUM-THROUGHPUT SCREENING DESIGN APPROACH FOR THE DEVELOPMENT OF HYDROXYMETHYLNITROFURAZONE (NFOH) NANOSTRUCTURED LIPID CARRIER FOR TREATING LEISHMANIASIS	43
2.1. INTRODUCTION.....	45
2.2. MATERIAL AND METHOD	47
2.2.1. <i>Material.....</i>	<i>47</i>

2.2.2. Selection of Liquid Lipids.....	47
2.2.3. Selection of Solid Lipid	48
2.2.4. Preparation of NLC-NFOH	49
2.2.5. Z-average, polydispersity index and potential zeta analysis.....	49
2.2.6. Determination of encapsulation efficiency (EE%) and drug loading (DL%)	50
2.2.7. NLC development and optimization.....	50
2.2.8. Determination of NFOH in plasma.....	51
2.3. RESULT	51
2.3.1. Selection of liquid lipid	51
2.3.2. Selection of solid lipids	52
2.3.3. NLC development and optimization.....	55
2.3.4. Determination of NFOH in plasma.....	59
2.4. DISCUSSION	60
2.5. CONCLUSION	63
2.6. REFERENCES.....	64
CHAPTER 3 : BIOANALYTICAL DEVELOPMENT OF HPLC METHOD FOR IDENTIFICATION AND QUANTIFICATION OF NFOH AND NF IN SERUM	71
3.1. INTRODUCTION.....	73
3.2. MATERIAL AND METHOD	74
3.2.1. Material.....	74
3.2.2. Apparatus and chromatographic conditions	74
3.2.3. Preparation of standard stock solution, working standard solution and serum sample.....	75
3.2.4. Bioanalytical method Development	75
3.2.5. HPLC method validation.....	75
3.2.5.1. Selectivity	Erro! Indicador não definido.
3.2.5.2. Carry-over	76
3.2.5.3. Matrix effect.....	76
3.2.5.4. Linearity and LLOQ	76
3.2.5.5. Accuracy and Precision	76
3.3. RESULT AND DISCUSSION	77
3.3.1. Development of method	77
3.3.2. HPLC method validation.....	78

3.3.2.1. Selectivity	78
3.3.2.1. Carryover.....	78
3.3.2.2. Matrix effect.....	79
3.3.2.3. Linearity and LLOQ	80
3.3.2.4. Accuracy and Precision	82
3.3.3. <i>Application</i>	83
3.4. CONCLUSION	83
3.5. REFERENCES.....	84
CHAPTER 4 : EVALUATION OF THE LYMPHATIC ABSORPTION OF A NANOSTRUCTURED LIPID CARRIER WITH HYDROXYMETHYLNITROFURAZONE (NFOH) AFTER ORAL ADMINISTRATION IN RATS.....	87
4.1. INTRODUCTION.....	89
4.2. MATERIAL AND METHOD	90
4.2.1. <i>Material</i>	90
4.2.2. <i>Preparation of NLC-NFOH and DMSO-NFOH</i>	90
4.2.3. <i>Cell Culture</i>	90
4.2.4. <i>Cytotoxicity</i>	91
4.2.5. <i>Animals</i>	91
4.2.6. <i>Analysis of NFOH presence in serum</i>	91
4.3. RESULT	92
4.3.1. <i>Cytotoxicity</i>	92
4.3.2. <i>Analysis of NFOH presence in serum</i>	92
4.4. DISCUSSION	94
4.5. CONCLUSION	95
4.6. REFERENCES.....	95
CHAPTER 5 : FINAL CONCLUSION	99

Chapter 1 : Promising nanotherapy in treating leishmaniasis

This study was published as Aline de Souza, Débora Soares Souza Marins, Samir Leite Mathias, Lis Marie Monteiro, Megumi Nishitani Yukuyama, Cauê Benito Scarim, Raimar Löbenberg, Nádia Araci Bou-Chacra, with the title of Promising nanotherapy in treating leishmaniasis in International Journal of Pharmaceutics, 2018, 547, 421-431.

Abstract

Leishmaniasis are infectious diseases caused by an intracellular protozoan in humans by 20 different species of *Leishmania* among more than 53 species. There are at least twelve million cases of infections worldwide and three hundred and fifty million people are at risk in at least 98 developing countries in Africa, South-East Asia, and the Americas. Only Brazil presented high burden for both visceral leishmaniasis (VL) and cutaneous (CL). Chemotherapy is the main means of dealing with this infection. Nevertheless, only a few effective drugs are available, and each has a particular disadvantage; toxicity and long-term regimens compromise most chemotherapeutic options, which decreases patient compliance and adherence to the treatment and consequently the emergence of drug-resistant strains. Nano drug delivery systems (NanoDDS) can direct antileishmanial drug substances for intracellular localization in macrophage-rich organs such as bone marrow, liver, and spleen. This strategy can improve the therapeutic efficacy and reduce the toxic effects of several antileishmanial drug substances. This review is an effort to comprehensively compile recent findings, with the aim of advancing understanding of the importance of nanotechnology for treating leishmaniases.

Keywords: nanotechnology, human leishmaniasis, treatment, nanotherapeutics, drug targeting, drug delivery systems.

1.1. Introduction

Neglected tropical diseases (NTDs) are a diverse group of infectious diseases that are predominant in the poorest parts of the world. These diseases are prevalent in tropical and subtropical areas due to insufficient health infrastructures. There are currently 20 NTDs prevalent in 149 countries, affecting approximately one billion people worldwide (WORLD HEALTH ORGANIZATION, 2016a). Among the NTDs, there are at least seven hundred thousand new leishmaniasis cases and twenty thousand deaths annually worldwide.

Leishmaniasis presents three main forms, visceral (VL), also known as kala-azar, cutaneous (CL) and mucocutaneous leishmaniasis (MCL). The average ratio of incidents between the cutaneous and visceral forms, respectively the common and the fatal form, is approximately 8 times (HERWALDT, 1999; WORLD HEALTH ORGANIZATION, 2017). There are approximately twelve million cases of infections worldwide and three hundred and fifty million people are at risk in 98 developing countries from Africa, South-East Asia and the Americas (AKHOUNDI et al., 2016; WORLD HEALTH ORGANIZATION, 2016b).

In 2015, six regions were reported to have higher cases of CL and VL by the WHO (Europe, Western Pacific, the Americas, Southeast Asia, eastern Mediterranean and Africa), 87 countries were considered endemic for CL and 75 for VL. Southeast Asia is the most affected by VL (9,250) followed by Africa (5,796) and eastern Mediterranean (4,501). For CL, the eastern Mediterranean is the most affected (139,033) followed by the Americas (46,304) and Africa (7,984) (WORLD HEALTH ORGANIZATION, 2017).

According to the World Health Organization (WHO), in 2015, 25 countries were considered a high-burden for leishmaniasis, which means they present over 100 cases of VL and over 2,500 cases of CL. Of these, 13 countries show high-burden of VL and 11, high burden of CL. Brazil is the only country to present high burden for both forms of Leishmaniasis (WORLD HEALTH ORGANIZATION, 2016b).

Considering the total number of cases of CL in the Americas, 70% were reported by Peru (5,459), Colombia (7,541), and Brazil (19,395). In the Americas,

69% of the cases of CL affect males and 12.7% occur in those younger than 10 years old. Secondary infection is reported in 54.2% of cases and is usually caused by *Staphylococcus aureus* (EKIZ et al., 2017). Another important reported coinfection was CL/human immunodeficiency virus (HIV), which is present in 198 of the cases (0.43%), of which 135 were reported in Brazil and 63 cases in Colombia (PAN AMERICAN HEALTH ORGANIZATION, 2017).

According to the Pan American Health Organization (PAHO), in 2015, among the 12 countries affected in the Americas by VL, 96% of the cases were reported in Brazil (3,289), with 268 deaths and a fatality rate of 7.7%. Of the total number of described cases, 64.64% (2,234) were men and 31.9% were children under five years old. For Venezuela, Honduras and Colombia, the infected children represent 59.5%, 83.3% and 95.2%, respectively. In this same year, 257 (7.4%) of VL/HIV coinfection cases were registered, including a single case in Venezuela, 12 in Paraguay and 244 of which were reported in Brazil (PAN AMERICAN HEALTH ORGANIZATION, 2017).

In Brazil the Northeast region is the most affected by VL, but the numbers have decreased from 2,022 in 2014 to 1,523 in 2016, a reduction of approximately 25%. Due to this decrease, the total number reported by Brazil also decreased in 2016 (3,200). However, all the other regions reported an increase of VL cases (BRASIL, 2017a) although the fatality rate decreased in 2015 (6.6%) compared to 2014 (7.8%) (BRASIL, 2017b). Despite these figures, the southern region of Brazil, comprising three of the ten wealthiest states, showed an increase of 40% in the fatality rate (BRASIL, 2017c). For CL, Brazil showed a decrease in all regions in 2016 (BRASIL, 2017d).

Chemotherapy is the main means of treating this infection. Nevertheless, only a few effective drugs are available and each one has a particular disadvantage and toxicity (PHAM; LOISEAU; BARRATT, 2013); long-term regimens compromise most chemotherapeutic options. Thus, the search for safer, more efficient, innovative, cost-effective therapies is urgently needed for treating leishmaniasis.

During the last decade, nanotechnology drug delivery systems (NanoDDS) have been used to enhance the performance of drugs in treating several diseases. Different nanotherapeutics have been approved by the FDA and are currently

available for clinical use (EIFLER; SHAD THAXTON, 2011). Therefore, this review is an effort to comprehensively compile the findings of recent studies while underscoring the importance of nanotechnology for treating leishmaniasis.

1.2. Leishmaniasis Infection

VL, CL and MCL are infections caused by intracellular protozoans in humans by 20 different species of *Leishmania* (World Health Organization, 2017) among more than 53 species (AKHOUNDI et al., 2016).

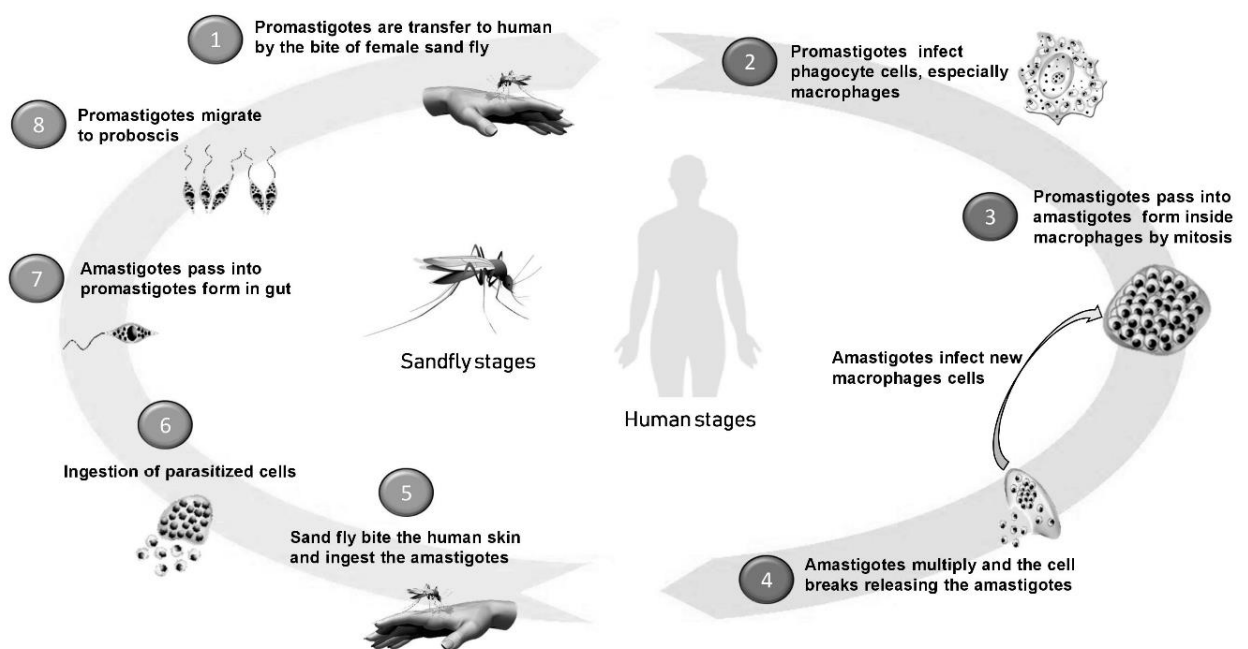
The transmission occurs through the bite of female phlebotomine sandflies (98 of 800 species infect humans) (AKHOUNDI et al., 2016; WORLD HEALTH ORGANIZATION, 2016b), The Old World is affected by the sandfly of the genus *Phlebotomus* (KEVRIC; CAPPEL; KEELING, 2015), and the New World by *Lutzomyia* (BORGHI et al., 2017). Moreover, leishmaniasis can be classified as anthroponotic or zoonotic, the natural reservoir is human or animal, respectively (WORLD HEALTH ORGANIZATION, 2016b).

The parasites have two life-cycles (Figure 1-1): an extracellular mobile stage (promastigote) exclusive to an invertebrate host and an intracellular (amastigote) non-mobile stage in a mammalian vertebrate host (BORGHI et al., 2017). In vertebrates, *Leishmania* parasites infect phagocyte cells, especially macrophages, which are considered to be the major cellular compartments for *Leishmania* in the mammalian vertebrate host (KOBETS; GREKOV; LIPOLDOVA, 2012). Promastigotes form, after infecting cells of the mononuclear phagocytic system, passing into the amastigote form and begin to multiply. Multiplication leads to rupture of the host cell releasing parasites, which infect other macrophages (BORGHI et al., 2017).

VL is generally caused by the *Leishmania donovani* complex, which includes the species *Leishmania infantum*, *Leishmania chagasi*, and *Leishmania donovani* (DE CARVALHO et al., 2013; SOARES-BEZERRA; LEON; GENESTRA, 2004) CL and MCL forms are caused by several *Leishmania* species, including *Leishmania tropica*, *Leishmania major*, *Leishmania amazonensis* (CL) and

Leishmania braziliensis (MINODIER; PAROLA, 2007). The lag period between developing cutaneous and mucosal lesions ranges from months to years (EKIZ et al., 2017).

Figure 1-1. Cycle of life of Leishmaniasis parasite



Source: De Souza, A. et. al., 2017

The cause of the appearance of mucocutaneous form can be associated with the species of parasite, and with the immunity of the host and the site of the primary lesion (CROVETTO-MARTÍNEZ et al., 2015). The MCL is the result of those species that can be disseminated by hematogenous or lymphatic system through the mucosal tissues of the mouth and/or upper respiratory tract (STRAZZULLA et al., 2013). Immunosuppressed patients can present similar conditions with different *Leishmania* species. Lesions above the waist, various or extensive primary lesions or delayed healing of primary CL can be also a risk factor (WORLD HEALTH ORGANIZATION, 2010a).

1.3. Overview of current chemotherapy

Historically, pentavalent antimonials (30 days, 20 mg/kg/day) are the gold standard for treating leishmaniasis (PALUMBO, 2010), which have been dispensed parenteral as first-line chemotherapy against all forms of leishmaniasis and still the drug of first choice for treatment (PHAM; LOISEAU; BARRATT, 2013). The two pentavalent antimonials available, sodium stibogluconate (Pentostan®) and meglumine antimoniate (Glucantime®), are not ideal due to their toxicity and the requirement of hospitalization for the administration (PALUMBO, 2010). The adverse effects of the drug include pancreatitis, cardiotoxicity, nephrotoxicity, hepatotoxicity (WORLD HEALTH ORGANIZATION, 2010a), which decreases patient compliance and adherence to the treatment and consequently the emergence of drug-resistant strains (JEBALI; KAZEMI, 2013).

Second-line recommended treatment consists of amphotericin B (AMB) deoxycholate (Fungizone®, 30 days with 1 mg/kg), liposomal amphotericin B (AmBisome®, single-dose 10mg/Kg), pentamidine (Pentam®, 3-5 days with 4 mg/kg), miltefosine (MILT) (Impavido®, 28 days with 1.5-2.5 mg/day) and paromomycin (PRM) (Humatin®, 21 days with 15 mg/kg/day). These drug substances can be used as combined therapy, which would increase efficacy and tolerance, reducing cost of the treatment and limit drug resistance (MCGWIRE; SATOSKAR, 2014; PHAM; LOISEAU; BARRATT, 2013; WORLD HEALTH ORGANIZATION, 2010a).

1.4. Recent advances in treating leishmaniasis: impact of nanotechnology

Among the new molecules, including those for the treatment of leishmaniasis approved for the development of new drugs, 40% presents low aqueous solubility. Additionally, considering those in the discovery pipeline, this figure raises to 90% (KALEPU; NEKKANTI, 2015). NanoDDS is an alternative and promising approach that allows improving the solubility characteristics of class II and IV drugs of the Biopharmaceutical Classification System. The solubility of the drug in

aqueous medium is determinant for its therapeutic efficacy (SAFFIE-SIEBERT; OGDEN; PARRY-BILLINGS, 2005; SHARMA; SHARMA; JAIN, 2016).

Furthermore, the use of NanoDDS can increase therapeutic efficacy by releasing leishmanicidal drug substances in macrophage-rich organs such as bone marrow, liver, and spleen. This strategy takes advantage of a particulate matter uptake mechanism by macrophages, which is the main phagocytic cell involved in leishmaniasis infection. These cells express receptors that efficiently internalize nanoparticles (NPs) in the range of 50-500 nm (SIEFERT et al., 2016). Phagocytosis, which allows nanoparticles to be engulfed, can increase intracellular drug concentration and a modified drug release can be achieved (RIBEIRO et al., 2014).

Thus, NanoDDS can direct antileishmanial drug substances for intracellular localization in its site of action, improving the efficacy and decreasing the toxic effects of these drugs (GUPTA; PAL; VYAS, 2010; SALOUTI; AHANGARI, 2014). In the last decade, several studies have proposed applying NanoDDS for treating leishmaniasis (KALANGI et al., 2016) using metallic, lipid, polymeric nanoparticles, liposome and nanocrystal.

In this review, the cutaneous leishmaniasis was targeted in 45.2% (14 of 31) of the studies, against 41.9% for visceral leishmaniasis. The others 12.9% (4 of 31) of the studies did not determine the target of the formulation. Among the nanostructures, the metallic nanoparticles were mostly tested for cutaneous leishmaniasis (73.3%), while the lipid and polymeric nanoparticles were most tested for visceral leishmaniasis (62.5%).

1.4.1. The role of metallic and metal oxide nanoparticle

In recent years, metallic nanoparticles have been a focus of interest because of their potential in theranostic nanomedicine (MODY et al., 2010; XIE; LEE; CHEN, 2010). Several chemical, physical and biological synthetic methods have been proposed in designing these nanoparticles (IRAVANI, 2011). Among these, the green synthesis method stands out, which is an ecofriendly and solvent-free approach (AROKIYARAJ et al., 2016; IRAVANI, 2011).

Considering the literature, several authors have reported the potential of inorganic nanoparticles against leishmanicidal activity when tested *in vivo*. Beheshti and collaborators (2013) reported that selenium nanoparticles (SeNPs) can inhibit the proliferation of the amastigote and promastigote forms of *Leishmania major* and limited the growth of CL in animal model. These nanoparticles were biosynthesized via *Bacillus* sp as described by Shakibaie et al. (2010). Also, it was possible to eliminate cutaneous lesions in infected BALB/c mice when SeNPs were administered after developing cutaneous lesions (Beheshti et al., 2013).

Silver nanoparticles (AgNPs) showed antimicrobial, antifungal, and antiviral properties (CHALOUPKA; MALAM; SEIFALIAN, 2010). Since 2009, AgNPs have been studied for treating and enhancing drug substance delivery against leishmaniasis (MOHEBALI et al., 2009), showing to be a highly effective trypanothione reductase inhibitor in *Leishmania donovani* infection (BAIOCCO et al., 2011). Complimentary investigations have demonstrated that it is possible to reduce the inhibitory concentration of miltefosine by half using AgNPs in synergy against *Leishmania* parasites. Kalangi et al. (2016) reported a green synthesis of AgNPs using dill leaf extract. The synergism of AgNPs associated with miltefosine was demonstrated by a decrease in IC₅₀ and increase (2-fold) in leishmanicidal activity (KALANGI et al., 2016).

Additionally, Allahverdiyev and collaborators (2011) reported the antileishmanial activity of AgNPs in the presence of ultraviolet (UV) light on amastigotes and promastigotes of *Leishmania tropica*. The findings indicated a significant decrease in antileishmanial activity by AgNPs. The proliferation and metabolic activity of the parasite in promastigotes was reduced by 1.5 to 3-fold, respectively, in the dark, and 2 to 6.5-fold, respectively, under UV light. Also, inhibition of amastigotes in host cells was most significant in the presence of UV light (Allahverdiyev et al., 2011). Given this, Mayelifar and coworkers (2015) showed the influence of a low dose ultraviolet B (UVB) radiation along with AgNPs in treating CL. These findings demonstrated the excellent pronounced inhibitory effect in the group that received AgNPs and phototherapy UVB. The results indicated synergism of UVB radiation with a cumulative dose of 150 mJ/cm² with AgNPs at a concentration of 2 mg/kg. AgNPs, UVB radiation or combined treatment were able to inhibit the growth of the cutaneous lesions and control infection (Mayelifar et al., 2015).

The use of nanoparticles under UV and infrared (IR) light has high toxicity by generating reactive oxygen species (ROS) causing the death of the organism. Jebali and Kazemi (2013) evaluated antileishmanial effects of some nanoparticles with AgNPs, AuNPs, TiO₂NPs, ZnONPs and MgONPs on *Leishmania major* parasites under UV, IR, and dark conditions. In this study, increased antileishmanial activity was observed for AgNPs, followed by AuNPs, TiO₂NPs, ZnONPs, and MgONPs. Thus, both UV and IR light improved antileishmanial properties of these nanoparticles, which must be considered in future studies (JEBALI; KAZEMI, 2013).

Allahverdiyev et al. (2013) observed the leishmanicidal effect of titanium dioxide and silver nanoparticles (TiAgNps) on the biological properties of *Leishmania infantum* and *Leishmania tropica* parasites. The study aimed to compare their metabolic activity, survival, and viability within host cells both in the presence of dark and UV light. The findings show that TiAgNps reduced viability rates of *Leishmania infantum* and *Leishmania tropica* promastigotes by 10 and 3-fold, respectively, in the dark, although these values decreased closely 20-fold for each species using UV light, in contrast to control (Allahverdiyev et al., 2013).

As alternative, metallic nanoparticles have been combined with bioactive compounds improving antileishmanial activity. Das and coworkers (2013) developed and evaluated gold nanoparticles conjugated with quercetin (QAuNP) against leishmanial macrophage infection. Macrophage uptake of gold nanoparticles and antileishmanial activity were studied against both the wild- and resistant-type parasites. The authors revealed antileishmanial activity of QAuNP against drug resistant strains with a high selectivity index (Das et al., 2013).

In a recent study, Abamor and Allahverdiyev (2016) proposed to investigate antileishmanial activity of TiAgNps, *in vitro*, in combination with essential oils of *Nigella sativa* obtained by different extraction methods. Its major constituent, thymoquinone, showed inhibitory effects on *Leishmania infantum* and *Leishmania tropica* parasites. An enhanced inhibitory effect of the combined agents on *Leishmania tropica* promastigotes (1.5-25 folds) and amastigotes (5-20 folds) was observed in contrast when the substances were used alone, while decreasing their toxicity to minimal levels. The presence of synergism was attributed to different action mechanisms of investigated agents (Abamor and Allahverdiyev, 2016).

In addition to metallic, metal oxide nanoparticles have shown to be a promising approach as an alternative to antibiotics in treating infectious diseases, interacting with vital mechanisms of infectious agents, such as DNA and enzymes, and disrupting their components (PANÁČEK et al., 2006).

Bafghi and coworkers (2015) showed the activity of magnesium oxide nanoparticles (MgONPs) and MgONPs coated with glucose (MONPCG) on *Leishmania major*. The authors evaluated cell viability and expression of two genes (GP63 and Cpb) after incubation with MgONPs and MONPCG. Thus, the expression of these genes was reduced with an increase of nanoparticle concentration. Consequently, the increase of incubation time led to reduction of their expression in MgONPs treated promastigotes; however, a reduction was not observed in MONPCG treated promastigotes (Bafghi et al., 2015).

Delavari et al. (2014) evaluated *in vitro* antileishmanial activity of zinc oxide nanoparticles (ZnONPs). ZnONPs showed dose dependent antileishmanial activity by induced apoptosis in *Leishmania major* (Delavari et al., 2014).

Zahir and collaborators (2015) proposed synthesizing AgNPs and titanium dioxide (TiO₂) nanoparticles using aqueous leaf extract of *Euphorbia prostrata*, which present antileishmanial activity. Comparing the metallic (AgNP) and metal oxide nanoparticles (AgONP), it was found that AgNPs were the most active against *Leishmania* parasites after 24 h exposure when it was evaluated *in vitro* antileishmanial activity. The authors also showed the unique trypanothione/trypanothione reductase system of *Leishmania* cells, which was expressively inhibited by synthesized AgNPs. Thus, these AgNPs presented promising leads for developing cost-effective and safer alternative treatment against VL (Zahir et al., 2015).

Metal oxide and metallic nanoparticles are widely used in various applications and usually classified as non-toxic due to the absence of toxicity of the bulk material. Nevertheless, these nanoparticles (NPs) naturally have toxicity to bacteria and fungi (DJURIŠIĆ et al., 2015). Toxicities associated with NPs in infectious agents are usually related to their causing damage such as generating ROS and oxidative DNA damage (NIAZI; GU, 2009). Additionally, NPs can be potentially dangerous to the central nervous system in some properties, such as

lysosome dysfunction, autophagy, oxidative stress, and the activation of certain signaling pathways (FENG et al., 2015).

Consensus on toxicity mechanisms remains inconclusive, with different studies demonstrating contradictory findings. The relation between the NP mechanisms and toxicity is complex and difficult to understand, demonstrating that there is need for further research in this area. Table 1.1 shows the metallic nanoparticles for treating leishmaniasis.

Metallic and metal oxide nanoparticles have potential to be developed for treating leishmaniasis, as shown in Table 1.1.

Table 1-1. Metallic and metal oxide nanoparticle delivery systems for treating leishmaniasis.

Drug / active Substance	Ref.	Size (nm)	IC ₅₀	Method of preparation
Selenium	(Beheshti et al., 2013)	80-220	$1.62 \pm 0.6 \mu\text{g/mL}$ promastigote $4.4 \pm 0.6 \mu\text{g/mL}$ amastigote	biosynthesized via <i>Bacillus sp.</i>
Silver Miltefosine	(Kalangi et al., 2016)	35	12.5 μM MILT + 50 μM AgNP promastigote	green synthesis
Quercetin Gold	(Das et al., 2013)	15.07	$15 \pm 3 \mu\text{M}$ wild type $40 \pm 8 \mu\text{M}$ sodium stibogluconate resistant strain $30 \pm 6 \mu\text{M}$ paromomycin-resistant strains	green synthesis
Zinc	(Delavari et al., 2014)	20	37.8 $\mu\text{g/mL}$ promastigote	from Selekchem Company, USA
Silver	(Zahir et al., 2015)	12.82 ± 2.50 83.22 ± 1.50	14.94 $\mu\text{g/mL}$ promastigote 3.89 $\mu\text{g/mL}$ amastigote	green synthesis

Ref.: reference; IC₅₀: 50% inhibitory concentrations; MILT: miltefosine; AgNP: silver nanoparticles.

1.4.2. Liposome: challenges and opportunities

Despite being invented over 50 years ago, there are only 15 liposome formulations on the market, mainly for anticancer therapy (BULBAKE et al., 2017). Since the 1970s, the efficacy of intravenous administration of liposomal formulations has improved together with a better understanding of the liposomal structure (LOPES et al., 2012). Liposomes are small artificial vesicles (80 nm to 100 μ m) consisting of concentric spheres of lipid bilayers created from cholesterol and phospholipids. The most common method used for liposome preparation is the thin-film hydration procedure (SHARMA; SHARMA, 1997). The lipids are dissolved in organic solvent, such as trichloromethane (CUI; ZHAO; LIN, 2015), chloroform (SOEMA et al., 2015) and a dry lipid film is then formed when the solvent evaporates (BANGHAM; STANDISH; WATKINS, 1965). The next step is to hydrate the film with an aqueous solution, such as a buffer solution pH 7-7.4, using a temperature higher than the lipid transition temperature (SHARMA; SHARMA, 1997).

Alterations in the pharmacokinetic and biodistribution profiles and/or in establishing a modified release of the drug due to association with these carrier systems lead to improvements in the pharmacological and therapeutic properties of the drugs. After *in vivo* administration and depending on their physicochemical properties, liposomes are perceived as external materials being cleared by cells of the mononuclear phagocytic system (KELLY; JEFFERIES; CRYAN, 2011), which are infected by parasites in leishmaniasis. Thus, the accumulation of antimicrobial drug substances through their combination with liposomes can deliver relevant benefits to the therapy (GASPAR et al., 2008a, 2008b).

The liposomal AMB (L-AMB) (AmBisome®), used for the treatment of systemic fungal infections, has become a standard treatment for VL (VAN DE VEN et al., 2012) and a second line treatment for CL. New et al. (1981) first reported L-AMB efficacy against leishmaniasis in 1981. Only almost two decades after this first study, in 1997, the FDA approved this product for treating this disease (VYAS; GUPTA, 2006).

L-AMB is composed of high transition temperature phospholipids and cholesterol, designed to incorporate AMB securely into the liposomal bilayer. The

AMB, after being released from the liposomes, is thought to transfer through the cell wall and bind to ergosterol in the parasite of *Leishmania* cell membrane. Hence, AMB forms aqueous pores within the plasma membrane and increase the permeability to monovalent cations and small metabolites (RAMOS et al., 1996). AMB also showed to have affinity to cholesterol of host macrophages cells (MOURI et al., 2008; READIO; BITTMAN, 1982), that is required to bind and internalize the parasite into macrophages (PUCADYIL et al., 2004). AMB sequester cholesterol from host macrophages cells and inhibit the infection of *Leishmania* (PAILA; SAHA; CHATTOPADHYAY, 2010). More recently, Chattopadhyay and Jafurulla (2011) proposed a novel AMB leishmanicidal mechanism, which included a combination of the interaction with ergosterol of *Leishmania* and the cholesterol of host macrophages.

The pharmacokinetics studies of L-AMB were performed in immunosuppressed patients with fungal infections. It has never been conducted in leishmaniasis patients (KIP et al., 2018) Pharmacokinetics studies revealed a statistically significant relationship between mean area under curve (AUC) and probability of nephrotoxicity and a non-linear pharmacokinetics (LESTNER et al., 2016). Seibel et al. (2017) showed that all immunosuppressed children (40), but three, had side effects after administration of L-AMB. The patients that received 10mg/kg of L-AMB presented more side effects than those who received 2.5 mg/kg. The study also showed a non-linear pharmacokinetics. Patients treated with 0.6 mg/kg of AMB ($0.060 \pm 0.01 \mu\text{g/mL}$) presented significantly higher C_{max} (mean \pm SD) than patients treated with 2 mg/kg of L-AMB ($0.016 \pm 0.004 \mu\text{g/mL}$) allowing reducing the side effects of AMB (BEKERSKY et al., 2002). For leishmaniasis, Wijnat et al. compared the skin pharmacokinetics of L-AMB with AMB, in murine models of *Leishmania major*. The study showed that after multiple administration, on day 10, the drug level in the lesion location was 3-fold higher for L-AMB than for AMB. The study also showed the linear correlation between dose level, intralesional AMB concentration and relative reduction in parasite load and lesion size.

However, the use of L-AMB continues to be restricted due to a major drawback; its repeated administration results in accumulation due to slow elimination from the body, finally directing to nephrotoxicity, in addition to its high cost (COSTA LIMA et al., 2014). For a patient weighing 35 kg, L-AMB costs US\$ 126 for a daily

treatment (10mg/kg), which means a 6.3-fold higher cost for AMB (30-day treatment, 1mg/kg, alternating days) (WORLD HEALTH ORGANIZATION, 2010b). However, Sundar et al. (2010) showed that a single-dose regimen of L-AMB (10mg/Kg) is effective, noninferior and less expensive to treatment with AMB deoxycholate (15 alternate-day infusions of 1mg/Kg during a 30-day hospital stay).

Several liposomal formulations have been described as an alternative to AmBisome®. Paromomycin (PRM) delivered by liposomes exposed preferential targeting of the antibiotic to the spleen, lungs and liver, relative to free PRM, which resulted in improved therapeutic efficacy and lower toxic effects in murine models infected with *Mycobacterium avium* and *Leishmania infantum* (GASPAR et al., 2015). Additionally, liposomal trifluralin (L-TFL) showed decrease in parasite loads in a murine visceral model of infection by *Leishmania donovani* (CARVALHEIRO et al., 2009).

Later, the same authors, Carvalheiro and coworkers (2015), developed trifluralin analogues liposomes, TFL-A3 and TFL-A6, to further enhance TFL antileishmanial activity. The efficacy of the liposomal formulations TFL-A3 and TFL-A6 were assessed *in vitro* against *Leishmania infantum* resulting in IC₅₀ 1.2±0.4 µM and IC₅₀ 1.8±1.3µM, respectively, and *in vivo* in a murine model of zoonotic visceral leishmaniasis. Furthermore, the findings reported trifluralin analogues were capable to target the intracellular amastigote form of *Leishmania infantum* in infected macrophages revealing the therapeutic activity of liposomal formulations (Carvalheiro et al., 2015).

1.4.3. The scope of lipid nanoparticle

Lipid colloidal drug carriers such as nanoemulsions (NE), solid lipid nanoparticle (SLN) and nanostructured lipid carrier (NLC) have been of great interest to drug delivery scientists mainly due to their versatile nature and interesting advantages as administration of poor water-soluble drug (DATE; JOSHI; PATRAVALE, 2007). These include a higher degree of safety, mainly biocompatibility and biodegradability, and the efficacy comprising their feasibility to be tailored for a

wide range of formulations according to the route of administration or disease (ATTAMA; MOMOH.; BUILDERS., 2012; YUKUYAMA et al., 2017).

These carriers have the potential to enable oral administration of antileishmanial drugs targeting the lymphatic system. Leishmaniasis disseminates through the lymphatic and vascular systems and infects monocytes and macrophages in liver, spleen, bone marrow and lymph nodes. Charman and Stella (1986) found that the solubility of the drug in triglycerides ($>50\text{mg/mL}$), and the octanol:water partition coefficient ($\log P > 5$) contributes to improve its absorption to lymphatic system. Later, Paliwal et al. (2009) and Caliph et al. (2000) showed that triglycerides with long chain are better transported to lymphatic system than the medium chain ones. Furthermore, Ibrahim et al. (2013) demonstrated the influence of the type and ratio of lipids in the pharmacokinetic of AMB after oral administration. This study showed that lipid-based formulation could point to higher steady state concentrations in the tissues after multiple doses, which can improve the destruction of leishmanial parasites. Recent advances in lipid-based nano formulations corroborated these findings. The lymphatic uptake and oral bioavailability of curcumin-SLN coated with N-carboxymethyl chitosan were 6.3-fold and 9.5-fold higher than that of free curcumin, respectively. These results suggest that SLN could be an efficient oral delivery system for curcumin (BAEK; CHO, 2017). Additionally, after oral administration in rats, topotecan (TPT), a water-soluble chemotherapeutic agent lipid nanoparticle allowed to enhance the intestinal lymphatic transport of TPT (WANG et al., 2017).

NEs are a colloidal particulate system, being submicron in size, with varying roles as carriers of drug substances. Their size ranges from 10 to 1000 nm (JAISWAL; DUDHE; SHARMA, 2015) and the main components are lipid liquid, surfactant and aqueous phase (GASCO; GALLARATE; PATTARINO, 1991). These components form a dispersion of two immiscible phases, which are kinetically stable and thermodynamically unstable. Under the selected surfactant type, they can be presented as oil-in-water (O/W) or water-in-oil (W/O) NE, or even generate a cationic or anionic NE (FRYD; MASON, 2012).

The SLN exchanges the liquid lipid of the emulsions by a solid lipid, which results in lipids being solid at room and body temperature. The mean diameter of the

NLS ranges from 40 to 1,000 nm (WEBER; ZIMMER; PARDEIKE, 2014; WISSING; MÜLLER, 2002). The NLC, the second generation of lipid nanoparticles, are composed of colloidal particles that present a matrix composed of a binary mixture of solid lipid with liquid lipid providing a less ordered structure but still solid in body temperature (POONIA et al., 2016).

Two main processes are required for obtaining NE, SLN and NLC: high- and low-energy methods. The first one, driven by mechanical force, comprises high-pressure homogenization, ultrasound and microfluidization. They involve mainly shearing, collision, and cavitation force for breaking down the droplets into a nanoscale range (ATTAMA; MOMOH.; BUILDERS., 2012; DATE; JOSHI; PATRAVALE, 2007; YUKUYAMA et al., 2017). The second one is driven by the physicochemical energy, which consists of the spontaneous curvature change of the phases to break down the particles to deliver the final nanodroplets, during the phase transition process. The low-energy process includes the phase inversion temperature and composition methods (PIT and PIC), spontaneous emulsification (ANTON; BENOIT; SAULNIER, 2008; KOROLEVA; YURTOV, 2012; YUKUYAMA et al., 2016) and the D-Phase emulsification method (SAGITANI; NABETA; NAGAI, 1991). Naseri et al. (2015) describe two other techniques for preparing SLN and NLC, solvent emulsification /evaporation and supercritical fluid extraction of emulsions (SFEE), both techniques use organic solvent to prepare the nanoparticles and each one uses different approaches to remove the solvents.

Mattos and collaborators (2015) successfully incorporated chalcone in nanoemulsions for topical administration in treating CL. This nanoemulsion improved activity against intracellular amastigotes of *L. amazonensis* in THP-1 cells. Additionally, considering the parasitic inhibition profile, this formulation demonstrated both stability and maintenance of leishmanicidal activity (MATTOS et al., 2015).

Lopes et al. (2012) proposed the encapsulated oryzalin containing dinitroanilines in SLN for parenteral administration. The formulation showed encapsulation efficiency > 75% without cytotoxicity effect for all concentrations tested indicating a very protective role to mammalian cells. Thus, suggesting that this strategy may improve the tolerability and therapeutic range of dinitroanilines.

Pham and coworkers (2014) proposed an SLN based on nanocochleates. These are stable cationic phospholipid precipitates with multilayered cylindrical structures, composed of positively charged calcium ions and negatively charged phospholipids (NAGARSEKAR et al., 2016) combining two drug substances: AMB and MILT, which could be administered by the oral route. After nanocochleate preparation, the encapsulation efficiency was 54% and 59% for AMB and MILT, respectively. Drug release is present preferentially in intestinal medium containing bile salts. The release rate of MILT was slightly higher than that of AMB, probably because of the amphiphilic mechanisms of the former. Therefore, AMB-MILT-loaded nanocochleates revealed to be a promising oral delivery system for VL therapy (Pham et al., 2014).

Jung and collaborators (2009) prepared the SLN which can entrap poor water-soluble drugs, AMB, with high drug entrapment efficiency by using solvent evaporation (SESE) and spontaneous emulsification low energy method. Entrapment efficiency of AMB in the SLN reached up to $76.5 \pm 5\%$. The cytotoxicity of AMB-entrapping SLN against normal kidney cells (293 cells) presented to be lower compared with those of the commercial AMB-products, Fungizone® and AmBisome®.

Kharaji and coworkers (2015) have reported PRM-SLN formulation containing 15% lipid composition, which showed efficacy in parasite inhibition. In another study, the authors (HEIDARI-KHARAJI et al., 2016) reported the PRM-SLN formulation as a novel drug delivery for treating leishmaniasis. The preparation was safe and inhibited the propagation of *L. major* parasites in infected mice. Thus, the authors have successfully demonstrated acceptable efficacy and safety of the PRM-SLN formulation as a novel drug against CL. PRM-loaded SLN may increase drug penetration into macrophages and efficient uptake by macrophages may explain the higher efficacy of this treatment (Heidari-Kharaji et al., 2016).

Buparvaquone application in leishmaniasis therapy has been limited by its poor-water solubility. Aiming to overcome this disadvantage, Monteiro et al. (2017b) first described a successful preparation of NLC containing buparvaquone. This drug delivery system has the potential to improve the availability of affordable therapy due

to the low cost of raw materials and the use of high-pressure homogenization, a scale-up feasible technology (Monteiro et al., 2017a).

NLCs have been proposed for treating various neglected diseases such as malaria (OMWOYO et al., 2016; PARASHAR; P; S R, 2016), Chagas disease (MORILLA; ROMERO, 2015; VARGAS DE OLIVEIRA et al., 2017), schistosomiasis (KOLENYAK-SANTOS et al., 2015), dengue fever (TSAI et al., 2012) and tuberculosis (BEG et al., 2018). However, this platform has been still poorly explored for treating leishmaniasis, as shown in Table 1.2.

Table 1-2 - Lipid matrix nanoparticle delivery systems for treating leishmaniasis.

Drug / active substance	Ref.	Size (nm)	PDI	Zeta Potential (mV)	EE%	Lipid	Class component	Method of preparation
Paromomycin	(Gaspar et al., 2015)	110	<0.1	-30±2	96±4	DPPC DPPG	LPS	Dehydration-rehydration method
Trifluralin	(Carvalho et al., 2009)	192 ± 7 and 187 ± 17	-----	40 ± 5 and 38 ± 4	80±6 and 81±12	DOPC DOPG	LPS	lipid film hydration with some modifications
Trifluralin analogues	(Carvalho et al., 2015)	170 - 200	< 0.2	- (30 a 47)	45 a 91	DMPC DMPG	LPS	lipid film-hydration method followed by extrusion
Chalcone	(Koester et al., 2015)	171.9±18.7	0.14±0.01	-39.43±3.56	-----	Soybean Lecithin	NE	spontaneous emulsification
Amphotericin B	(Jung et al., 2009)	84.4±6.0	-----	-50.4±5.0	76.5±5	DPPC CHOL DSPE DPPA	SLN	SESE method
Oryzalin	(Lopes et al., 2012)	< 140	< 0.2	-35	>75	Tripalmitin	SLN	emulsification-solvent
Amphotericin B and Miltefosine	(Pham et al., 2014)	250±2	< 0.1	-2.3±0.6	$\frac{54 \text{ AMB}}{59 \text{ MILT}}$	CHOL DOPS	SLN	hydrogel method

Drug / active substance	Ref.	Size (nm)	PDI	Zeta Potential (mV)	EE%	Lipid	Class component	Method of preparation
Paromomycin	(Heidari-Kharaji et al., 2016)	120	0.67±0.05	532.43±164.40	42 - 46	CHOL	SLN	modified HSH microemulsion technique
Buparvaquone	(Monteiro et al., 2017a)	< 350	< 0.3	< -21.0	100	Miglyol 182 Softisan 154 WitepsolE 85	NLC	high-pressure homogenizer method

Ref.: references; DPPG: dipalmitoyl phosphatidylglycerol, DPPC: dipalmitoyl phosphatidylcholine, DMPC: dimyristoylphosphatidylcholine, DMPG: dimyristoylphosphatidylglycerol, DOPC: dioleoylphosphatidylcholine, DOPG: dioleoylphosphatidylglycerol, DPPC: 1,2-dipalmitoyl-sn-glycero-3-phosphocholine, CHOL: cholesterol, DPPA: 1,2-dipalmitoyl-sn-glycero-3-phosphate (monosodium salt), DOPS: dioleoylphosphatidylserine, DSPE: 1,2-distearoyl-sn-glycero-3-phosphoethanolamine-N-[methoxy(polyethylene glycol)-2000] (ammonium salt), Chalcone: (E)-3-(3-nitrophenyl)-1-(3,4,5-trimethoxyphenyl) prop-2-en-1-one, LPS: liposome, NLC: nanostructured lipid carriers, SLN: solid lipid nanoparticles, NE: nanoemulsions, SESE: spontaneous emulsification and solvent evaporation, HSH: high shear homogenization, EE%: encapsulation efficiency and PDI: polydispersity index.

1.4.4. Polymeric nanoparticle: synthetic and natural matrices

Polymeric nanoparticles are solid colloidal particles, with size of less than 1 μm , made of various biocompatible polymeric matrices (DATE; JOSHI; PATRAVALE, 2007). The drug may be dissolved, retained or adsorbed in the polymer matrix, or in the case of nanocapsules, solubilized in the oily nucleus (DIMER et al., 2013). Polymeric particles have capacity to impact specific drug release kinetic patterns and increase biocompatibility. Biodegradable polymers include synthetic polymers such as polyalkylcyanoacrylates (PACA), poly (lactic acid) (PLA), poly (n-butyl cyanoacrylate) (PBCA), poly (lactide-co-glycolide) (PLGA), poly (caprolactone) (PCL), poly (glycolic acid) (PGA), poly (amino acids) and natural polymers such as gelatin, albumin, chitosan, and alginate (BANIK; FATTAHI; BROWN, 2016).

Different methods have been employed to load antileishmanial drug substances into polymeric nanoparticles such as emulsion or microemulsion polymerization (MONTEIRO et al., 2017a), interfacial polymerization (CHAUBEY; MISHRA, 2014) and precipitation polymerization (KUMAR et al., 2015). Their major drawbacks refer to inadequate biodegradability and/or the possible presence of organic solvent toxic residues (AHLIN GRABNAR; KRISTL, 2011). The removal of solvent represents a time-consuming procedure and any residue can pose a risk to the patient.

Despite a diverse number of polymer molecular structures, most of them (probably > 95%) are not suitable for clinical use. Different weight, architecture and the specific linking chemistry used during the polymer conjugation can impact in safety and efficacy. The discussion of an appropriate regulatory framework has become fundamental (DUNCAN, 2011). Gaspar and Duncan (2009) described the challenges of the regulatory agencies and the importance to treat each polymer used in therapeutic as unique, based on route of administration, doses, dosing frequency and proposal clinical use.

De Carvalho et al. (2013) developed AMB nanoencapsulated in PLGA and dimercaptosuccinic acid (DMSA) nanoparticles (Nano-D-AMB). Its efficacy was evaluated in treating CL. Because hyperthermia based on magnetic nanoparticles

results in controlled release of the drug (DE CARVALHO et al., 2013; KUMAR; MOHAMMAD, 2011), magnetic citrate-coated nanoparticles (Nano-D-AMB-MG) were combined in this nanosystem, in an attempt to improve the release of AMB by magneto hyperthermia. Although Nano-D-AMB-MG showed the same potential as free D-AMB in reducing cutaneous leishmaniasis lesions, the Nano-D-AMB-MG treatment promoted significantly greater reductions in the number of parasites and in cell viability than free D-AMB. This suggests that these NPs were more efficacious than free D-AMB therapy, allowing the dose frequency required to reach the same therapeutic level to be reduced, and thus favoring an extended dosing interval (DE CARVALHO et al., 2013).

Rifampicin (RIF) is well-known and described as an antituberculosis drug; its antileishmanial activity has been reported (NEUBER, 2008). Chaubey and Misha (2014) developed a novel RIF-loaded mannose-conjugated chitosan nanoparticulate system targeting macrophages for treating visceral leishmaniasis. This targeted delivery system was efficient, viable, safe and affordable. Ex vivo pharmacokinetic and biodistribution studies resulted in an expressive increased concentration of RIF in liver and spleen. The cellular drug uptake was 16.2 times higher than that of the free drug (Chaubey and Mishra, 2014).

Kumar et al. (2015) developed PLGA-PEG encapsulated AMB nanoparticles to target the macrophage of visceral leishmaniasis infected tissues. This system showed cytotoxicity of extracellular promastigote 1.4-fold lower than free AMB. In addition, amastigote inhibition in the splenic tissue was expressively higher than with conventional AMB ($93.02 \pm 6.63\%$ versus $74.42 \pm 14.78\%$). Thus, AMB encapsulated PLGA-PEG NPs showed to have greater potential than free AMB in terms of therapeutic efficacy in *in vitro* and *in vivo* studies (Kumar et al., 2015).

Monteiro and coworkers (2017a) prepared hydroxymethylnitrofurazone (NFOH), a drug candidate, PBCA nanoparticle presenting encapsulation efficiency of $64.47 \pm 0.43\%$. Where PBCA-NFOH-NPs demonstrated IC₅₀ values of $0.33 \mu\text{M}$ and $4.90 \mu\text{M}$ for amastigotes and promastigotes of *L. amazonensis*, respectively. The selectivity index was 370.6 for PBCA-NFOH-NPs, which was a 49-fold increase than free NFOH. The activity of PBCA-NFOH-NPs presented great efficacy for delivery

aimed at macrophages (Monteiro et al., 2017b). The authors have filed a patent application for this invention (BR 10 2014 007923-8).

In a similar way, Britti et al. (2015) claimed ownership of intellectual property WO 2015 177820 where polymer nanoparticles are employed as an effective vehicle for compounds based on antimony and antimonials, such as Glucantime®. The system was prepared from an aqueous nucleus in which the active ingredient is entrapped, surrounded by a polymeric biocompatible and biodegradable shell based on PLA. This invention claims that the system allows reduction of cellular toxicity in treating this disease since the active ingredient is carried and concentrated only within the macrophages, avoiding systemic effects related to the therapy with antimonial medications (BRITTI et al., 2015).

Table 1.3 presents the properties of polymer nanoparticles for treating leishmaniasis. As can be observed, there are few studies proposing these nanoparticles possibly because of their limitations. In all procedures, the use of organic solvents was necessary with the exception of the method described by Monteiro and coworkers (2017a).

Table 1-3 - Polymeric nanoparticle delivery systems for treating leishmaniasis.

Drug / active substance	Ref.	Size (nm)	PDI	Zeta Potential (mV)	EE%	Polymers	Method of preparation
AMB	(De Carvalho et al., 2013)	456.60±133.60	0.431±0.001	-32.60 ±4.64	----	PLGA DMSA	method described by Amaral et al., with slight modification
AMB-MG		675.20±40.28	0.584±0.001	-28.00±4.86			prepared by chemical condensation reaction of aqueous ions in alkaline medium
RIF	(Chaubey and Mishra, 2014)	215.2±2.4	0.109±0.18	26.2±1.7	39.1±6.3	Chitosan Mannose	inducing the gelation method with suitable modifications
AMB	(Kumar et al., 2015)	30-35	----	----	----	PLGA	precipitation method
NFOH	(Monteiro et al., 2017b)	151.50±61.97	0.104±0.01	-10.10±6.47	64.47±0.43	PBCA	anionic emulsion polymerization method

Ref.: references; AMB: desoxycholate amphotericin B, AMB-MG: desoxycholate amphotericin B with magnetic citrate-coated maghemite, DMSA: dimercaptosuccinic acid, PLGA: poly (glycolic acid) (PGA), PBCA: poly (n-butyl cyanoacrylate), RIF: rifampicin, NFOH: hydroxymethylnitrofurazone, EE%: encapsulation efficiency and PDI: polydispersity index.

1.4.5. Nanocrystal, an encapsulating-carrier free nanoparticle

Nanocrystals are drug particles with crystalline or amorphous character in the submicron or nanometric range, generally between 100 and 500 nm. The nanocrystals are solids formed by a network of atoms, ions or molecules, usually obtained by direct crystallization (bottom-up approach) or grinding (fragmentation) of the material (top-down approach) (MÜLLER; GOHLA; KECK, 2011; SHEGOKAR; MÜLLER, 2010), composed exclusively of the drug (MÜLLER; GOHLA; KECK, 2011; SINHA; MÜLLER; MÖSCHWITZER, 2013) prepared in dispersion media using stabilizers (surfactants and / or polymers), resulting in a colloidal system. Thus, in the liquid medium, this system is called a nanosuspension (MÜLLER; GOHLA; KECK, 2011; RABINOW, 2004).

Poor water-soluble drug substances represent 40% of the top 200 oral medicines marketed in the US, 33% of drug substances listed in the US Pharmacopeia, 75% of drug candidates under development and 90% of molecules in the discovery pipeline (RODRIGUEZ-ALLER et al., 2015). Nanocrystals can improve the dissolution velocity and the saturation solubility of these drugs. The essence of the nanonization of poor water-soluble drug substances rests mainly on Noyes-Whitney equations Noyes and Whitney (1897) and Prandtl (1904). These equations describe how a decrease in particle size facilitates increasing the surface area and reducing the thickness of the diffusion layer, and thus, provides an increase in dissolution rate.

An additional advantage of nanocrystals refers to their greater adhesiveness compared to particles in the micrometer range in the biological membrane and surface of the gastrointestinal tract. As a result, drug absorption can be increased independent of the fed or fasting state (MÜLLER; GOHLA; KECK, 2011). However, it is important to ensure the physical chemical properties of the drug nanocrystal during the manufacturing process and in storage throughout its shelf life (CHEN et al., 2017) since these characteristics are critical for drug dissolution velocity in the nanosuspension.

Kayser et al (2003) develop a nanosuspension of AMB by high-pressure homogenization, using polysorbate 80 and poloxamer P188. This formulation

showed to be more active than micronized AMB for visceral leishmania model, after oral administration in rats. The reduction of parasite in liver was 28.6%. In our group, Marins et al. (2017) reported a successful formulation using NFOH and polysorbate 80. NFOH, a nitrofurazone reciprocal prodrug, is a promising drug candidate, which presented potential use in treating Chagas disease and leishmaniasis (CHUNG et al., 2003).

1.5. Final considerations and future trends

Considering the advantages and limitations, it is possible to identify a tendency in research into NanoDDS for treating leishmaniasis. Different nanosystems have been proposed in the last decade such as metallic, polymeric and lipid nanoparticles, liposomes and nanocrystals. Metallic nanoparticles have potential application as diagnostic and chemotherapeutic agents, although their toxicity has aroused concern. The synthetic polymers can be a challenge to regulatory agencies due to their diversity and consequent impact in safety and efficacy. Besides, natural polymers and their derivatives can present a high degree of variability due to it being obtained from an animal source.

A feasible industrial-scale manufacturing process allows an economically viable NanoDDS, which can be successfully introduced to the clinic and market. For this reason, the lipid nanoparticles obtained by high-pressure homogenization have been considered a promising delivery system. This well-established reliable and scale-up technology has the potential to improve the availability of affordable medicines. Besides this, for preparation the use of organic solvent is not necessary. However, this technology is not recommended for thermolabile and volatile drugs. Drug nanocrystal, an encapsulating-carrier free nanoparticle, can also be produced using this technology.

Nanosystems have the potential to play a key role in a major shift in treating leishmaniasis through macrophage-targeted delivery. It can reduce the duration of the treatment and frequency of administration by improving the adherence of patients to the therapy. A considerable number of studies demonstrate the *in vivo* efficacy of these therapies; however only liposomes (AmBisome®) have reached the market. Unfortunately, this product is not affordable, preventing long-term availability

of treatment and currently only benefiting a small proportion of patients worldwide. The present study revealed diverse innovative nanotherapies that are potentially safe and effective, which can provide an alternative for necessary competition to reduce the price of leishmaniasis treatment using state-of-art technology.

1.6. References

- ABAMOR, E. S.; ALLAHVERDIYEV, A. M. A nanotechnology based new approach for chemotherapy of Cutaneous Leishmaniasis: TIO₂@AG nanoparticles - Nigella sativa oil combinations. **Experimental Parasitology**, v. 166, p. 150–163, 1 jul. 2016.
- AHLIN GRABNAR, P.; KRISTL, J. The manufacturing techniques of drug-loaded polymeric nanoparticles from preformed polymers. **Journal of Microencapsulation**, v. 28, n. 4, p. 323–335, 17 jun. 2011.
- AKHOUNDI, M. et al. A Historical Overview of the Classification, Evolution, and Dispersion of Leishmania Parasites and Sandflies. **PLoS Neglected Tropical Diseases Academic Press**. 3 mar. 2016.
- ALLAHVERDIYEV, A. M. et al. Antileishmanial effect of silver nanoparticles and their enhanced antiparasitic activity under ultraviolet light. **International journal of nanomedicine**, v. 6, p. 2705–2714, 2011.
- ALLAHVERDIYEV, A. M. et al. Investigation of antileishmanial activities of Tio₂@Ag nanoparticles on biological properties of L. tropica and L. infantum parasites, *in vitro*. **Experimental Parasitology**, v. 135, n. 1, p. 55–63, 1 set. 2013.
- ANTON, N.; BENOIT, J. P.; SAULNIER, P. Design and production of nanoparticles formulated from nano-emulsion templates-A review. **Journal of Controlled Release**, v. 128, n. 3, p. 185–199, 2008.
- AROKIYARAJ, S. et al. Green synthesis of metallic nanoparticles using plant compounds and their applications: Metallic nanoparticles synthesis using plants. In: BOUOUDINA, M. (Ed.). . **Emerging Research on Bioinspired Materials Engineering**. 1. ed. Hershey: IGI Global, 2016. p. 1–34.
- ATTAMA, A.; MOMOH., M.; BUILDERS., P. Lipid Nanoparticulate Drug Delivery Systems: A Revolution in Dosage Form Design and Development. In: SEZER, A. D.

(Ed.). . **Recent Advances in Novel Drug Carrier Systems**. 1. ed. InTech, 2012. p. 107–140.

BAEK, J. S.; CHO, C. W. Surface modification of solid lipid nanoparticles for oral delivery of curcumin: Improvement of bioavailability through enhanced cellular uptake, and lymphatic uptake. **European Journal of Pharmaceutics and Biopharmaceutics**, v. 117, p. 132–140, 1 ago. 2017.

BAFGHI, A. F. et al. Magnesium oxide nanoparticles coated with glucose can silence important genes of *Leishmania major* at sub-toxic concentrations. **Colloids and Surfaces B: Biointerfaces**, v. 136, p. 300–304, 1 dez. 2015.

BAIOCCO, P. et al. Inhibitory effect of silver nanoparticles on trypanothione reductase activity and *Leishmania infantum* proliferation. **ACS Medicinal Chemistry Letters**, v. 2, n. 3, p. 230–233, 10 mar. 2011.

BANGHAM, A. D.; STANDISH, M. M.; WATKINS, J. C. Diffusion of univalent ions across the lamellae of swollen phospholipids. **Journal of Molecular Biology**, v. 13, n. 1, p. 238–252, 1 ago. 1965.

BANIK, B. L.; FATTAHI, P.; BROWN, J. L. Polymeric nanoparticles: The future of nanomedicine. **Wiley Interdisciplinary Reviews: Nanomedicine and Nanobiotechnology**, v. 8, n. 2, p. 271–299, 1 mar. 2016.

BEG, S. et al. Nanoemulsion for the Effective Treatment and Management of Anti-tubercular Drug Therapy. **Recent Patents on Anti-Infective Drug Discovery**, v. 12, n. 2, p. 85–94, 3 maio 2018.

BEHESHTI, N. et al. Efficacy of biogenic selenium nanoparticles against *Leishmania major*. *In vitro* and *in vivo* studies. **Journal of Trace Elements in Medicine and Biology**, v. 27, n. 3, p. 203–207, 2013.

BEKERSKY, I. et al. Plasma protein binding of amphotericin B and pharmacokinetics of bound versus unbound amphotericin B after administration of intravenous liposomal amphotericin B (AmBisome) and amphotericin B deoxycholate. **Antimicrobial Agents and Chemotherapy**, v. 46, n. 3, p. 834–840, 1 mar. 2002.

BORGHI, S. M. et al. Leishmania infection: painful or painless? **Parasitology Research**, v. 116, n. 2, p. 465–475, 9 fev. 2017

BRASIL. **Casos confirmados de Leishmaniose Visceral, Brasil, Grandes Regiões e Unidades Federativas Ministério da Saúde de 1990 a 2016.** Disponível em: <<http://portalarquivos.saude.gov.br/images/pdf/2017/setembro/14/LV-Casos.pdf>>.

BRASIL. **Casos de leishmaniose visceral no Brasil, 1980 a 2015.** Disponível em: <<https://portalarquivos.saude.gov.br/images/pdf/2017/marco/03/LV-Graficos-e-Mapas.pdf>>.

BRASIL. **Letalidade de Leishmaniose Visceral. Brasil, Grandes Regiões e Unidades Federadas. 2000 a 2016.** Ministério da Saúde, p. 1, 2017c.

BRASIL. **Casos de Leishmaniose Tegumentar. Brasil, Grandes Regiões e Unidades Federadas. 1990 a 2016.** Disponível em: <<http://portalarquivos.saude.gov.br/images/pdf/2017/setembro/14/LT-Casos.pdf>>.

BRITTI, D. et al. **Nanoparticulate systems for vehiculating drugs for the treatment of leishmania infection-related pathologies.**, 2015.

BULBAKE, U. et al. Liposomal Formulations in Clinical Use: An Updated Review. **Pharmaceutics**, v. 9, n. 4, p. 12, 27 mar. 2017.

CALIPH, S. M.; CHARMAN, W. N.; PORTER, C. J. H. Effect of short-, medium-, and long-chain fatty acid-based vehicles on the absolute oral bioavailability and intestinal lymphatic transport of halofantrine and assessment of mass balance in lymph-cannulated and non-cannulated rats. **Journal of Pharmaceutical Sciences**, v. 89, n. 8, p. 1073–1084, 1 ago. 2000.

CARVALHEIRO, M. et al. Trifluralin liposomal formulations active against *Leishmania donovani* infections. **European Journal of Pharmaceutics and Biopharmaceutics**, v. 71, n. 2, p. 292–296, 1 fev. 2009.

CARVALHEIRO, M. et al. Hemisynthetic trifluralin analogues incorporated in liposomes for the treatment of leishmanial infections. **European Journal of Pharmaceutics and Biopharmaceutics**, v. 93, p. 346–352, 26 maio 2015.

CHALOUPKA, K.; MALAM, Y.; SEIFALIAN, A. M. Nanosilver as a new generation of nanoprodut in biomedical applications. **Trends in Biotechnology**, v. 28, n. 11, p. 580–588, 1 nov. 2010.

CHARMAN, W. N. A.; STELLA, V. J. Estimating the maximal potential for intestinal lymphatic transport of lipophilic drug molecules. **International Journal of Pharmaceutics**, v. 34, n. 1–2, p. 175–178, 1 dez. 1986.

CHATTOPADHYAY, A.; JAFURULLA, M. A novel mechanism for an old drug: Amphotericin B in the treatment of visceral leishmaniasis. **Biochemical and Biophysical Research Communications**, v. 416, n. 1–2, p. 7–12, 9 dez. 2011.

CHAUBEY, P.; MISHRA, B. Mannose-conjugated chitosan nanoparticles loaded with rifampicin for the treatment of visceral leishmaniasis. **Carbohydrate Polymers**, v. 101, n. 1, p. 1101–1108, 30 jan. 2014.

CHEN, M.-L. et al. Development Considerations for Nanocrystal Drug Products. **The AAPS Journal**, n. 9, 2017.

CHUNG, M. C. et al. Synthesis and *in vitro* evaluation of potential antischistosomal hydroxymethylnitrofurazone (NFOH-121): A new nitrofurazone prodrug. **Bioorganic and Medicinal Chemistry**, v. 11, n. 22, p. 4779–4783, 2003.

COSTA LIMA, S. A. et al. Crucial CD8⁺ T-lymphocyte cytotoxic role in amphotericin B nanospheres efficacy against experimental visceral leishmaniasis. **Nanomedicine: Nanotechnology, Biology, and Medicine**, v. 10, n. 5, p. e1021–e1030, 1 jul. 2014.

CROVETTO-MARTÍNEZ, R. et al. Mucocutaneous leishmaniasis must be included in the differential diagnosis of midline destructive disease: Two case reports. **Oral Surgery, Oral Medicine, Oral Pathology and Oral Radiology**, v. 119, n. 1, p. e20–e26, 1 jan. 2015.

CUI, H.; ZHAO, C.; LIN, L. The specific antibacterial activity of liposome-encapsulated Clove oil and its application in tofu. **Food Control**, v. 56, p. 128–134, 1 out. 2015.

DAS, S. et al. One pot synthesis of gold nanoparticles and application in chemotherapy of wild and resistant type visceral leishmaniasis. **Colloids and Surfaces B: Biointerfaces**, v. 107, p. 27–34, 1 jul. 2013.

DATE, A. A.; JOSHI, M. D.; PATRAVALE, V. B. Parasitic diseases: Liposomes and polymeric nanoparticles versus lipid nanoparticles. **Advanced Drug Delivery Reviews**, v. 59, n. 6, p. 505–521, 10 jul. 2007.

DE CARVALHO, R. F. et al. Leishmanicidal activity of amphotericin B encapsulated in PLGA-DMSA nanoparticles to treat cutaneous leishmaniasis in C57BL/6 mice. **Experimental Parasitology**, v. 135, n. 2, p. 217–222, out. 2013.

DE MATTOS, C. B. et al. Nanoemulsions containing a synthetic chalcone as an alternative for treating cutaneous leishmaniasis: Optimization using a full factorial design. **International Journal of Nanomedicine**, v. 10, p. 5529–5542, 1 set. 2015.

DELAVARI, M. et al. *In vitro* study on cytotoxic effects of ZnO nanoparticles on promastigote and amastigote forms of *Leishmania major* (MRHO/IR/75/ER). **Iranian Journal of Parasitology**, v. 9, n. 1, p. 6–13, 2014.

DIMER, F. A. et al. IMPACTOS DA NANOTECNOLOGIA NA SAÚDE: PRODUÇÃO DE MEDICAMENTOS. *Química Nova*, v. 36, n. 10, p. 1520–1526, 2013.

DJURIŠIĆ, A. B. et al. Toxicity of Metal Oxide Nanoparticles: Mechanisms, Characterization, and Avoiding Experimental Artefacts. **Small**, v. 11, n. 1, p. 26–44, 7 jan. 2015.

DUNCAN, R. Polymer therapeutics as nanomedicines: New perspectives. **Current Opinion in Biotechnology**, v. 22, n. 4, p. 492–501, 1 ago. 2011.

EIFLER, A. C.; SHAD THAXTON, C. Nanoparticle therapeutics: FDA approval, clinical trials, regulatory pathways, and case study. In: HURST, S. (Ed.). . **Biomedical Nanotechnology. Methods in Molecular Biology (Methods and Protocols)**. 1. ed. Humana Press, 2011. v. 726p. 325–338.

EKIZ, O. et al. Mucocutaneous leishmaniasis with marked facial disfigurement. **Indian journal of dermatology, venereology and leprology**, v. 83, n. 1, p. 91–93, 2017.

FENG, X. et al. Central nervous system toxicity of metallic nanoparticles. **International Journal of Nanomedicine**, v. 10, p. 4321–4340, 2015.

FRYD, M. M.; MASON, T. G. Advanced Nanoemulsions. **Annual Review of Physical Chemistry**, v. 63, n. 1, p. 493–518, 5 maio 2012.

GASCO, M. R.; GALLARATE, M.; PATTARINO, F. *In vitro* permeation of azelaic acid from viscosized microemulsions. **International Journal of Pharmaceutics**, v. 69, n. 3, p. 193–196, 20 mar. 1991.

GASPAR, M. et al. Developments on Drug Delivery Systems for the Treatment of Mycobacterial Infections. **Current Topics in Medicinal Chemistry**, v. 8, n. 7, p. 579–591, 28 mar. 2008a.

GASPAR, M. M. et al. Rifabutin encapsulated in liposomes exhibits increased therapeutic activity in a model of disseminated tuberculosis. **International Journal of Antimicrobial Agents**, v. 31, n. 1, p. 37–45, 1 jan. 2008b.

GASPAR, M. M. et al. Targeted delivery of paromomycin in murine infectious diseases through association to nano lipid systems. **Nanomedicine: Nanotechnology, Biology, and Medicine**, v. 11, n. 7, p. 1851–1860, 1 out. 2015.

GASPAR, R.; DUNCAN, R. Polymeric carriers: Preclinical safety and the regulatory implications for design and development of polymer therapeutics. **Advanced Drug Delivery Reviews**, v. 61, n. 13, p. 1220–1231, 12 nov. 2009.

GUPTA, S.; PAL, A.; VYAS, S. P. Drug delivery strategies for therapy of visceral leishmaniasis. **Expert Opinion on Drug Delivery**, v. 7, n. 3, p. 371–402, mar. 2010

HEIDARI-KHARAJI, M. et al. Solid lipid nanoparticle loaded with paromomycin: *in vivo* efficacy against *Leishmania tropica* infection in BALB/c mice model. **Applied Microbiology and Biotechnology**, v. 100, n. 16, p. 7051–7060, 2016.

HERWALDT, B. L. Leishmaniasis. **Lancet**, v. 354, n. 9185, p. 1191–1199, 2 out. 1999.

IBRAHIM, F. et al. Pharmacokinetics and tissue distribution of amphotericin B following oral administration of three lipid-based formulations to rats. **Drug Development and Industrial Pharmacy**, v. 39, n. 9, p. 1277–1283, 18 set. 2013.

IRAVANI, S. Green synthesis of metal nanoparticles using plants. **Green Chemistry**, v. 13, n. 10, p. 2638–2650, 10 jan. 2011.

JAISWAL, M.; DUDHE, R.; SHARMA, P. K. Nanoemulsion: an advanced mode of drug delivery system. **3 Biotech**, v. 5, n. 2, p. 123–127, 1 abr. 2015.

JEBALI, A.; KAZEMI, B. Nano-based antileishmanial agents: A toxicological study on nanoparticles for future treatment of cutaneous leishmaniasis. **Toxicology in vitro**, v. 27, n. 6, p. 1896–1904, 1 set. 2013.

JUNG, S. H. et al. Amphotericin B-entrapping lipid nanoparticles and their *in vitro* and *in vivo* characteristics. **European Journal of Pharmaceutical Sciences**, v. 37, n. 3–4, p. 313–320, 28 jun. 2009.

KALANGI, S. K. et al. Biocompatible silver nanoparticles reduced from *Anethum graveolens* leaf extract augments the antileishmanial efficacy of miltefosine. **Experimental Parasitology**, v. 170, p. 184–192, 1 nov. 2016.

KALEPU, S.; NEKKANTI, V. Insoluble drug delivery strategies: Review of recent advances and business prospects. **Acta Pharmaceutica Sinica B**, v. 5, n. 5, p. 442–453, 2015.

KAYSER, O. et al. Formulation of amphotericin B as nanosuspension for oral administration. **International Journal of Pharmaceutics**, v. 254, n. 1, p. 73–75, 18 mar. 2003.

KELLY, C.; JEFFERIES, C.; CRYAN, S.-A. Targeted Liposomal Drug Delivery to Monocytes and Macrophages. **Journal of Drug Delivery**, v. 2011, p. 11, 2011.

KEVRIC, I.; CAPPEL, M. A.; KEELING, J. H. New World and Old World Leishmania Infections: A Practical Review. **Dermatologic Clinics**, v. 33, n. 3, p. 579–593, 2015.

KHARAJI, M. H. et al. Drug Targeting to Macrophages With Solid Lipid Nanoparticles Harboring Paromomycin: an *In vitro* Evaluation Against *L. major* and *L. tropica*. **AAPS PharmSciTech**, n. 12, p. 13–15, 2015.

KIP, A. E. et al. Clinical Pharmacokinetics of Systemically Administered Antileishmanial Drugs. **Clinical Pharmacokinetics**, v. 57, n. 2, p. 151–176, 1 fev. 2018.

KOBETS, T.; GREKOV, I.; LIPOLDOVA, M. Leishmaniasis: Prevention, Parasite Detection and Treatment. **Current Medicinal Chemistry**, v. 19, n. 10, p. 1443–1474, 2012.

KOLENYAK-SANTOS, F. et al. Nanostructured lipid carriers as a strategy to improve the *in vitro* schistosomiasis activity of Praziquantel. **Journal of Nanoscience and Nanotechnology**, v. 15, n. 1, p. 761–772, 1 jan. 2015.

KOROLEVA, M. Y.; YURTOV, E. V. Nanoemulsions: the properties, methods of preparation and promising applications. **Russian Chemical Reviews**, v. 81, n. 1, p. 21–43, 31 jan. 2012.

KUMAR, C. S. S. R.; MOHAMMAD, F. Magnetic nanomaterials for hyperthermia-based therapy and controlled drug delivery. **Advanced Drug Delivery Reviews**, v. 63, n. 9, p. 789–808, 14 ago. 2011.

KUMAR, R. et al. Study the effects of PLGA-PEG encapsulated Amphotericin B nanoparticle drug delivery system against *Leishmania donovani*. **Drug Delivery**, v. 22, n. 3, p. 383–388, 3 abr. 2015.

LESTNER, J. M. et al. Population pharmacokinetics of liposomal amphotericin B in immunocompromised children. **Antimicrobial Agents and Chemotherapy**, v. 60, n. 12, p. 7340–7346, 1 dez. 2016.

LOPES, R. et al. Lipid nanoparticles containing oryzalin for the treatment of leishmaniasis. **European Journal of Pharmaceutical Sciences**, v. 45, n. 4, p. 442–450, 12 mar. 2012.

MARINS, D.; ARAÚJO, GABRIEL., LÖBENBERG, R.; BOU-CHACRA, N. A. **Hydroxymethylnitrofurazone Nanocrystals (NFOH): A Promising Therapeutic Approach in the Treatment of Leishmaniasis**. AAPS Annual Meeting and Exposition. **Anais**. San Diego: 2017

MAYELIFAR, K. et al. Ultraviolet B efficacy in improving antileishmanial effects of silver nanoparticles. **Iranian journal of basic medical sciences**, v. 18, n. 7, p. 677–83, jul. 2015.

MCGWIRE, B. S.; SATOSKAR, A. R. Leishmaniasis: Clinical syndromes and treatment. **QJM**, v. 107, n. 1, p. 7–14, 2014.

MINODIER, P.; PAROLA, P. Cutaneous leishmaniasis treatment. **Travel Medicine and Infectious Disease**, v. 5, p. 150–158, out. 2007.

MODY, V. et al. Introduction to metallic nanoparticles. **Journal of Pharmacy and Bioallied Sciences**, v. 2, n. 4, p. 282, 2010.

MOHEBALI, M. et al. Nanosilver in the treatment of localized cutaneous leishmaniasis caused by *Leishmania major* (MRHO/IR/75/ER): An *in vitro* and *in vivo* study. **Daru**, v. 17, n. 4, p. 285–289, 13 dez. 2009.

MONTEIRO, L. M. et al. Buparvaquone Nanostructured Lipid Carrier: Development of an Affordable Delivery System for the Treatment of Leishmaniasis. **BioMed Research International**, v. 2017, p. 1–11, 2017a.

MONTEIRO, L. M. et al. Targeting *Leishmania amazonensis* amastigotes through macrophage internalisation of a hydroxymethylnitrofurazone nanostructured polymeric system. **International Journal of Antimicrobial Agents**, v. 50, n. 1, p. 88–92, 2017b.

MORILLA, M. J.; ROMERO, E. L. Nanomedicines against Chagas disease: an update on therapeutics, prophylaxis and diagnosis. **Nanomedicine**, v. 10, n. 3, p. 465–481, 24 fev. 2015.

MOURI, R. et al. Complex formation of amphotericin B in sterol-containing membranes as evidenced by surface plasmon resonance. **Biochemistry**, v. 47, n. 30, p. 7807–7815, 29 jul. 2008.

MÜLLER, R. H.; GOHLA, S.; KECK, C. M. State of the art of nanocrystals - Special features, production, nanotoxicology aspects and intracellular delivery. **European Journal of Pharmaceutics and Biopharmaceutics**, v. 78, n. 1, p. 1–9, 2011.

NAGARSEKAR, K. et al. Understanding cochleate formation: Insights into structural development. **Soft Matter**, v. 12, n. 16, p. 3797–3809, 28 abr. 2016.

NASERI, N.; VALIZADEH, H.; ZAKERI-MILANI, P. Solid Lipid Nanoparticles and Nanostructured Lipid Carriers: Structure, Preparation and Application. **Tabriz University of Medical Sciences**, v. 5, n. 3, p. 305–313, 2015.

NEUBER, H. Leishmaniasis. **JDDG - Journal of the German Society of Dermatology**, v. 6, n. 9, p. 754–765, 2008.

NEW, R. R. C.; CHANCE, M. L.; HEATH, S. Antileishmanial activity of amphotericin and other antifungal agents entrapped in liposomes. **Journal of Antimicrobial Chemotherapy**, v. 8, n. 5, p. 371–381, 1 nov. 1981.

NIAZI, J. H.; GU, M. B. Toxicity of metallic nanoparticles in microorganisms- A review. In: Y.J., K. et al. (Eds.). . **Atmospheric and Biological Environmental Monitoring**. 1. ed. Springer, Dordrecht, 2009. p. 193–206.

NOYES, A. A.; WHITNEY, W. R. The rate of solution of solid substances in their own solutions. **Journal of the American Chemical Society**, v. 19, n. 12, p. 930–934, 1897.

OMWOYO, W. N. et al. Development, characterization and antimalarial efficacy of dihydroartemisinin loaded solid lipid nanoparticles. **Nanomedicine: Nanotechnology, Biology, and Medicine**, v. 12, n. 3, p. 801–809, 1 abr. 2016.

PAILA, Y. D.; SAHA, B.; CHATTOPADHYAY, A. Amphotericin B inhibits entry of *Leishmania donovani* into primary macrophages. **Biochemical and Biophysical Research Communications**, v. 399, n. 3, p. 429–433, 2010.

PALIWAL, R. et al. Effect of lipid core material on characteristics of solid lipid nanoparticles designed for oral lymphatic delivery. **Nanomedicine: Nanotechnology, Biology, and Medicine**, v. 5, n. 2, p. 184–191, 1 jun. 2009.

PALUMBO, E. Treatment strategies for mucocutaneous leishmaniasis. **Journal of Global Infectious Diseases**, v. 2, n. 2, p. 147, 2010.

PAN AMERICAN HEALTH ORGANIZATION. **Leishmaniasis: Epidemiological report of the Americas Number 5**, 2017. Disponível em: <www.paho.org>. Acesso em: 13 abr. 2021.

PANÁČEK, A. et al. Silver colloid nanoparticles: Synthesis, characterization, and their antibacterial activity. **Journal of Physical Chemistry B**, v. 110, n. 33, p. 16248–16253, 24 ago. 2006.

PARASHAR, D.; P, A. N.; S R, M. R. Development of artemether and lumefantrine co-loaded nanostructured lipid carriers: physicochemical characterization and *in vivo* antimalarial activity. **Drug Deliv**, v. 23, n. 1, p. 1071–7544, 2016.

PHAM, T. T. H. et al. Development of antileishmanial lipid nanocomplexes. **Biochimie**, v. 107, n. Part A, p. 143–153, 1 dez. 2014.

PHAM, T. T. H.; LOISEAU, P. M.; BARRATT, G. Strategies for the design of orally bioavailable antileishmanial treatments. **International Journal of Pharmaceutics**, v. 454, n. 1, p. 539–552, 15 set. 2013.

POONIA, N. et al. Nanostructured lipid carriers: versatile oral delivery vehicle. **Future Science OA**, v. 2, n. 3, p. FSO135, 2016.

PRANDTL; L. Ueber flussigkeitsbewegung bei sehr kleiner reibung. **Verhandl. III, Internat. Math.-Kong., Heidelberg, Teubner, Leipzig, 1904**, p. 484–491, 1904.

PUCADYIL, T. J. et al. Cholesterol is required for *Leishmania donovani* infection: Implications in leishmaniasis. **Molecular and Biochemical Parasitology**, v. 133, n. 2, p. 145–152, 1 fev. 2004.

RABINOW, B. E. Nanosuspensions in drug delivery. **Nature Reviews Drug Discovery**, v. 3, p. 785–796, 2004.

RAMOS, H. et al. Amphotericin B kills unicellular leishmanias by forming aqueous pores permeable to small cations and anions. **Journal of Membrane Biology**, v. 152, n. 1, p. 65–75, 1996.

READIO, J. D.; BITTMAN, R. Equilibrium binding of amphotericin B and its methyl ester and borate complex to sterols. **BBA - Biomembranes**, v. 685, n. 2, p. 219–224, 23 fev. 1982.

RIBEIRO, T. G. et al. An optimized nanoparticle delivery system based on chitosan and chondroitin sulfate molecules reduces the toxicity of amphotericin B and is effective in treating tegumentary leishmaniasis. **International journal of nanomedicine**, v. 9, p. 5341–5353, 2014.

RODRIGUEZ-ALLER, M. et al. Strategies for formulating and delivering poorly water-soluble drugs. **Journal of Drug Delivery Science and Technology**, v. 30, p. 342–351, 1 dez. 2015.

SAFFIE-SIEBERT, R.; OGDEN, J.; PARRY-BILLINGS, M. Nanotechnology approaches to solving the problems of poorly water-soluble drugs. **Drug Discovery World**, v. 6, n. 3, p. 71–76, 2005.

SAGITANI, H.; NABETA, K.; NAGAI, M. A New Preparing Method for Fine O/W Emulsions by D Phase Emulsification and Their Application to Cosmetic Industry. **Journal of Japan Oil Chemists' Society**, v. 40, n. 11, p. 988–994, 1991.

SALOUTI, M.; AHANGARI, A. Nanoparticle based Drug Delivery Systems for Treatment of Infectious Diseases. In: SEZER, A. D. (Ed.). **Application of Nanotechnology in Drug Delivery**. 1. Ed. InTech, 2014. p. 155–192.

SEIBEL, N. L. et al. Safety, tolerability, and pharmacokinetics of liposomal amphotericin b in immunocompromised pediatric patients. **Antimicrobial Agents and Chemotherapy**, v. 61, n. 2, 1 fev. 2017.

SHAKIBAIE, M. et al. Biosynthesis and recovery of selenium nanoparticles and the effects on matrix metalloproteinase-2 expression. **Biotechnology and Applied Biochemistry**, v. 56, n. 1, p. 7–15, 14 maio 2010.

SHARMA, A.; SHARMA, U. S. Liposomes in drug delivery: Progress and limitations. **International Journal of Pharmaceutics**, v. 154, n. 2, p. 123–140, 26 ago. 1997.

SHARMA, M.; SHARMA, R.; JAIN, D. K. Nanotechnology Based Approaches for Enhancing Oral Bioavailability of Poorly Water Soluble Antihypertensive Drugs. **Scientifica**, v. 2016, p. 1–11, 2016.

SHEGOKAR, R.; MÜLLER, R. H. Nanocrystals: Industrially feasible multifunctional formulation technology for poorly soluble actives. **International Journal of Pharmaceutics**, v. 399, n. 1–2, p. 129–139, 2010.

SIEFERT, A. L. et al. Immunomodulatory nanoparticles ameliorate disease in the Leishmania (Viannia) panamensis mouse model. **Biomaterials**, v. 108, p. 168–176, 1 nov. 2016.

SINHA, B.; MÜLLER, R. H.; MÖSCHWITZER, J. P. Bottom-up approaches for preparing drug nanocrystals: Formulations and factors affecting particle size. **International Journal of Pharmaceutics**, v. 453, n. 1, p. 126–141, 2013.

SOARES-BEZERRA, R. J.; LEON, L.; GENESTRA, M. Recent advances on leishmaniasis chemotherapy: Intracellular molecules as a drug target. **Revista Brasileira de Ciencias Farmaceuticas/Brazilian Journal of Pharmaceutical Sciences**, v. 40, n. 2, p. 139–149, 2004.

SOEMA, P. C. et al. Predicting the influence of liposomal lipid composition on liposome size, zeta potential and liposome-induced dendritic cell maturation using a design of experiments approach. **European Journal of Pharmaceutics and Biopharmaceutics**, v. 94, p. 427–435, 10 jul. 2015.

STRAZZULLA, A. et al. Mucosal leishmaniasis: An underestimated presentation of a neglected disease. **BioMed Research International**, v. 2013, 2013.

SUNDAR, S. et al. Single-Dose Liposomal Amphotericin B for Visceral Leishmaniasis in India. **New England Journal of Medicine**, v. 362, n. 6, p. 504–512, 11 fev. 2010.

TSAI, M. J. et al. Baicalein loaded in tocol nanostructured lipid carriers (tocol NLCs) for enhanced stability and brain targeting. **International Journal of Pharmaceutics**, v. 423, n. 2, p. 461–470, 28 fev. 2012.

VAN DE VEN, H. et al. PLGA nanoparticles and nanosuspensions with amphotericin B: Potent *in vitro* and *in vivo* alternatives to Fungizone and AmBisome. **Journal of Controlled Release**, v. 161, n. 3, p. 795–803, 10 ago. 2012.

VARGAS DE OLIVEIRA, E. C. et al. Development and Evaluation of a Nanoemulsion Containing Ursolic Acid: a Promising Trypanocidal Agent: Nanoemulsion with Ursolic Acid Against *T. cruzi*. **AAPS PharmSciTech**, v. 18, n. 7, p. 2551–2560, 1 out. 2017.

VYAS, S. P.; GUPTA, S. Optimizing efficacy of amphotericin B through nanomodification. **International Journal of Nanomedicine**, v. 1, n. 4, p. 417–432, 2006.

WANG, W. et al. Preparation and Characterization of Minoxidil Loaded Nanostructured Lipid Carriers. **AAPS PharmSciTech**, v. 18, n. 2, p. 509–516, 2017.

WEBER, S.; ZIMMER, A.; PARDEIKE, J. Solid Lipid Nanoparticles (SLN) and Nanostructured Lipid Carriers (NLC) for pulmonary application: A review of the state of the art. **European Journal of Pharmaceutics and Biopharmaceutics**, v. 86, n. 1, p. 7–22, 2014.

WISSING, S. A.; MÜLLER, R. H. The influence of the crystallinity of lipid nanoparticles on their occlusive properties. **International Journal of Pharmaceutics**, v. 242, n. 1–2, p. 377–379, ago. 2002.

WORLD HEALTH ORGANIZATION. **Control of the leishmaniasis: report of a meeting of the WHO expert committee on the control of leishmaniasis. Control of the leishmaniasis: report of a meeting of the WHO expert committee on the control of leishmaniasis.** Geneva: World Health Organization, 2010a. Disponível em: <<https://www.cabdirect.org/cabdirect/abstract/20123045323>>. Acesso em: 27 maio. 2019.

WORLD HEALTH ORGANIZATION. **Costs of medicines in current use for the treatment of leishmaniasis** Technical Report series (TRS) Geneva, 2010b. Disponível em: <https://www.who.int/leishmaniasis/research/978_92_4_12_949_6_Annex6.pdf?ua=1>. Acesso em: 13 abr. 2021.

WORLD HEALTH ORGANIZATION. **Neglected tropical diseases.** Disponível em: <http://www.who.int/neglected_diseases/diseases/en/#>. Acesso em: 18 nov. 2016a.

WORLD HEALTH ORGANIZATION. Leishmaniasis in high-burden countries: an epidemiological update based on data reported in 2014. **Weekly epidemiological record**, v. 91, n. 5, p. 287–96, 2016b.

WORLD HEALTH ORGANIZATION. Weekly epidemiological record; Global leishmaniasis, 2006-2015: a turning point in leishmaniasis surveillance. **Weekly epidemiological record**, v. 92, n. 38, p. 557–572, 2017.

XIE, J.; LEE, S.; CHEN, X. Nanoparticle-based theranostic agents. **Advanced Drug Delivery Reviews**, v. 62, n. 11, p. 1064–1079, 2010.

YUKUYAMA, M. N. et al. Nanoemulsion: Process selection and application in cosmetics - A review. **International Journal of Cosmetic Science**, v. 38, n. 1, p. 13–24, 2016.

YUKUYAMA, M. N. et al. Challenges and Future Prospects of Nanoemulsion as a Drug Delivery System. **Current Pharmaceutical Design**, v. 23, n. 3, p. 495–508, 2017.

ZAHIR, A. A. et al. Green synthesis of silver and titanium dioxide nanoparticles using Euphorbia prostrata extract shows shift from apoptosis to G0/G1 arrest followed by necrotic cell death in *Leishmania donovani*. **Antimicrobial Agents and Chemotherapy**, v. 59, n. 8, p. 4782–4799, 1 ago. 2015.

Chapter 2 : A new medium-throughput screening design approach for the development of hydroxymethylnitrofurazone (NFOH) nanostructured lipid carrier for treating leishmaniasis

This study was published as Aline de Souza, Megumi Nishitani Yukuyama, Eduardo José Barbosa, Lis Marie Monteiro, Ana Cristina Breithaupt Faloppa, Leandro Augusto Calixto, Gabriel Lima de Barros Araújo, Nikoletta Fotaki, Raimar Löbenberg, Nádia Araci Bou-Chacra. With the title of A new medium-throughput screening design approach for the development of hydroxymethylnitrofurazone (NFOH) nanostructured lipid carrier for treating leishmaniasis in *Colloids and Surfaces B: Biointerfaces*, 2020, 111097.

Abstract

Hydroxymethylnitrofurazone (NFOH) is a nitrofurazone derivative and has potential use in treating leishmaniasis. However, due to low water solubility and bioavailability, NFOH has failed in *in vivo* tests. Nanostructured lipid carrier (NLC) is an alternative to overcome these limitations by improving pharmacokinetics and modifying drug delivery. This work is focused on developing a novel NFOH-loaded NLC (NLC-NFOH) using a D-optimal mixture statistical design and high-pressure homogenization, for oral administration to treat leishmaniasis. The optimized NLC-NFOH consisted of Mygliol® 840, Gelucire® 50/13, and Precirol® ATO 5 as lipids. These lipids were selected using a rapid methodology Technobis Crystal 16TM, microscopy, and DSC. Different tools for selecting lipids provided relevant scientific knowledge for the development of the NLC. NLC-NFOH presented a z-average of 198.6 ± 5.4 nm, PDI of 0.11 ± 0.01 , and zeta potential of -13.7 ± 0.7 mV. A preliminary *in vivo* assay was performed by oral administration of NLC-NFOH (2.8 mg/kg) in one healthy male Wistar rat (341g) by gavage. Blood from the carotid vein was collected, and the sample was analyzed by HPLC. The plasma concentration of NFOH after 5h of oral administration was 0.22 µg/mL. This same concentration was previously found using free NFOH in the DMSO solution (200mg/kg), which is an almost 100-fold higher dose. This study allowed a design space development approach of the first NLC-NFOH with the potential to treat leishmaniasis orally.

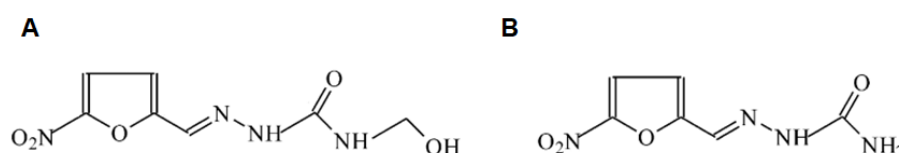
Keywords: Leishmaniasis; Nanoparticle(s); Drug delivery system(s), Lipid-based formulation(s); Nanostructured lipid carrier; Hydroxymethylnitrofurazone

2.1. Introduction

Leishmaniasis is a neglected tropical disease, in which the parasite infects macrophages in liver, spleen, bone marrow, and lymph nodes (DE SOUZA et al., 2018). Currently, the first-line treatment for leishmaniasis is pentavalent antimonials administered via parenteral: meglumine antimoniate (Glucantime[®], Sanofi Aventis, 81 mg/mL, solution) and sodium stibogluconate (Pentostam[™], Glaxo Smith Kline, 100 mg/mL, solution for injection). Other alternative drugs may include pentamidine and amphotericin B, also administered parenterally (WORLD HEALTH ORGANIZATION, 2015). However, they require the administration of high and repeated doses and at least 20 days of treatment and hospitalization (DE SOUZA et al., 2018; MARQUELE-OLIVEIRA et al., 2016). Additionally, these medicines show side effects such as pancreatitis, cardiotoxicity, nephrotoxicity and hepatotoxicity and induction of drug-resistant strains (WORLD HEALTH ORGANIZATION, 2010).

Hydroxymethylnitrofurazone (NFOH) (Figure 2-1A) has been a promising alternative for treating leishmaniasis. Chung et al (2003) first obtained this compound, using a molecular modification of nitrofurazone (NF) (Figure 2-1B), a topical antimicrobial agent. NFOH showed high activity in cultures of the infected cell of *Trypanosoma cruzi* and lower toxicity compared to NF. It also shows activity against *L. amazonensis*, which was confirmed by *in vitro* test using NFOH- poly n-butyl cyanoacrylate (PBCA) nanoparticles (MONTEIRO et al., 2017a). Despite this promising efficacy, the low water solubility of NFOH has limited its therapeutic use (MONTEIRO et al., 2017a).

Figure 2-1. Chemical structure of hydroxymethylnitrofurazone (A) and nitrofurazone (B).



Source: Adapted from CHUNG et al., 2003.

In search of new approaches to overcome this limitation, nanostructured lipid systems have promising qualities. They have a distinctive record in improving pharmacokinetics, modifying drug delivery, and can be used to target the drug at a specific site (BELOQUI et al., 2016; MARQUELE-OLIVEIRA et al., 2016). Thus, it is possible to increase efficacy, reduce toxicity, and reduce the frequency and duration of treatment (LIU; JIANG, 2017). Also, nanostructured preparations can increase the time of drug circulation in the body and encapsulated lipophilic molecules (ZULFIQAR et al., 2017). Among the alternatives there are nanoemulsion (NE), solid lipid nanoparticles (SLN), and nanostructured lipid carriers (NLC), the second generation of solid lipid nanoparticles.

NLC is comprised of colloidal particles that present a matrix composed of a binary mixture of solid lipid and liquid lipid giving rise to a less ordered structure, solid at room and body temperature (POONIA et al., 2016). This feature allows higher encapsulation efficiency compared to conventional SLN (NASERI; VALIZADEH; ZAKERI-MILANI, 2015). NLC can be prepared using high pressure homogenization, a scale up feasible technology (MONTEIRO et al., 2017b). NLC has many advantages, such as low production cost, no need for organic solvents, and high stability. Additionally, Monteiro et al. showed that NLC loaded with buparvaquone improved the *in vitro* activity against *Leishmania infantum* (MONTEIRO et al., 2019). Similar results were revealed using amphotericin B-NLC and cedrol-NLC. These nanosystems show better activity against *Leishmania sp* after oral administration in an animal model compared to the free drugs (KAR et al., 2017; TAN; ROBERTS; BILLA, 2020).

However, a systematic rational approach is required in developing NLC to select its proper components and their concentration. The lipids with higher drug solubility can increase the drug loading, encapsulation efficiency and enhance the stability of nanoparticles (NEGI; JAGGI; TALEGAONKAR, 2014; TAMJIDI et al., 2013). Thus, this task is a critical part of the formulation development.

Moreover, the concept of space design in pharmaceutical development has been considered an important stage of quality by design. Design space offers quality assurance and process understanding by a multivariate combination and interaction of input variables (JAIN; SOOD; GOWTHAMARAJAN, 2015; YUKUYAMA

et al., 2019). It can be achieved using design of experiments (DoE). The applicability of DoE has increased due to its ease in overcoming limitations and time-consuming methodologies (MONTEIRO et al., 2017b; VALICHERLA et al., 2016; YUKUYAMA et al., 2019). Therefore, this work is focused on developing a novel NFOH-loaded NLC for oral administration to treat leishmaniasis, using a design space approach.

2.2. Material and Method

2.2.1. Material

Hydroxymethylnitrofurazone was synthesized as previously described by Chung et al. (2003). Hydrogenated palm oil (Softisan® 154 and Dynasan® P60), tristearin (Dynasan® 118) and saturated fatty acid triglycerides (Witepsol® E85) were kindly donated by IOI Oleo Chemical (Germany). Lauroyl polyoxyl-32 glycerides (Gelucire® 44/14), stearyl polyoxyl-32 glycerides (Gelucire® 50/13), glyceryl dibehenate (Compritol® 888) and glyceryl distearate (Precirol® ATO 5) were kindly donated by Gattefossé (France). Oleic acid, glyceryl caprylate/caprate (Capmul® MCM EP), glyceryl tricaprylate/tricaprate (Captex® 300 EP/NF) and triglycerides of oleic acid (Captex® GTO) were kindly donated by Abitec (USA). Super refined cottonseed, safflower, corn, olive, soybean, and sesame oils were kindly donated by Croda (UK). Stearyl alcohol, buriti oil, wheat germ oil, hazelnut oil, grape seed oil, sunflower oil and isopropyl palmitate were kindly donated by Mapric (Brazil). Propylene glycol dicaprylate/dicaprate (Miglyol® 840) and Capric and caprylic acid esters (Miglyol® 812) were kindly donated by IOI Oleo Chemical. Phosphatidylcholine from soybean (Lipoid® S100) were kindly donated by LIPOID GMBH. Methanol and Acetonitrile HPLC grade were purchased from JTBaker. Purified water was prepared using Milli-Q quality (Millipore, USA). All other reagents were at least analytical grade and were used without further purification.

2.2.2. Selection of Liquid Lipids

The equipment, Crystal 16™ (Crystal Pharmatech Inc., USA), was used to determine the liquid lipid that solubilized the highest quantity of NFOH. For the test, 5.0 mg of NFOH was added to 1.0 g of liquid lipid in a 2.0 mL vial. The parameters

used were: 700 rpm, at 80°C for one h, with a heating and cooling ramp of 2.7°C/min. The second step for selection was performed as follows: 200 mg of Lipoid® S100 were added to the previous vials, under the same conditions described above. According to the equipment manufacturer's guidelines, the lipids presenting turbidity were excluded from the experiment. In the third step, the optimized proportion of Lipoid® S100: liquid lipid was investigated. Therefore, the selected liquid lipids and the suitable proportion of Lipoid®: liquid lipid were tested using different concentrations of NFOH (1.0-12.0 mg/g of lipid). The system with the highest concentration of the solubilization NFOH was selected.

The quantification of NFOH was performed using spectrophotometry UV/vis Evolution series 201 (Thermo Fisher Scientific, Waltham, MA, USA) operated at 370 nm. The sample was prepared with the addition of NFOH in excess to the liquid lipid and placed in a magnetic stirrer at 80°C. After 1 h, aliquots were filtered through a PVDF membrane of 0.22- μ m pore size and diluted in acetonitrile.

2.2.3. Selection of Solid Lipid

NFOH solubility in solid lipids was evaluated according to Kasongo et al (2011). NFOH was added to the solid lipid in a concentration of 0.001% (w/w); this preparation was heated 10°C above the melting point of each lipid, under constant shaking. Aliquots were taken and observed by an optical microscope Olympus CK2 (Japan); the NFOH concentration was adjusted until crystals were observed.

Additionally, drug solubility and crystallization behavior in solid lipids were carried out by using differential scanning calorimetry (DSC), according to Monteiro et al (MONTEIRO et al., 2017b). The NFOH, solid lipids, 1:1 physical mixtures (PM) and the mixtures of selected lipids thermal behavior were characterized in a DSC 4,000 Perkin Elmer cell (Perkin Elmer Corp., Norwalk, CT, USA), under a dynamic N₂ atmosphere (50 mL/min), using a sealed aluminum pan with about 2.0 mg of samples. DSC curves were obtained at a heating rate of 10°C/min, and the temperature ranged from 25 to 290°C. An empty sealed pan was used as a reference.

The onset temperature, maximum peak in the melting range (T_{peak}) and melting enthalpy (ΔH_m) were calculated using the software provided by PerkinElmer.

The crystallinity indices (CI) of NFOH were calculated in percentage according to the following Equation 2-1 (FREITAS; MÜLLER, 1999; SOUTO; MÜLLER, 2005),

$$CI (\%) = (\Delta H_{NFOH \text{ PM}} * D) / (\Delta H_{NFOH \text{ 100\%}}) * 100 \quad \text{Equation 2-1}$$

where $\Delta H_{NFOH \text{ PM}}$ is the enthalpy of fusion (J.mg⁻¹) of NFOH in the binary physical mixture of NFOH and solid lipid, $\Delta H_{NFOH \text{ 100\%}}$ is the enthalpy of fusion (J.mg⁻¹) of pure drug. D is the dilution of NFOH in the solid lipids, in this case, 1:1, D=2.

2.2.4. Preparation of NLC-NFOH

A total of 50.0g of the formulation was prepared using the selected liquid lipid, solid lipids and poloxamer 188. The oil and aqueous phases were heated to 80°C using RTC basic IKA® magnetic stirrer at 300 rpm until complete dissolution. Then, the aqueous phase was dispersed in the oil phase, and mixed by a mechanical homogenizer at 8000 rpm (Ultraturrax, IKA) for 5 min. The coarse emulsion was passed through a high-pressure homogenizer using Nano DeBEE® (BEE International, Inc. USA) using five successive cycles at 600 bar (MONTEIRO et al., 2017b).

2.2.5. Z-average, polydispersity index and potential zeta analysis

The z-average of the nanostructured lipid carriers was assessed by photon correlation spectroscopy (PCS) using Zetasizer ZS90 (Malvern Instruments, Malvern, UK) at 25°C and a 90° detection angle. The equipment was also used to measure the zeta potential (ZP). ZP measurements were carried out in purified water with a conductivity adjusted to 50 µS.cm⁻¹ by adding NaCl 0.2% (w/v), to avoid ZP fluctuations caused by the difference in conductivity (n = 3). The pH of formulations was determined using a pH measurement system (MP 220, Mettler Toledo® Inc, Columbus, OH, US) previously calibrated at 20°C. The particle size of the optimized NLC-NFOH was also determined by laser-based particle size analyzer CILAS 1090 (Orleans, France) in aqueous medium.

2.2.6. Determination of encapsulation efficiency (EE%) and drug loading (DL%)

NLC-NFOH was ultrafiltrated using Amicon Ultra-0.5 mL Ultracel-10 membrane 50 kDa centrifugal filters (Millipore Merck, USA). Then, the filter was centrifuged at 590 g for 30 min. The supernatant and the filtrate were suitably diluted and analyzed for NFOH in spectrophotometry method as described earlier. The EE% and DL% were determined using the equation 2-2 and equation 2-3, respectively.

$$EE\% = (W_{\text{total}} - W_{\text{free}}) / (W_{\text{total}}) \times 100 \quad \text{Equation 2-2}$$

$$DL\% = (W_{\text{total}} - W_{\text{free}}) / W_{\text{lipid}} \times 100 \quad \text{Equation 2-3}$$

Where W_{total} is weight of initial NFOH added, W_{free} is the weight of free drug detected in the filtrate after centrifugation and W_{lipid} is the weight of lipid at the formulation.

2.2.7. NLC development and optimization

An extreme vertex experiment, with five-factor, grade 3, two-level D-Optimal mixture statistical design was used to evaluate the lipids and surfactant concentration effects on NLC z-average using Minitab® 18 software (State College PA, USA). To design the mathematical model the following restrictions were used: 2.0% to 5.0% w/w of Gelucire® 50/13 concentration and $\leq 8.0\%$ w/w of Precirol® ATO 5 + Miglyol® 840 concentration. The independent variables are shown in Table 2.1 and the dependent variable (response) was z-average. A total of 45 experiments were designed by Minitab 18 (Table 2.3).

Table 2-1. Variables and level of extreme vertex experiment in developing NLC-NFOH.

Independent Variables	Coded Level	
	-1	+1
Gelucire® 50/13 (Gel)	2.0	5.0
Precirol® ATO 5 (Prec)	0.0	7.0
Miglyol® 840 (Mig)	2.0	9.0
Poloxamer® 188 (Pol)	0.0	3.0
Water	86.0	90.0

2.2.8. Determination of NFOH in plasma

The Ethics Committee approved the animal experiment protocol (protocol n°1155/2019). NLC-NFOH (2.8 mg/kg) was administered to one healthy male Wistar rat (341g) by gavage. After 5 h blood from the carotid vein was collected. A blood sample was collected to heparin tubes (10 µl, 500 IU/mL). Plasma samples were obtained immediately by centrifuging at 8000 rpm for 10 min, and stored at -20°C until further analysis by HPLC (KIMURA et al., 1997). Plasma samples (200 µL) were mixed with acetonitrile (200 µL), to precipitate proteins, then centrifuged at 10000 rpm for 10 min. The supernatant was transferred to a vial insert and analyzed in HPLC.

The quantification of NFOH in plasma was performed according to Monteiro et al (MONTEIRO et al., 2015). The Shimadzu HPLC-UV system consisted of a CBM-20A controller, LC-20AT-pump, SPD-20A detector, and SIL-20AC sampler LC Solution software (version 1.25SP4) was applied for data collecting and processing. The mobile phase consisted of acetonitrile: water (20:80) at a flow rate of 1.2 mL/min and the UV detector at 265 nm. The volume of injection was 20 µl. The method was linear ($r = 0.9997$) in the concentration range of 10 - 0.1 µg/mL.

2.3. Result

2.3.1. Selection of liquid lipid

Crystal 16TM detects the turbidity of the solution through a laser that passes through the vials. The clearer the solution, the higher the solubility of the drug

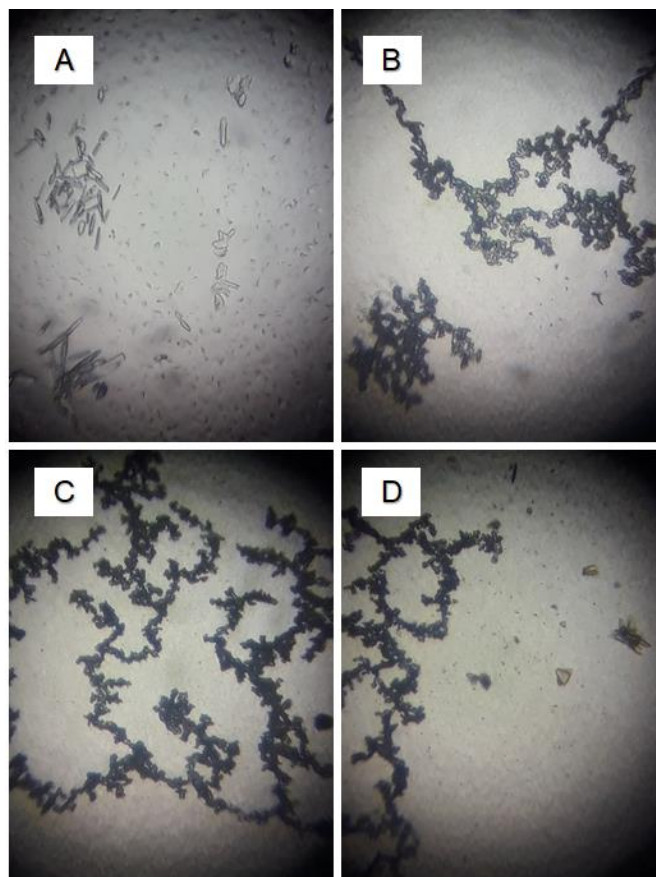
in the oil. In the first screening, none of the 23 oils tested showed a 100% clear solution. In the second screening, Lipoid® S100, a solubilizer agent, was added to improve the solubility of NFOH in these oils. Buriti oil, grape seed oil, Miglyol® 840, Capmul® MCM, Captex® 300 and Miglyol® 812 showed 100% clear solution. The interaction of Lipoid® S100 and the oils helped solubilize the NFOH. The proportion of Lipoid® S100 and liquid lipid was optimized to 1:9.

To determine if the selected liquid lipids were able to solubilize more than 5.0 mg/g of drug substance, different vials with variable amounts of NFOH (6.0 to 12.0 mg/g) were evaluated in a Crystal 16TM instrument. The maximum amount of NFOH solubilized in Miglyol® 840 was 8.0 mg/g. This solubilized concentration remains after cooling the solution. For the Miglyol® 812, the maximum quantity of solubilized NFOH was 6.0 mg/g. The NFOH quantification by spectroscopy in Miglyol® 840 and Miglyol® 812 were 14.0 mg/g and 10.2 mg/g, respectively. Due to the superior NFOH solubility, Miglyol® 840 was chosen as the liquid lipid for the preparation of nanostructure lipid carrier.

2.3.2. Selection of solid lipids

Eight solid lipids were analyzed by microscopy to evaluate the solubility of NFOH. NFOH was soluble in all the lipids tested at 1.0 mg/g, except for Gelucire® 44/10. Microscopy revealed Gelucire® 50/13 was the only solid lipid to solubilize 2.0 mg/g of NFOH. Figure 2-2 showed the microscopy of NFOH in Gelucire® 50/13.

Figure 2-2. Optical micrographs (x10) of (A) NFOH; (B) Gelucire® 50/13; (C) Gelucire® 50/13 and NFOH (2.0mg/g) and (D) Gelucire® 50/13 and NFOH (10mg/g).



Source: the author

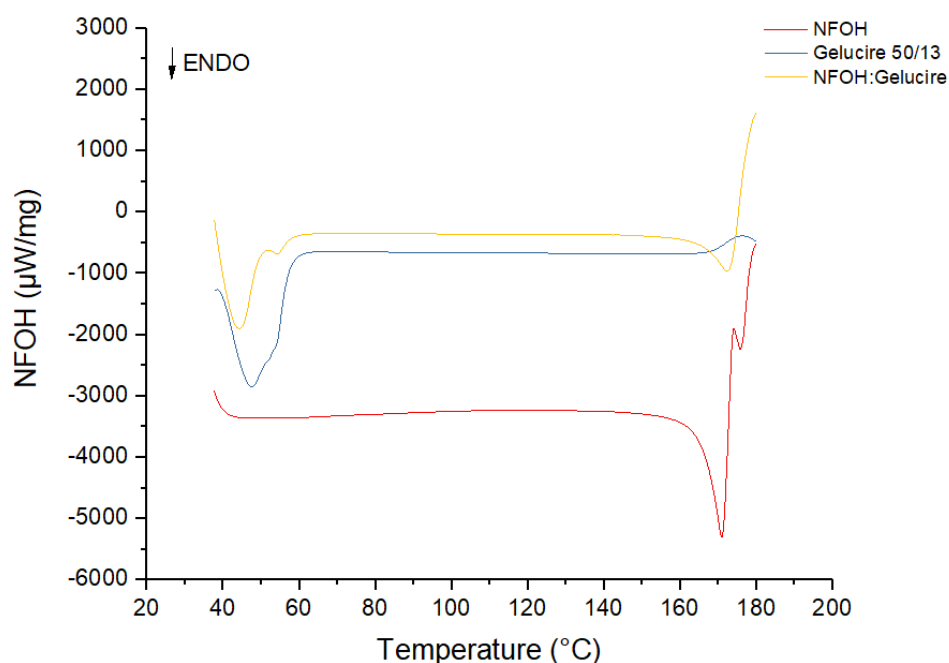
The melting enthalpy obtained from DSC data and the Crystallinity index (CI) of NFOH and solid lipids mixtures were used to select the best solid lipid (Table 2.2). The pure drug presents ΔH_{NFOH} 12.8 (kJ/mg); the greater the reduction in CI, the better the ability of the lipid to solubilize the drug (MONTEIRO et al., 2017b). Gelucire® 50/13 mixture (Figure 2-3) resulted in the lowest CI of NFOH, of 63.5 which is in consonance with the microscopic screening. Thus, it was the chosen SL for the preparation of nanostructure lipid carrier. Precirol® ATO 5, presenting the second-best CI (96.1%) was also chosen.

Table 2-2. Enthalpy of fusion (kJ/mg) and crystallinity index to determine NFOH solubility in solid lipids by differential scanning calorimetry.

Lipids	$\Delta H_{\text{NFOH-PM}}$ (kJ/mg)	CI (%)
Gelucire® 50/13	4.0	63.5
Precirol® ATO 5	6.2	96.1
Compritol® 888	6.2	97.2
Witepsol® E85	6.5	101.4
Softsan® 154	6.9	108.2
Dynasan® 118	7.2	112.0
Dynasan® P60	8.3	129.6

NFOH:Hydroxymethylnitrofurazone; NFOH-PM:NFOH and lipid physical mixture (1:1); CI: crystallinity index = (NFOH enthalpy of fusion in lipid mixture*dilution/NFOH enthalpy of fusion (J/mg))*100.

Figure 2-3. DSC curves of hydroxymethylnitrofurazone (NFOH), Gelucire® 50/13, and NFOH and Gelucire® 50/13 – physical mixture (PM) obtained at $\beta = 10^\circ\text{C}/\text{min}$.



Source: the author.

2.3.3. NLC development and optimization

The restrictions were determined in a preliminary study. Gelation was observed in a mixture composed of Precirol® ATO 5 and Miglyol® 840 at the ratio of 4:1. However, when Gelucire® 50/13 was added to this mixture, the gelation was not observed (data not shown). The addition of surfactants can also avoid the gelation (SOUTO; ALMEIDA; MÜLLER, 2007). Thus, Gelucire® 50/13 was added to all formulations of statistical design. The Z-average ranged from 100.9 nm to 294.0 nm and Pdl from 0.12 to 0.66 (Table 2.3).

Table 2-3. Experimental matrix of extreme vertex experiment, with five-factor, grade 3, two-level D-Optimal mixture statistical design and values of z-average and PDI of NLC-NFOH

	Gelucire® 50/13 (% w/w)	Precirol® ATO 5 (% w/w)	Miglyol® 840 (% w/w)	Poloxamer® (% w/w)	Water (% w/w)	z-average (nm)	PDI
1	2.00	0.00	8.00	0.00	90.00	140.40	0.19
2	2.00	7.00	2.00	3.00	86.00	191.10	0.23
3	5.00	3.00	2.00	0.00	90.00	115.00	0.15
4	5.00	0.00	6.00	3.00	86.00	131.60	0.16
5	2.00	3.50	5.50	0.00	89.00	208.90	0.12
6	2.00	3.00	5.00	3.00	87.00	164.60	0.45
7	2.00	0.00	9.00	3.00	86.00	178.40	0.20
8	2.00	6.00	2.00	0.00	90.00	250.90	0.29
9	5.00	4.00	2.00	3.00	86.00	153.10	0.31
10	3.50	0.00	7.50	1.50	87.50	142.00	0.19
11	3.50	5.50	2.00	0.00	89.00	201.70	0.16
12	5.00	0.00	5.00	3.00	87.00	138.80	0.17
13	3.50	4.50	2.00	3.00	87.00	111.40	0.24
14	5.00	0.00	6.00	0.00	89.00	100.90	0.17
15	2.00	0.00	9.00	0.00	89.00	138.20	0.18
16	2.00	6.00	2.00	1.50	88.50	188.50	0.78
17	2.00	3.50	5.50	3.00	86.00	182.39	0.42
18	2.00	7.00	2.00	0.00	89.00	294.00	0.27
19	2.75	4.75	3.25	2.25	87.00	163.12	0.66
20	3.50	0.00	7.00	0.00	89.50	118.50	0.18
21	2.00	0.00	8.50	1.50	88.00	155.40	0.19
22	5.00	0.00	5.00	0.00	90.00	102.30	0.13

	Gelucire® 50/13 (% w/w)	Precirol® ATO 5 (% w/w)	Miglyol® 840 (% w/w)	Poloxamer® (% w/w)	Water (% w/w)	z-average (nm)	PDI
23	2.00	6.00	2.00	3.00	87.00	158.70	0.17
24	2.75	1.25	6.75	2.25	87.00	134.20	0.13
25	2.00	0.00	8.00	3.00	87.00	178.00	0.16
26	2.00	7.00	2.00	1.50	87.50	210.40	0.27
27	2.00	6.50	2.00	0.00	89.50	274.60	0.31
28	4.25	2.75	3.25	2.25	87.50	143.40	0.21
29	5.00	3.50	2.00	0.00	89.50	131.20	0.15
30	5.00	4.00	2.00	1.50	87.50	117.70	0.19
31	2.75	4.25	3.25	0.75	89.00	179.87	0.43
32	4.25	3.25	3.25	0.75	88.50	127.30	0.17
33	3.50	0.00	7.00	3.00	86.50	161.20	0.18
34	5.00	3.00	2.00	3.00	87.00	153.64	0.22
35	2.00	3.00	5.00	0.00	90.00	218.80	0.16
36	5.00	2.00	4.00	0.00	89.00	144.70	0.30
37	2.00	6.50	2.00	3.00	86.50	183.20	0.18
38	5.00	1.75	3.75	3.00	86.50	145.60	0.19
39	3.50	4.50	2.00	0.00	90.00	192.10	0.13
40	2.75	1.25	6.25	0.75	89.00	130.40	0.19
41	5.00	3.00	2.00	1.50	88.50	164.40	0.29
42	5.00	0.00	5.50	1.50	88.00	118.00	0.15
43	3.50	5.50	2.00	3.00	86.00	136.00	0.39
44	3.50	0.00	6.50	1.50	88.50	144.10	0.17
45	3.50	2.75	4.75	3.00	86.00	121.90	0.19

NFOH: hydroxymethylnitrofur; PDI: polydispersity index

The R-square (R^2), adjusted- R^2 (adj- R^2) and predicted R^2 (pred- R^2) were 89.54%, 87.21% and 83.67%, respectively. The normal probability plot of the residuals was approximately linear revealing a normally distributed behavior (data not shown). The linear model was significant ($p < 0.05$; $\alpha = 0.05$) (Table 2-4). The mathematical model (Equation 2-4) showed the influence of independent variables for the z-average. The interaction of Gelucire® 50/13+Precirol® ATO 5, Gelucire® 50/13+Miglyol® 840, and Precirol® ATO 5 + Poloxamer® 188 resulted in a synergy that helped decrease the z-average. Interestingly, the mix of the three compounds, Gelucire® 50/13+Precirol® ATO 5+Poloxamer® 188, showed the opposite response,

significantly increasing the z-average. Table 2.5 shows the optimized formulations with a z-average less than 200 nm (monomodal distribution), which verified the validity of the mathematical model. The contour plots are presented in Figure 2-4. The EE% of F1 and F2 were 58.8% and 61.7%, respectively and DL% were 21.6% and 34.5%, respectively.

Table 2-4. Analysis of variance for z-average

SOURCE OF VARIATION	DF	SS (adj)	MS (adj)	F-value	p-value
Model	8	71519	8939.9	38.52	0.001
Linear	4	22542	5635.5	24.28	0.001
Gelucire® 50/13* Precirol® ATO 5	1	4567	4567.1	19.68	0.001
Gelucire® 50/13* Miglyol® 840	1	1923	1923.0	8.29	0.007
Precirol® ATO 5* Poloxamer® 188	1	12569	12569.1	54.16	0.001
Gelucire® 50/13* Precirol® ATO 5*	1	1925	1929.5	8.25	0.007
Error	36	8355	232.1	-	-
Total SS	44	79874	-	-	-
S= 15.2345	$R^2 = 89.54\%$	$\text{Adj-}R^2 = 87.21$		$\text{Pred-}R^2$	=

DF = degrees of freedom, SS = sequential sums of squares, MS = sequential mean squares, F-Value = value on the F distribution, p-Value = lack-of-fit adjustment, S = standard error of the regression, R^2 = multiple correlation coefficient, $\text{adj-}R^2$ = adjusted multiple correlation coefficient, $\text{pred-}R^2$ = predicted correlation coefficient.

$$\text{Z-average} = +3210 \cdot \text{Gel} + 4970 \cdot \text{Prec} + 2216 \cdot \text{Mig} + 1124 \cdot \text{Pol} - 8.4 \cdot \text{Water} - 98856 \cdot \text{Gel} \cdot \text{Prec} - 60703 \cdot \text{Gel} \cdot \text{Mig} - 98279 \cdot \text{Prec} \cdot \text{Pol} + 1351126 \cdot \text{Gel} \cdot \text{Prec} \cdot \text{Pol}$$

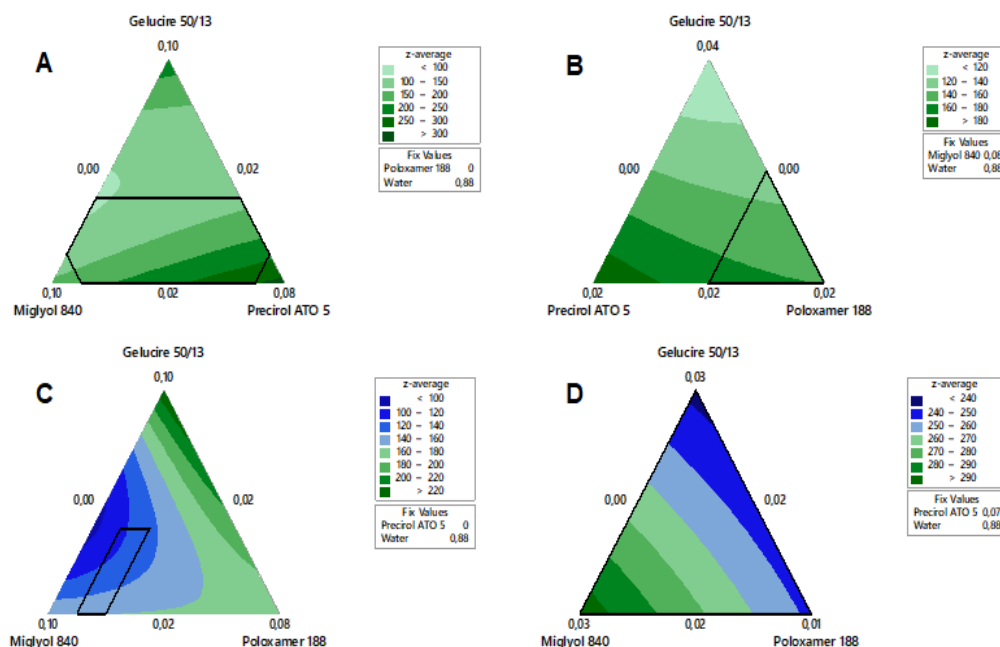
Equation 2-4

Table 2-5. Observed and predicted z-average, polydispersity index (PDI) and zeta potential (ZP) results from NLC-NFOH for F1 and F2.

	F1	F2
	(% w/w)	(% w/w)
Gelucire® 50/13	4.70	2.30
Precirol® ATO 5	2.45	3.70
Miglyol® 840	3.00	4.00
Poloxamer® 188	1.00	0.00
Water	88.85	90.00
Observed z-average (nm) ± SD	135.3 ± 2.1	198.6 ± 5.4
Predicted z-average (nm)	134.9	198.7
PDI ± SD	0.23 ± 0.02	0.11 ± 0.01
ZP (mV) ± SD	-13.7 ± 0.9	-13.7 ± 0.7
pH	4.92	4.98

PDI: polydispersity index; ZP: zeta potential; SD: Standard deviation.

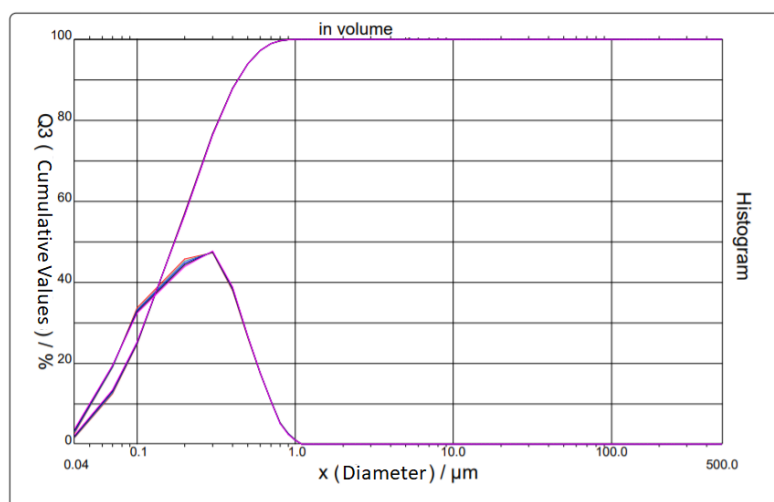
Figure 2-4. Contour plots of the NLC-NFOH mathematical model for z-average, containing the following variables: Gelucire® 50/13, Precirol® ATO 5, Miglyol® 840, Poloxamer® 188, and Water



Source: The Author.

F2 particle size was also determined using a laser-based particle size analyzer. The diameter 50%, $d(50)$, was 170 nm and the media size was 220 nm (Figure 2-5).

Figure 2-5. Distribution of the particle size for NLC-NFOH (F2) by the liquid diffraction dispersion laser method.

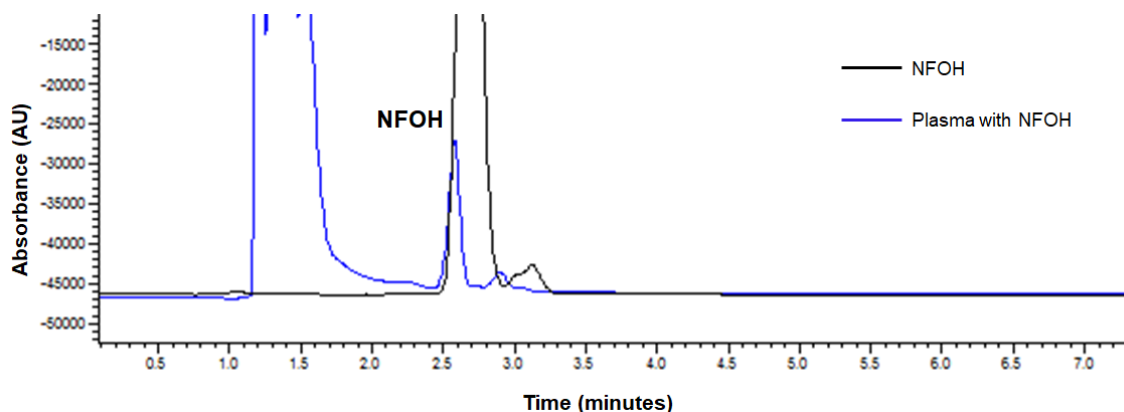


Source: The Author.

2.3.4. Determination of NFOH in plasma

The NFOH was successfully detected in animal after oral administration of F2. The time of retention of NFOH was 2.6 minutes for NFOH solution and NFOH in plasma (Figure 2-6). The plasma concentration of NFOH after 5h of oral administration in rat was 0.22 $\mu\text{g/mL}$.

Figure 2-6. Chromatogram of hydroxymethylnitrofurazone (NFOH) in rat plasma after oral administration of NLC-NFOH.



Source: The Author.

2.4. Discussion

The use of different tools for selecting lipids provided relevant scientific knowledge for the development of the NLC. Shake flask and spectrophotometry are the conventional approaches used to select liquid lipids (BALGURI; ADELLI; MAJUMDAR, 2016). However, the use of Crystal 16™ helped to screen a large number of liquid lipids in a short time, low amount, without the use of organic solvent. Microscopy is also frequently used to select solid lipids (KASONGO et al., 2011; MÜLLER; GOHLA; KECK, 2011; PATIL-GADHE; POKHARKAR, 2016), but it presents some limitations such as being time-consuming, presenting semi-quantitative results, and the experience of the analyst (MONTEIRO et al., 2017b). DSC used in this study could overcome these limitations. Thus, the association of these methods is substantial in saving time, material and labor.

The first selected liquid lipid was Miglyol® 840, a diester related to medium chain triglycerides (propylene glycol dicaprylate / dicaprinate) (COLE; CADÉ; BENAMEUR, 2008). It has been used for developing formulations in oral, (SAKLOETSAKUN et al., 2013; SALUNKHE; BHATIA; BHATIA, 2016; WANG et al., 2011) ophthalmic (SHEN et al., 2009, 2010), subcutaneous (SALUNKHE; BHATIA; BHATIA, 2016), dermatological (MAHJOUR et al., 1993) and transdermal applications (ZHANG et al., 2013a, 2013b). In order to increase the solubility of NFOH in Miglyol® 840, Lipoid® S100 was added. Lipoid® S100 is a lecithin derived

from soybeans and contains 100% phosphatidylcholine, one of the main naturally occurring phospholipids. Lipoid® S100 offers a high transition phase temperature preventing leakage of drugs from the lipid matrix, and can therefore increase encapsulation efficiency (LI et al., 2016). In addition, when added to formulations, it can increase the oral bioavailability of drugs (JAWAHAR et al., 2018; ZHOU et al., 2015). Despite these advantages, this component is highly susceptible to oxidation (JIN; LU; JIANG, 2016). Therefore, it is desirable to use the smallest amount of Lipoid® S100 suitable to solubilized NFOH.

Gelucire® 50/13 was selected due to the superior ability to solubilize NFOH among the solid lipids tested, and its lower CI. This lipid is a mixture of propylene glycol mono, di and triglycerides and mono and diesters of palmitic (C 16) and stearic (C 18) acids, it has a melting point of around 50°C, and hydrophilic-lipophilic balance (HLB) of 13. It is an amphiphilic lipid compound that has been used to increase the oral bioavailability of hydrophobic drugs (DE OLIVEIRA ELOY et al., 2012; EL-BADRY; FETIH; FATHY, 2009; JIMÉNEZ DE LOS SANTOS et al., 2017). In addition, it has been used as solid lipid and surfactant in the preparation of lipid nanostructures (DATE et al., 2011; GARG et al., 2016; HAZZAH et al., 2015). Precirol® ATO 5 is composed of esters of palmitic (C16) and stearic (C18) acids, used to modify the release of drugs (AGRAWAL; PETKAR; SAWANT, 2010; JANNIN; POCHARD; CHAMBIN, 2006; ZHAO et al., 2015) and to increase oral bioavailability of drugs (LI et al., 2015; RAMALINGAM; KO, 2016).

Lipid polymorphism can induce gelation and instability of formulation (HELGASON et al., 2008; SZNITOWSKA et al., 2017). Precirol® ATO 5 and Gelucire® 50/13 present 3 and 4 polymorphic forms, respectively (DATE et al., 2011). The interaction between these two components suppressed the polymorphism. Hazza et al (HAZZAH et al., 2015). demonstrated an increase in the z-average due to the interaction between Gelucire® 50/13 and Precirol® ATO 5. This confirms the findings of Jeon et al. (JEON et al., 2013), which revealed Precirol® ATO 5 is the main constituent of the particle walls. Gelucire® 50/13 molecules intercalate between Precirol® ATO 5 by Van der Waals forces between their lipophilic long hydrocarbon chain. When the concentration of Gelucire® 50/13 increases, the Gelucire® 50/13 molecules interact between themselves leading to a z-average increase. Thus,

Gelucire® 50/13, as stabilizer, can provide suitable colloidal stability. Additionally, it can slow down the expulsion of the encapsulated drug (DATE et al., 2011).

In the present study, when Gelucire® 50/13 concentration increased from 2.0 to 5.0%, the NLC-NFOH z-average decreased, contrary to Jeon's study. This can be attributed to the addition of Miglyol® 840 to the formulation. This liquid lipid decreased the crystallinity of solid lipids reducing the particle size (SOUTO et al., 2004). Furthermore, Precirol® ATO 5 (HLB = 2) may facilitate emulsification efficiency when combining with Miglyol® 840, leading to a lower particle size (SHEN et al., 2010).

The use of a design space allowed for a systematic rational approach in the development of NLC-NFOH. The knowledge of the attributes that influence the z-average of the formulation provided an optimized NLC. Thus, the mathematical model demonstrated the predicted z-average similar to the observed values (Table 2.2). Two preparations were selected to verify the model: F1 and F2. Gelucire® 50/13 (2.30 to 4.70% w/w) acted as solid lipid and also as a stabilizer for the formulation. The F2, without Poloxamer® 188, presented stability of three months (Table 2.6). Poloxamer was intended to act as gelation inhibitor in this system; however, the applied concentration of Gelucire® 50/13 seemed to be enough for this proposal. Therefore, the preparation F2 was chosen for the *in vivo* preliminary assay.

Table 2-6. Stability of NLC-NFOH, F2 formulation:

Time (Days)	z-average (nm) ± SD	PDI ± SD	ZP (mV) ± SD
1	198.6 ± 5.4	0.11 ± 0.01	-13.7 ± 0.7
7	212.9 ± 1.1	0.07 ± 0.03	-12.0 ± 0.4
14	226.4 ± 3.4	0.10 ± 0.01	-13.6 ± 0.4
21	225.7 ± 4.3	0.09 ± 0.01	-13.8 ± 0.3
30	239.0 ± 5.1	0.09 ± 0.03	-13.3 ± 0.5
45	240.5 ± 5.6	0.11 ± 0.01	-12.8 ± 0.6
60	249.4 ± 5.1	0.11 ± 0.03	-8.3 ± 0.4
90	248.2 ± 2.0	0.17 ± 0.02	-11.2 ± 1.1

PDI: polydispersity index; ZP: zeta potential; SD: Standard deviation

The plasma concentration analysis of NFOH using Wistar rats (approx. 250g) was also performed and determined by Serafin et al. (SERAFIM et al., 2013); the authors found a plasma concentration of 0.25 mg/mL at 5h, which is similar to the concentration determined in our study (0.22 mg/mL) using NLC-NFOH at 2.8 mg/Kg. Thus, it was possible to achieve a similar plasma concentration using an almost 100-fold lower dose with DL% of 34.5%(w/w). These preliminary results indicate that NLC might improve oral absorption of NFOH. The Lipid-based formulation can enhance the solubility and bioavailability of poorly soluble drugs by keeping drugs solubilized in the gastrointestinal tract by enhancing mucosal adhesion and/or gradually releasing drug molecules from the lipid matrix. Also, these formulations can improve therapeutic profiles compared to the free drug due to its protection from chemical and enzymatic degradation (KOLLIPARA; GANDHI, 2014; SEVERINO et al., 2012). Fathi et al. (FATHI et al., 2018) and Kar et al. (KAR et al., 2017) showed an initial burst in the drug release profile study; this can be associated with the entrapped drug on the surface of the nanoparticle. A similar feature might be attributed to NLC-NFOH due to the presence of 40% of free drug in the aqueous phase. Additionally, both studies showed a sustained drug released, attributed, probably to the lipophilic nature of the drug and the lipid-based formulation. Therefore, our group is encouraged to continue researching the influence of NLC, aiming to enhance NFOH bioavailability.

2.5. Conclusion

A rational approach allowed to successfully develop the first stable NLC-NFOH. The D-Optimal mixture statistical design was effectively used to optimize the formulation. Besides, within the design space, it was possible to have a better understanding of the attributes that influence the z-average of the formulation. Gelucire® 50/13 decreased the z-average, while the addition of Precirol® ATO 5 increased the z-average. Additionally, the preliminary experiment of NLC-NFOH in rats demonstrated the presence of NFOH in plasma at a lower concentration of oral administration, compared to other studies. Under these promising results, we consider the NLC-NFOH as a potential candidate of oral

2.6. References

- AGRAWAL, Y.; PETKAR, K. C.; SAWANT, K. K. Development, evaluation and clinical studies of Acitretin loaded nanostructured lipid carriers for topical treatment of psoriasis. **International Journal of Pharmaceutics**, v. 401, n. 1–2, p. 93–102, 30 nov. 2010.
- BALGURI, S. P.; ADELLI, G. R.; MAJUMDAR, S. Topical ophthalmic lipid nanoparticle formulations (SLN, NLC) of indomethacin for delivery to the posterior segment ocular tissues. **European Journal of Pharmaceutics and Biopharmaceutics**, v. 109, p. 224–235, 1 dez. 2016.
- BELOQUI, A. et al. Nanostructured lipid carriers: Promising drug delivery systems for future clinics. **Nanomedicine: Nanotechnology, Biology, and Medicine**, v. 12, n. 1, p. 143–161, 2016.
- CHUNG, M. C. et al. Synthesis and *in vitro* evaluation of potential antichagasic hydroxymethylnitrofurazone (NFOH-121): A new nitrofurazone prodrug. **Bioorganic and Medicinal Chemistry**, v. 11, n. 22, p. 4779–4783, 2003.
- COLE, E. T.; CADÉ, D.; BENAMEUR, H. **Challenges and opportunities in the encapsulation of liquid and semi-solid formulations into capsules for oral administration** *Advanced Drug Delivery Reviews*, 2008. Disponível em: <<https://www.sciencedirect.com/science/article/pii/S0169409X07003171>>. Acesso em: 3 jul. 2018
- DATE, A. A. et al. Lipid nanocarriers (GeluPearl) containing amphiphilic lipid Gelucire 50/13 as a novel stabilizer: fabrication, characterization and evaluation for oral drug delivery. **Nanotechnology**, v. 22, n. 27, 8 jul. 2011.
- DE OLIVEIRA ELOY, J. et al. Solid Dispersion of Ursolic Acid in Gelucire 50/13: a Strategy to Enhance Drug Release and Trypanocidal Activity. **AAPS PharmSciTech**, v. 13, n. 4, p. 1436–1445, 16 dez. 2012.
- DE SOUZA, A. et al. **Promising nanotherapy in treating leishmaniasis** *International Journal of Pharmaceutics* Elsevier B.V., , 25 ago. 2018a.
- DE SOUZA, A. et al. Promising nanotherapy in treating leishmaniasis. **International Journal of Pharmaceutics**, v. 547, n. 1–2, p. 421–431, 25 ago. 2018b.

EL-BADRY, M.; FETIH, G.; FATHY, M. Improvement of solubility and dissolution rate of indomethacin by solid dispersions in Gelucire 50/13 and PEG4000. **Saudi Pharmaceutical Journal**, v. 17, n. 3, p. 217–225, 1 jul. 2009.

FATHI, H. A. et al. Nanostructured lipid carriers for improved oral delivery and prolonged antihyperlipidemic effect of simvastatin. **Colloids and Surfaces B: Biointerfaces**, v. 162, p. 236–245, 1 fev. 2018.

FREITAS, C.; MÜLLER, R. H. Correlation between long-term stability of solid lipid nanoparticles (SLN™) and crystallinity of the lipid phase. **European Journal of Pharmaceutics and Biopharmaceutics**, v. 47, n. 2, p. 125–132, 1 mar. 1999.

GARG, N. K. et al. Nanostructured lipid carrier mediates effective delivery of methotrexate to induce apoptosis of rheumatoid arthritis via NF- κ B and FOXO1. **International Journal of Pharmaceutics**, v. 499, n. 1–2, p. 301–320, 29 fev. 2016.

HAZZAH, H. A. et al. Gelucire-Based Nanoparticles for Curcumin Targeting to Oral Mucosa: Preparation, Characterization, and Antimicrobial Activity Assessment. **Journal of Pharmaceutical Sciences**, v. 104, n. 11, p. 3913–3924, nov. 2015.

HELGASON, T. et al. Influence of polymorphic transformations on gelation of tripalmitin solid lipid nanoparticle suspensions. **JAACS, Journal of the American Oil Chemists' Society**, v. 85, n. 6, p. 501–511, 2008.

JAIN, K.; SOOD, S.; GOWTHAMARAJAN, K. Optimization of artemether-loaded NLC for intranasal delivery using central composite design. **Drug Delivery**, v. 22, n. 7, p. 940–954, 3 out. 2015.

JANNIN, V.; POCHARD, E.; CHAMBIN, O. Influence of poloxamers on the dissolution performance and stability of controlled-release formulations containing Precirol® ATO 5. **International Journal of Pharmaceutics**, v. 309, n. 1–2, p. 6–15, 17 fev. 2006.

JAWAHAR, N. et al. Enhanced oral bioavailability of an antipsychotic drug through nanostructured lipid carriers. **International Journal of Biological Macromolecules**, v. 110, p. 269–275, 15 abr. 2018.

JEON, H. S. et al. A retinyl palmitate-loaded solid lipid nanoparticle system: Effect of surface modification with dicetyl phosphate on skin permeation *in vitro* and anti-wrinkle effect *in vivo*. **International Journal of Pharmaceutics**, v. 452, n. 1–2, p.

311–320, 16 ago. 2013.

JIMÉNEZ DE LOS SANTOS, C. J. et al. Enhancement of albendazole dissolution properties using solid dispersions with Gelucire 50/13 and PEG 15000. **Journal of Drug Delivery Science and Technology**, v. 42, p. 261–272, 1 dez. 2017.

JIN, H.-H.; LU, Q.; JIANG, J.-G. Curcumin liposomes prepared with milk fat globule membrane phospholipids and soybean lecithin. **Journal of Dairy Science**, v. 99, n. 3, p. 1780–1790, 1 mar. 2016.

KAR, N. et al. Development and evaluation of a cedrol-loaded nanostructured lipid carrier system for *in vitro* and *in vivo* susceptibilities of wild and drug resistant *Leishmania donovani* amastigotes. **European Journal of Pharmaceutical Sciences**, v. 104, p. 196–211, 15 jun. 2017.

KASONGO, W. K. et al. Selection and Characterization of Suitable Lipid Excipients for use in the Manufacture of Didanosine-Loaded Solid Lipid Nanoparticles and Nanostructured Lipid Carriers. **Journal of Pharmaceutical Sciences**, v. 100, n. 12, p. 5185–5196, 2011.

KIMURA, E. et al. Pharmacokinetic profile of piroxicam β -cyclodextrin, in rat plasma and lymph. **General Pharmacology**, v. 28, n. 5, p. 695–698, 1 maio 1997.

KOLLIPARA, S.; GANDHI, R. K. Pharmacokinetic aspects and *in vitro*–*in vivo* correlation potential for lipid-based formulations. **Acta Pharmaceutica Sinica B**, v. 4, n. 5, p. 333–349, 1 out. 2014.

LI, W. et al. Enhanced bioavailability of tripterine through lipid nanoparticles using broccoli-derived lipids as a carrier material. **International Journal of Pharmaceutics**, v. 495, n. 2, p. 948–955, 30 nov. 2015.

LI, X. et al. Mucoadhesive dexamethasone acetate-polymyxin B sulfate cationic ocular nanoemulsion - Novel combinatorial formulation concept. **Pharmazie**, v. 71, n. 6, p. 327–333, 2016.

LIU, L.; JIANG, C. Drug Delivery Strategies Based on Nanotechnology for Cancer Immunotherapy. **Current Organic Chemistry**, v. 21, n. 1, p. 34–44, 2017.

MAHJOUR, M. et al. Effects of propylene glycol diesters of caprylic and capric acids (Miglyol® 840) and ethanol binary systems on *in vitro* skin permeation of drugs.

International Journal of Pharmaceutics, v. 95, n. 1–3, p. 161–169, 30 jun. 1993.

MARQUELE-OLIVEIRA, F. et al. Physicochemical characterization by AFM, FT-IR and DSC and biological assays of a promising antileishmania delivery system loaded with a natural Brazilian product. **Journal of Pharmaceutical and Biomedical Analysis**, v. 123, p. 195–204, 2016.

MONTEIRO, L. M. et al. Reverse phase high-performance liquid chromatography for quantification of hydroxymethylnitrofurazone in polymeric nanoparticles. **Brazilian Journal of Pharmaceutical Sciences**, v. 51, n. 3, p. 561–568, 2015.

MONTEIRO, L. M. et al. Targeting Leishmania amazonensis amastigotes through macrophage internalisation of a hydroxymethylnitrofurazone nanostructured polymeric system. **International Journal of Antimicrobial Agents**, v. 50, n. 1, p. 88–92, 2017a.

MONTEIRO, L. M. et al. Buparvaquone Nanostructured Lipid Carrier : Development of an Affordable Delivery System for the Treatment of Leishmaniasis. **BioMed Research International**, v. 2017, p. 1–11, 2017b.

MONTEIRO, L. M. et al. Co-delivery of buparvaquone and polymyxin B in a nanostructured lipid carrier for leishmaniasis treatment. **Journal of Global Antimicrobial Resistance**, v. 18, p. 279–283, 1 set. 2019.

MÜLLER, R. H.; GOHLA, S.; KECK, C. M. State of the art of nanocrystals - Special features, production, nanotoxicology aspects and intracellular delivery. **European Journal of Pharmaceutics and Biopharmaceutics**, v. 78, n. 1, p. 1–9, 2011.

NASERI, N.; VALIZADEH, H.; ZAKERI-MILANI, P. Solid Lipid Nanoparticles and Nanostructured Lipid Carriers : Structure , Preparation and Application. **Tabriz University of Medical Sciences**, v. 5, n. 3, p. 305–313, 2015.

NEGI, L. M.; JAGGI, M.; TALEGAONKAR, S. Development of protocol for screening the formulation components and the assessment of common quality problems of nano-structured lipid carriers. **International Journal of Pharmaceutics**, v. 461, n. 1–2, p. 403–410, 30 jan. 2014.

PATIL-GADHE, A.; POKHARKAR, V. Pulmonary targeting potential of rosuvastatin loaded nanostructured lipid carrier: Optimization by factorial design. **International Journal of Pharmaceutics**, v. 501, n. 1–2, p. 199–210, 2016.

POONIA, N. et al. Nanostructured lipid carriers: versatile oral delivery vehicle. **Future Science OA**, v. 2, n. 3, p. FSO135, 2016.

RAMALINGAM, P.; KO, Y. T. Improved oral delivery of resveratrol from N-trimethyl chitosan-g-palmitic acid surface-modified solid lipid nanoparticles. **Colloids and Surfaces B: Biointerfaces**, v. 139, p. 52–61, 1 mar. 2016.

SAKLOETSAKUN, D. et al. Combining two technologies: Multifunctional polymers and self-nanoemulsifying drug delivery system (SNEDDS) for oral insulin administration. **International Journal of Biological Macromolecules**, v. 61, p. 363–372, 1 out. 2013.

SALUNKHE, S. S.; BHATIA, N. M.; BHATIA, M. S. Implications of formulation design on lipid-based nanostructured carrier system for drug delivery to brain. **Drug Delivery**, v. 23, n. 4, p. 1306–1316, 31 jul. 2016.

SERAFIM, E. O. P. et al. Pharmacokinetics of hydroxymethylnitrofurazone, a promising new prodrug for chagas' disease treatment. **Antimicrobial Agents and Chemotherapy**, v. 57, n. 12, p. 6106–6109, 2013.

SEVERINO, P. et al. Current State-of-Art and New Trends on Lipid Nanoparticles (SLN and NLC) for Oral Drug Delivery. **Journal of Drug Delivery**, v. 2012, 2012.

SHEN, J. et al. Mucoadhesive effect of thiolated PEG stearate and its modified NLC for ocular drug delivery. **Journal of Controlled Release**, v. 137, n. 3, p. 217–223, 2009.

SHEN, J. et al. Incorporation of liquid lipid in lipid nanoparticles for ocular drug delivery enhancement. **Nanotechnology**, v. 21, n. 2, p. 025101, 15 jan. 2010.

SOUTO, E. B. et al. Development of a controlled release formulation based on SLN and NLC for topical clotrimazole delivery. **International Journal of Pharmaceutics**, v. 278, n. 1, p. 71–77, 2004.

SOUTO, E. B.; ALMEIDA, A. J.; MÜLLER, R. H. **Lipid nanoparticles (SLN®, NLC®) for cutaneous drug delivery: Structure, protection and skin effects** *Journal of Biomedical Nanotechnology*, 1 dez. 2007. Disponível em: <<http://openurl.ingenta.com/content/xref?genre=article&issn=1550-7033&volume=3&issue=4&spage=317>>. Acesso em: 10 maio. 2019

SOUTO, E. B.; MÜLLER, R. H. SLN and NLC for topical delivery of ketoconazole. **Journal of Microencapsulation**, v. 22, n. 5, p. 501–510, 3 ago. 2005.

SZNITOWSKA, M. et al. The effect of a lipid composition and a surfactant on the characteristics of the solid lipid microspheres and nanospheres (SLM and SLN). **European Journal of Pharmaceutics and Biopharmaceutics**, v. 110, p. 24–30, 1 jan. 2017.

TAMJIDI, F. et al. Nanostructured lipid carriers (NLC): A potential delivery system for bioactive food molecules. **Innovative Food Science & Emerging Technologies**, v. 19, p. 29–43, 1 jul. 2013.

TAN, J. S. L.; ROBERTS, C.; BILLA, N. Pharmacokinetics and tissue distribution of an orally administered mucoadhesive chitosan-coated amphotericin B-Loaded nanostructured lipid carrier (NLC) in rats. **Journal of Biomaterials Science, Polymer Edition**, v. 31, n. 2, p. 141–154, 22 jan. 2020.

VALICHERLA, G. R. et al. Formulation optimization of Docetaxel loaded self-emulsifying drug delivery system to enhance bioavailability and anti-tumor activity. **Scientific Reports**, v. 6, n. 1, p. 26895, 31 jul. 2016.

WANG, Y. et al. Enhanced oral bioavailability of tacrolimus in rats by self-microemulsifying drug delivery systems. **Drug Development and Industrial Pharmacy**, v. 37, n. 10, p. 1225–1230, 26 out. 2011.

WORLD HEALTH ORGANIZATION. **Control of the leishmaniasis: report of a meeting of the WHO expert committee on the control of leishmaniasis. Control of the leishmaniasis: report of a meeting of the WHO expert committee on the control of leishmaniasis**. Geneva: World Health Organization, 2010. Disponível em: <<https://www.cabdirect.org/cabdirect/abstract/20123045323>>. Acesso em: 27 maio. 2019.

WORLD HEALTH ORGANIZATION. **Investing to overcome the global impact of neglected tropical diseases: third report on neglected diseases 2015**. Geneva: World Health Organization, 2015. Disponível em: <http://www.who.int/neglected_diseases>

YUKUYAMA, M. N. et al. Olive oil nanoemulsion preparation using high-pressure homogenization and d-phase emulsification – A design space approach. **Journal of**

Drug Delivery Science and Technology, v. 49, p. 622–631, fev. 2019.

ZHANG, Y. et al. Nonaqueous Gel for the Transdermal Delivery of a DTPA Penta-ethyl Ester Prodrug. **The AAPS Journal**, v. 15, n. 2, p. 523–532, 7 abr. 2013a.

ZHANG, Y. et al. Transdermal prodrug delivery for radionuclide decorporation: Nonaqueous gel formulation development and *in vitro* and *in vivo* assessment. **Drug Development Research**, v. 74, n. 5, p. 322–331, ago. 2013b.

ZHAO, X. et al. Codelivery of doxorubicin and curcumin with lipid nanoparticles results in improved efficacy of chemotherapy in liver cancer. **International journal of nanomedicine**, v. 10, p. 257–70, 2015.

ZHOU, X. et al. Nanostructured lipid carriers used for oral delivery of oridonin: An effect of ligand modification on absorption. **International Journal of Pharmaceutics**, v. 479, n. 2, p. 391–398, 20 fev. 2015.

ZULFIQAR, B. et al. Nanomedicine and cancer immunotherapy: focus on indoleamine 2,3-dioxygenase inhibitors. **OncoTargets and Therapy**, v. 10, p. 463–476, 2017.

Chapter 3 : Bioanalytical Development of HPLC method for identification and quantification of NFOH and NF in serum

This study will be submitted as Aline de Souza, Megumi Nishitani Yukuyama, Maria Karilly Lima de Almeida, Nádia Araci Bou-Chacra, Leandro Augusto Calixto. With the title of Bioanalytical Development of HPLC method for identification and quantification of NFOH and NF in serum in Biomedical Chromatography.

Abstract

Hydroxymethylnitrofurazone (NFOH) is a prodrug synthesized from the original nitrofurazone compound (NF). NFOH has showed activity *in vivo* against *Trypanosoma cruzi*, *in vitro* activity against *Leishmania amazonensis*, but less toxicity than NF. This study aims to develop and evaluate some analytical figures of merit of a bioanalytical method using HPLC to quantify NFOH and NF. The mobile phase consisted of acetonitrile: water (20:80 v/v), Zorbax SB-C18, 5 μ m, (4.6x250mm) was used as HPLC column, with a flow rate of 1.2 ml/min, at UV detection of 370 nm. The linearity obtained for NFOH and NF was in the range of 0.025 to 3.0 μ g/mL with a correlation coefficient > 0.98. The precision (RSD) was 2.44 to 13.77% for NFOH and 2.61 to 18.42%; the accuracy was 2.66 to 14.28% for NFOH and 2.09 to 19.06% for NF. In conclusion, this developed method could be applied effectively for the evaluation of NF, and NFOH in serum.

Keywords: Bioanalytical method, HPLC, leishmaniasis, lymphatic system, nanostructured lipid carrier

3.1. Introduction

Hydroxymethylnitrofurazone (NFOH) (Figure 3-1A) was first obtained by Chung et al. (2003) using a molecular modification of the original nitrofurazone compound (NF) (Figure 3-1B). NF is an antimicrobial agent primarily active against Gram-positive microorganisms and used only in topical infections due to its adverse effects. Due to the low aqueous solubility and high toxicity of NF, a prodrug (NFOH) was developed to overcome these issues. The pharmacokinetics showed that NFOH converted in NF after hydrolysis *in vitro* and *in vivo* studies. NFOH showed activity against *Trypanosoma cruzi* and less toxicity than NF (CHUNG et al., 2003; SERAFIM et al., 2013). Besides, it showed *in vitro* activity against *Leishmania amazonensis* (MONTEIRO et al., 2017).

Leishmaniasis is a neglected disease and presents two primary clinical forms: cutaneous leishmaniasis (CL) and visceral leishmaniasis (VL). In 2018, 10 countries (Afghanistan, Algeria, Bolivia, Brazil, Colombia, the Islamic Republic of Iran, Iraq, Pakistan, Peru, the Syrian Arab Republic, and Tunisia) reported more than 5000 cutaneous leishmaniasis cases. This represents over 85% of global reported CL incidence. Moreover, over 90% of global VL cases were reported from seven countries: Brazil, Ethiopia, India, Kenya, Somalia, South Sudan, and Sudan (WORLD HEALTH ORGANIZATION, 2020).

Leishmaniasis is transmitted by the bite of female phlebotomine sandflies. After the bite, the promastigote infects dendritic cells and macrophages, and the parasite transforms into an amastigote. The multiplication of amastigotes forms leads to the rupture of the cells, disseminating the infection through the lymphatic and vascular systems targeting the spleen, liver, and bone marrow. Thus, causing hepatosplenomegaly and enlarged lymph nodes (lymphadenopathy) (CHAPPUIS et al., 2007).

Thus, it is essential to deliver the drug substance to these specific organs, aiming for therapeutic efficacy. The lipid-based nanostructured system has demonstrated its potential as a lymphatic drug delivery system (CHAUDHARY et al., 2014; KHAN et al., 2013). These nanoparticles also can overcome the hurdles of poorly water-soluble drugs, such as NFOH (0.992 mg/mL). The oral drug lymphatic delivery is favored by ingestion of triglycerides (CHARMAN; STELLA, 1986;

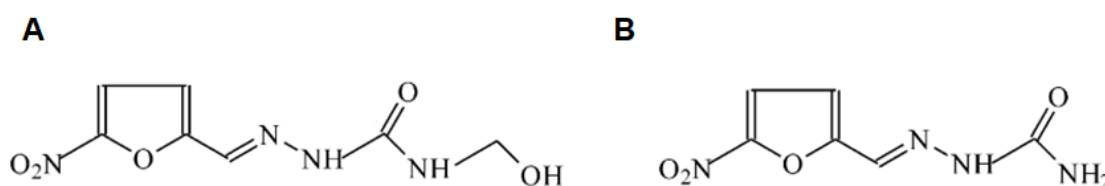
CHAUDHARY et al., 2014). The drugs with solubility in triglycerides higher than 50 mg/mL and a log $P > 5$ are prone to reach the lymphatic system after oral administration (SATO et al., 2018). Thus, a promising oral nanostructured lipid carrier containing NFOH (NLC-NFOH) using this lipid has already been described in the literature (DE SOUZA et al., 2020). Therefore, this formulation was administrated in rats orally, targeting their lymphatic system. This study aims to develop and evaluate some analytical figures of merit to validate a sensitive bioanalytical method using HPLC to quantify NFOH and NF in serum.

3.2. Material and Method

3.2.1. Material

Hydroxymethylnitrofurazone (NFOH) was obtained by synthesis (CHUNG et al., 2003). Acetonitrile HPLC grade was purchased from JT Baker. Purified water was prepared using Milli-Q quality (Millipore, USA). All other reagents were analytical grade. NLC-NFOH was prepared as described by De Souza et al. (2020).

Figure 3-1. Chemical structure of hydroxymethylnitrofurazone (A) and nitrofurazone (B)



Source: Adapted from (CHUNG et al., 2003)

3.2.2. Apparatus and chromatographic conditions

The chromatographic system was Shimadzu HPLC-UV system consisted of a CBM-20A controller, LC-20AT-pump, SPD-20A detector, and SIL-20AC sampler. LC Solution software (version 1.25SP4) was applied for data collecting and processing. Chromatographic separation was performed on Zorbax SB-C18, 5 μ m, (4.6x250mm) HPLC column. The mobile phase consisted of acetonitrile: water

(20:80) at a flow rate of 1.2 mL/min and the UV detector at 370 nm. The volume of injection was 20 µL.

3.2.3. Preparation of standard stock solution, working standard solution and serum sample

Standard stock solutions of NFOH and NF (100 µg/mL) were prepared in acetonitrile. The solutions were sonicated for 10 min to aid dissolution and kept under refrigeration at 5°C. Working standard solution was freshly prepared daily by appropriately diluting the stock solutions with water. The final concentration of standard NFOH and NF solution was 5.0 µg/mL.

The animal experiment was approved by The Ethics Committee (protocol n°1155/2019). The blood was collected from carotid vein. Serum samples were obtained by centrifugation (8000 rpm, 10 min), and it was stored at -20°C for further analysis by HPLC (KIMURA et al., 1997). Acetonitrile (200 µL) were added to serum samples (100 µL) to precipitate proteins, this solution was vortex by one minute, centrifuged at 12500 rpm for 20 min, and then the supernatant was analyzed in HPLC.

3.2.4. Bioanalytical method Development

Monteiro et al. (2015) method was modified and adjusted to provided separation among NFOH, NF and interferences from serum. The 200 to 600 nm screening using UV-vis spectrophotometer (Evolution series 201, Thermo Scientific Inc. USA) was performed to define the best wavelength.

3.2.5. HPLC method validation

Method validation was based on Bioanalytical Method Validation Guidance for Industry from Food and Drug Administration (FDA, 2018).

3.2.5.1. Selectivity

Selectivity evaluates the ability of the method to differentiate the analyte at the presence blank of the biological matrix. Figure 3-3 shows there are no interferences at the retention time of NFOH and NF.

3.2.5.2. Carry-over

During the validation, the carryover evaluated the alteration of a measured concentration due to residual analyte from a preceding sample. Two injections of the blank sample were run before the upper limit of quantification (ULOQ) and two injections after ULOQ.

3.2.5.3. Matrix effect

The low-quality control (LQC) and high-quality control samples (HQC) concentration level were evaluated in water in triplicate compared to the serum matrix. Furthermore, Equation 3-1 shows the matrix effect factor (MEF). And the DPR of the MEF was used to calculate the matrix effect.

$$\text{MEF} = \frac{\text{Analyte response at serum}}{\text{Analyte response at water}} \quad \text{Equation 3-1}$$

3.2.5.4. Linearity and LLOQ

The linearity of the method was evaluated at seven different concentrations in triplicate, ranging from 0.025 to 3.0 µg/mL for NFOH and NF to obtain the linear curve in serum. The lower limit of quantification (LLOQ) will be considered the lowest concentration of the calibration standard.

3.2.5.5. Accuracy and Precision

The method was evaluated for accuracy and precision by analyzing LLOQ, LQC, medium quality control (MQC), and HQC concentration level within calibration curve (0.025 µg/mL; 0.25 µg/mL; 1.0 µg/mL; 2.5 µg/mL) in serum. Five replicates

were analyzed on the same day for intra-day analysis. The precision was expressed as percent relative standard deviation (Equation 3-2) and the accuracy as percent recovery (Equation 3-3).

$$RSD = \frac{\text{Standard deviation}}{\text{Experimental Average Concentration}} * 100 \quad \text{Equation 3-2}$$

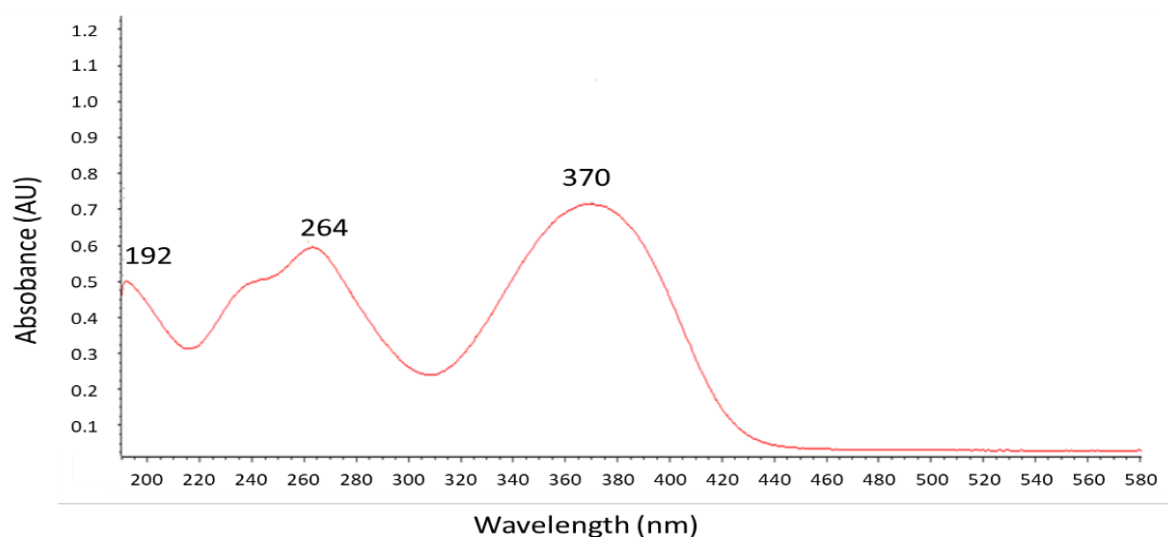
$$\% \text{ Recovery} = \frac{(\text{Experimental Average Concentration} - \text{Teoric Value})}{\text{Teoric Value}} * 100 \quad \text{Equation 3-3}$$

3.3. Result and Discussion

3.3.1. Development of method

Preliminarily, we used the method development by Monteiro et al. (2015). Due to the interferents at the 265nm wavelength at the same retention time as NFOH and NF, the 370nm wavelength was chosen (Figure 3-2).

Figure 3-2. Maximum NFOH (5.0µg/mL) absorbance in the range of 190-600 nm.



Source: The Author.

To develop the bioanalytical method, it is essential to have a pretreatment of biological matrices to remove proteins and other impurities (SAHU et al., 2018). Protein precipitation is one technique used to remove the complex biogenic compounds that can interact with the drugs (KISHIKAWA; EL-MAGHRABEY; KURODA, 2019). For this work, it was used acetonitrile to precipitate the proteins. Different proportion of serum and acetonitrile (1:1; 1:2; 1:3 and 1:4) was used to achieve satisfied chromatographic conditions. The precipitation of all the proteins prevents clogging and the deterioration of the HPLC column. However, if there is a high acetonitrile volume, the resolution of the peaks might be compromised, and the drug may be diluted, impairing its detection. After some tests, the proportion chosen was 1:2 (serum: acetonitrile).

During the development of the method, the volume of injection was also studied. Moreover, it was injected 20 and 50 μ L. Due to the acetonitrile solution to prepare the samples, the high injection volume altered the resolution of the peaks. This phenomenon occurs because the higher strength of the organic solvent compared to the mobile phase leads a portion of the sample more quickly through the column, forming wide peaks (PEPERMANS et al., 2021). Thus, the volume of 20 μ L of injection was selected.

3.3.2. HPLC method validation

3.3.2.1. Selectivity

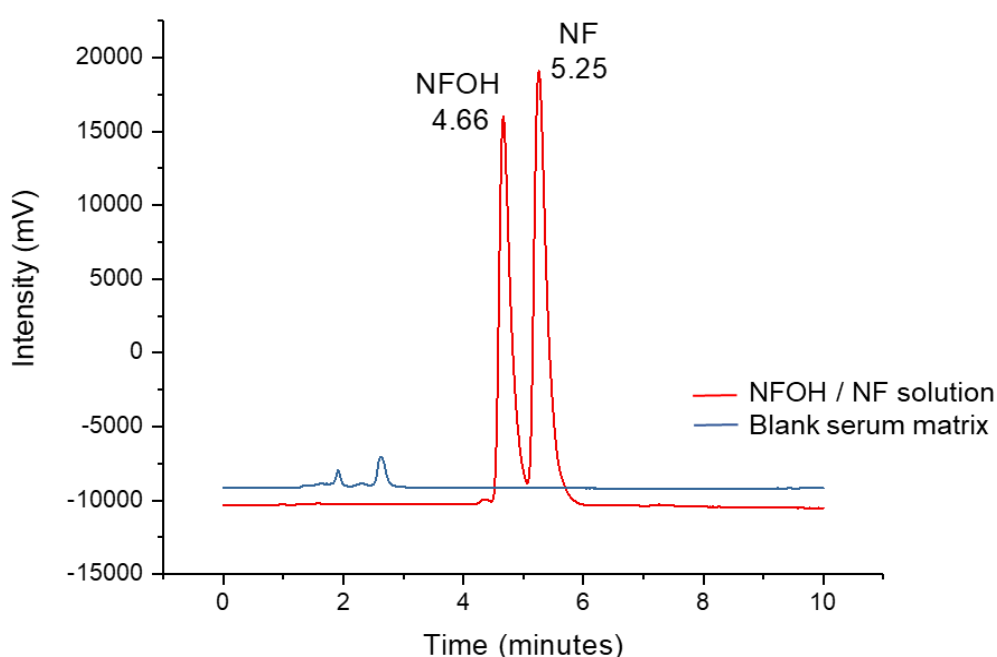
Selectivity evaluates the ability of the method to differentiate the analyte at the presence blank of the biological matrix. Figure 3-3 shows there are no interferences at the retention time of NFOH and NF.

3.3.2.1. Carryover

The carryover is the effect generated by the appearance or increase of the analyte caused by contamination from previous runs. For NFOH, there was no carryover. Thus, it was possible to use the LLOQ for NFOH quantification analyzes in serum. The same did not occur with NF, which showed a carryover effect, influencing its quantification in the samples. This may have occurred because NF is more apolar

(Log P_{NF} 0.23), than NFOH (Log P_{NFOH} - 0.19), requiring washing during the run to reduce the carryover (CHUNG et al, 2003). The method is intended to quantify especially the NFOH.

Figure 3-3. Chromatogram of hydroxymethylnitrofurazone (NFOH) and nitrofurazone (NF) standards solution (5.0 $\mu\text{g/mL}$) and blank serum matrix. Chromatographic conditions: Mobile Phase - acetonitrile:water (20:80); wavelength= 370nm; volume of injection= 20 μL .



Source: The Author.

3.3.2.2. Matrix effect

The matrix effect is an alteration in response due to the presence of interferent substances in the sample. The percent relative standard deviation (RSD) of the MEF for all samples must not exceed 15% (FDA, 2018). The RSD found for LQC (0.25 $\mu\text{g/mL}$) were 13.07% and 6.26% for NFOH and NF, respectively. Moreover, RSD found for HQC (2.50 $\mu\text{g/mL}$) were 7.39% and 13.73% for NFOH and NF, respectively.

3.3.2.3. Linearity and LLOQ

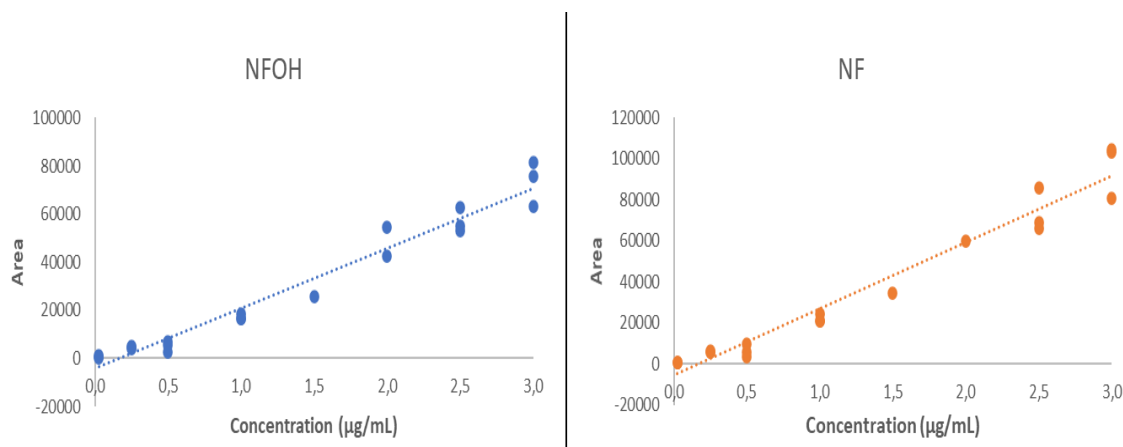
The analytical curve was built using seven data points in triplicate injection of matrix spiked with NFOH and NF. The curve range was 0.025 – 3.0 µg/mL for NFOH and NF with good linearity ($r > 0.98$) using a ponderation of $1/x^2$. The results are presented in Table 3-1 and Figure 3-4. Table 3-2 and Table 3-3 shows the analysis of variance ($p < 0.05$, $\alpha = 0.5$) for NFOH and NF, respectively. The evaluation of the regression efficiency showed F-value greater than the tabulated for NFOH and NF. The analysis of Lack of Fit (error associated with the model) shows the error is not associated with the model, with $p > 0.05$, and F-value lesser than the $F_{\text{tabulated}}$, for both substances.

Table 3-1. Linear regression for the curve calibration of hydroxymethylnitrofurazone (NFOH) and nitrofurazone (NF) in rat serum.

Parameter	Statistical Data	
	NFOH	NF
Concentration range (µg/mL)	0.025 – 3.00	0.025 – 3.00
Intercept	- 4.2	93.7
Slope (S)	20904	25992
Coefficient of correlation (r)	0.98	0.98
Residual SD of regression line (σ)	4216.02	4570.16
LLOQ (µg/mL)	0.025	0.025

LLOQ: lower limit of quantification; NFOH: hydroxymethylnitrofurazone; NF: nitrofurazone.

Figure 3-4. Linear regression for the curve calibration of hydroxymethylnitrofurazone (NFOH) and nitrofurazone (NF) in rat serum.



Source: The Author.

Table 3-2. Analysis of variance for NFOH analysis.

SOURCE OF VARIATION	DF	SS (adj)	MS (adj)	F-value	F _{tabulated}	p-value
Regression	1	6115314474	6115314474	344.04	4.543	0.000
Concentration (µg/mL)	1	6115314474	6115314474	344.04	-	0.000
Error	15	266622522	17774835	-		-
Lack-of-fit	5	158449861	31689972	2.93	3.326	0.070
Pure error	10	108172661	10817266	-	-	
Total	16	6381936996	-	-	-	-

DF = degrees of freedom, SS = sequential sums of squares, MS = sequential mean squares, F-Value = value on the F distribution, p-Value = lack-of-fit adjustment.

Table 3-3. Analysis of variance for NF analysis.

SOURCE OF VARIATION	DF	SS (adj)	MS (adj)	F-value	F _{tabulated}	p-value
Regression	1	8156370154	8156370154	390.51	4.600	0.000
Concentration (µg/mL)	1	8156370154	8156370154	390.51	-	0.000
Error	14	292408901	20886350	-	-	-
Lack-of-fit	5	182907145	36581429	3.01	3.482	0.072
Pure error	9	109501755	12166862	-	-	-
Total	15	8448877905	-	-	-	-

DF = degrees of freedom, SS = sequential sums of squares, MS = sequential mean squares, F-Value = value on the F distribution, p-Value = lack-of-fit adjustment.

3.3.2.4. Accuracy and Precision

The precision is the proximity of results obtained by repeated measurements in different concentrations from the same matrix. Furthermore, the accuracy is evaluated by the proximity of the values between the test and the reference (FDA, 2018). According to the FDA, the acceptance criteria are 15% for RSD or %Recovery for all concentrations except for LLOQ accepted 20%. The method showed to be in accordance with the legislation (Table 3-2).

Table 3-4. Precision and Accuracy of NFOH and NF at serum.

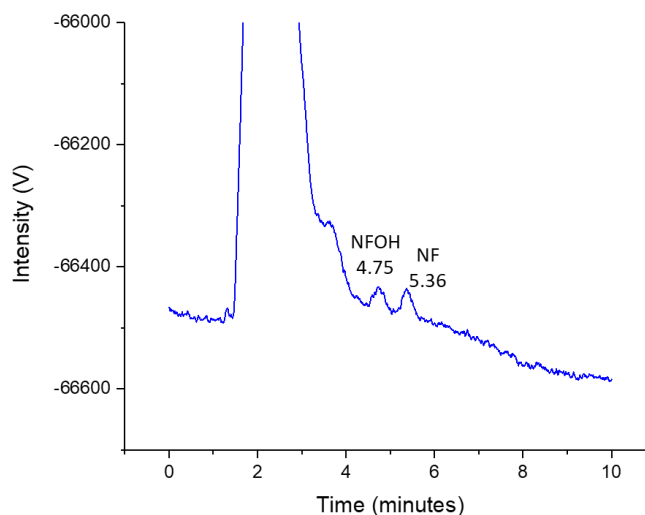
	Concentration (µg/mL)	Precision (RSD)	Accuracy (%Recovery)
NFOH	0.025	10.96	2.66
	0.25	13.71	-10.52
	1.00	6.29	-7.95
	2.50	2.44	14.28
NF	0.025	18.42	19.06
	0.25	6.41	-9.20
	1.00	9.60	-2.09
	2.50	2.61	11.83

NFOH: Hydroxymethylnitrofurazone; NF: nitrofurazone; RSD: relative Standard Deviation.

3.3.3. Application

The application of the method quantified NFOH in rat serum after oral administration of NLC-NFOH showed a concentration of $0.029 \pm 0.004 \mu\text{g/mL}$. The chromatogram did not show interfering peaks, enabling quantification within the method range (Figure 3-5).

Figure 3-5. Chromatogram of rat serum after oral administration of nanostructured lipid carrier with NFOH. Chromatographic conditions: Mobile Phase - acetonitrile:water (20:80); wavelength= 370nm; volume of injection= 20 μL .



Source: The Author.

3.4. Conclusion

The developed bioanalytical method to quantify NFOH in serum using HPLC/UVvis showed selectivity, linearity, accuracy and precision. And also showed no carryover and matrix effect. The preparation of the sample was simple and suitable for the analysis. Besides, the proposed method was simple, fast and efficient to separate NFOH and NF. The bioanalytical method can be used for quantification of NFOH in serum.

3.5. References

- CHAPPUIS, F. et al. Visceral leishmaniasis: what are the needs for diagnosis, treatment and control? **Nature Reviews Microbiology**, v. 5, p. S7–S16, 1 nov. 2007.
- CHARMAN, W. N. A.; STELLA, V. J. Estimating the maximal potential for intestinal lymphatic transport of lipophilic drug molecules. **International Journal of Pharmaceutics**, v. 34, n. 1–2, p. 175–178, 1 dez. 1986.
- CHAUDHARY, S. et al. Recent approaches of lipid-based delivery system for lymphatic targeting via oral route. **Journal of Drug Targeting**, v. 22, n. 10, p. 871–882, 22 dez. 2014.
- CHUNG, M. C. et al. Synthesis and *in vitro* evaluation of potential antichagasic hydroxymethylnitrofurazone (NFOH-121): A new nitrofurazone prodrug. **Bioorganic and Medicinal Chemistry**, v. 11, n. 22, p. 4779–4783, 2003.
- DE SOUZA, A. et al. A new medium-throughput screening design approach for the development of hydroxymethylnitrofurazone (NFOH) nanostructured lipid carrier for treating leishmaniasis. **Colloids and Surfaces B: Biointerfaces**, v. 193, 2020.
- FDA. Bioanalytical Method Validation Guidance for Industry. **U.S. Department of Health and Human Services, Food and Drug Administration**, p. 1–41, 2018.
- KHAN, A. A. et al. Advanced drug delivery to the lymphatic system: lipid-based nanoformulations. **International journal of nanomedicine**, v. 8, p. 2733–2744, 2013.
- KIMURA, E. et al. Pharmacokinetic profile of piroxicam β -cyclodextrin, in rat plasma and lymph. **General Pharmacology**, v. 28, n. 5, p. 695–698, 1 maio 1997.
- KISHIKAWA, N.; EL-MAGHRABEY, M. H.; KURODA, N. Chromatographic methods and sample pretreatment techniques for aldehydes determination in biological, food, and environmental samples. **Journal of Pharmaceutical and Biomedical** v. 175, p. 112782, 25 out. 2019..
- MONTEIRO, L. M. et al. Reverse phase high-performance liquid chromatography for quantification of hydroxymethylnitrofurazone in polymeric nanoparticles. **Brazilian Journal of Pharmaceutical Sciences**, v. 51, n. 3, p. 561–568, 2015.

MONTEIRO, L. M. et al. Targeting *Leishmania amazonensis* amastigotes through macrophage internalisation of a hydroxymethylnitrofurazone nanostructured polymeric system. **International Journal of Antimicrobial Agents**, v. 50, n. 1, p. 88–92, 2017.

PEPERMANS, V. et al. Detailed numerical study of the peak shapes of neutral analytes injected at high solvent strength in short reversed-phase liquid chromatography columns and comparison with experimental observations. **Journal of Chromatography A**, v. 1643, p. 462078, 26 abr. 2021.

SAHU, P. K. et al. An overview of experimental designs in HPLC method development and validation. **Journal of Pharmaceutical and Biomedical Analysis**, v. 147, p. 590–611, 5 jan. 2018.

SATO, Y. et al. Enhancement of lymphatic transport of lutein by oral administration of a solid dispersion and a self-microemulsifying drug delivery system. **European Journal of Pharmaceutics and Biopharmaceutics**, v. 127, p. 171–176, 1 jun. 2018.

SERAFIM, E. O. P. et al. Pharmacokinetics of hydroxymethylnitrofurazone, a promising new prodrug for chagas' disease treatment. **Antimicrobial Agents and Chemotherapy**, v. 57, n. 12, p. 6106–6109, 2013.

WORLD HEALTH ORGANIZATION. **WHO | Leishmaniasis - Global Health Observatory (GHO) data**. Disponível em:

<https://www.who.int/gho/neglected_diseases/leishmaniasis/en/>. Acesso em: 6 maio. 2020.

Chapter 4 : Evaluation of the lymphatic absorption of a nanostructured lipid carrier with hydroxymethylnitrofurazone (NFOH) after oral administration in rats

This study will be submitted as Aline de Souza, Megumi Nishitani Yukuyama, Cristiano Jesus Correia, Paulo Cesar Cotrim, Edite Kanashiro, Ana Cristina Breithaupt Faloppa, Nádia Araci Bou-Chacra. With the title of Evaluation of the lymphatic absorption of nanostructured lipid carrier with hydroxymethylnitrofurazone (NFOH) after oral administration in rats in AAPS PharmSciTech or International Journal of Pharmaceutics.

Abstract

This study demonstrates the influence of nanostructured lipid carrier with hydroxymethylnitrofurazone (NLC-NFOH) at the chylomicron's secretion using the chylomicron blocking flow in a rat model. NLC-NFOH (2.8 mg/kg) was administered to animals by gavage, and the blocking flow of the chylomicrons model was performed with an intraperitoneal injection of cycloheximide. The presence of NFOH in serum was evaluated with and without the injection of cycloheximide. NLC-NFOH and blank-NLC showed more than 90% viable cells at the maximum concentration used (2560 μ M). NFOH and NF were detected at 1h after the gavage of DMSO-NFOH or NLC-NFOH, with or without the pretreatment with cycloheximide. The concentration found for DMSO-NFOH and NLC-NFOH were 0.0316 and 0.0291 μ g/mL, respectively. The NLC presented the NFOH absorption by the lymphatic system, demonstrated by blocking chylomicrons flow.

Keywords: Lymphatic system, Hydroxymethylnitrofurazone, nanostructured lipid carrier, cycloheximide, chylomicrons

4.1. Introduction

The lymphatic system is formed for different organs, such as lymph nodes, spleen, thymus, tonsil, and bone marrow. The lymphatic vascular system extends to all human body (MOORE JR.; BERTRAM, 2018). It has three main functions, first maintain the water balance. Second, to circulate immune cells and to present antigen for immune activation. Moreover, third, it is responsible for the absorption of long-chain fatty acids, triglycerides, cholesterol esters, lipid-soluble vitamins, and xenobiotics (KHAN et al., 2013; TREVASKIS; KAMINSKAS; PORTER, 2015).

Enterocytes make the absorption of lipids by the lymphatic system. The digestion starts with the action of hydrolysis enzymes that reduces triglycerides (TG) (primary lipid of the diet) in monoglycerides (MG) and fatty acids (FA). The bile secretion is stimulated by lipids in GI tract, providing the solubilization of the poorly water-soluble fatty acid, monoglyceride, and diglyceride products (PORTER; TREVASKIS; CHARMAN, 2007). The resynthesized TG form a core lipid with lipoprotein (chylomicrons), then are liberated in the interstitial space going to the lacteals or lymphatic system (CHAUDHARY et al., 2014).

Lipid-based drug delivery systems (LBDDS) have gained importance in the last decade due to biocompatibility and conformability (HARSHITA et al., 2020). They can be used in different routes, different diseases, and a variety of pharmaceutical forms, vaccine, and others (GALVÃO et al., 2020; PINDIPROLU et al., 2020; ZHUANG et al., 2010)

The use of LBDDS active enterocyte transport mechanisms at the absorption site. They also make the drug solubilization in the intestine favorable for their transport through the lymphatic system and, consequently, the systemic availability of the drug, avoiding first-pass metabolism (PATEL et al., 2018). LBDDS increases the bioavailability of BCS classification class II and IV drugs.

Nanostructured lipid carriers (NLC) are colloidal particles composed of a binary mixture of solid lipid and liquid lipid, and the particle is solid at room and body temperature (POONIA et al., 2016). They have several advantages: the production is cost-effective, no need to use organic solvents, high stability, control of drug release, and stability during storage (MENNINI et al., 2016). Thus, this work aims to demonstrate the influence of nanostructured lipid carrier with

hydroxymethylnitrofurazone (NLC-NFOH) at the chylomicron's secretion using the chylomicron blocking flow in a rat model.

4.2. Material and Method

4.2.1. Material

Hydroxymethylnitrofurazone (NFOH) synthesized in accordance with Chung et al. (2003). Stearoyl polyoxyl-32 glycerides (Gelucire® 50/13) and glyceryl distearate (Precirol® ATO 5) were kindly donated by Gattefossé (France). IOI Oleo Chemical kindly donated propylene glycol dicaprylate/dicaprate (Miglyol® 840). Phosphatidylcholine from soybean (Lipoid® S100) was kindly donated by LIPOID GMBH. Acetonitrile HPLC grade were purchased from JTBaker. Purified water was prepared using Milli-Q quality (Millipore, USA). MTT reagent [3-(4,5-dimethylthiazol-2-yl)-2,5-diphenyl tetrazolium bromide], PMA; 0.5µM [phorbol 12-myristate 13-acetate] were all from Sigma-Aldrich (St Louis, MO). RPMI 1640 culture medium was purchased from Merck Millipore (Darmstadt, Germany). Cycloheximide was purchased from Chem Index. All other reagents were at least analytical grade.

4.2.2. Preparation of NLC-NFOH and DMSO-NFOH

NLC-NFOH (0.56 mg/mL). was prepared heating the aqueous and oil phases were at 80°C using RTC basic IKA® magnetic stirrer (300 rpm) until complete dissolution of NFOH. Then, the phases were mixed and taking to Ultraturrax (IKA) at 8000 rpm for 5 min. For five successive cycles at 600 bar, the coarse emulsion was homogenized by high-pressure using Nano DeBEE® (BEE International, Inc. USA) using (DE SOUZA et al., 2020). DMSO-NFOH (0.56 mg/mL). was prepared dissolving NFOH in DMSO.

4.2.3. Cell Culture

Human monocyte cell line THP-1 was supplemented with 10% fetal bovine serum, L-glutamine (10.0 µg/mL), and RPMI for the culture of the cell line. THP-1

cells were incubated with PMA for 24h to induce the transformation of monocytes to macrophages before the cytotoxicity assay.

4.2.4. Cytotoxicity

For evaluation of cytotoxic effects, free NFOH, NLC-NFOH, and blank NLC (5–2560 μ M) were added to well with THP-1 cells. They were incubated with RMPI 1640 medium at 37°C with 5% CO₂ for 24h. The next day MTT solution (5.0 mg/mL) was added to each well and incubated. After 4h, sodium lauryl sulfate (20% w/v) was added and the absorbance was determined at 595 nm. Experiments were performed in replicates of six (Monteiro et al. 2017).

4.2.5. Animals

Male Wistar rats (50-60 days, n=24) were kept in a 23 \pm 2°C, 12 h light-dark cycle, with free access to food and water. All rats received humane care in compliance with the “Principles of Laboratory Animal Care” formulated by the National Society for Medical Research and the ‘Guide for the Care, and the “Use of Laboratory Animals” prepared by the Institute of Laboratory Animal Resources, published by the National Institute of Health (NIH Publication No. 86-23, revised 1996). The Ethics Committee approved the animal experiment protocol (protocol n°1155/2019). All rats were fasting the night before the administration of the formulation. The animals were divided into three groups according to the time of maintenance after gavage: 1, 4, or 6 hours.

4.2.6. Analysis of NFOH presence in serum

NLC-NFOH or DMSO-NFOH (2.8 mg/kg) was administered to animals by gavage. After administration, all animals were anesthetized with isoflurane (5%) in a closed glass chamber and maintained with 2% using an anesthesia mask. After the respective time, the rats were submitted to euthanasia through total blood exsanguination. Blood samples were centrifuged at 2500 rpm for 15 min, and the serum was stored at -20°C until further analysis by HPLC. (Chapter 3, section 3.2.2)

In order to evaluate the induction of the secretion of chylomicrons *in vivo*, the blocking flow of the chylomicrons model (FU et al., 2013) was performed. After the serum analysis, the collection time with the highest concentration of NFOH was selected to follow the *in vivo* assays. The animals were treated with an intraperitoneal injection of cycloheximide (3.0 mg/kg), dissolved in saline (3.0 mg/mL). After 60 min, NLC-NFOH or DMSO-NFOH was administered to animals by gavage, and the collection of blood was proceeded as before.

4.3. Result

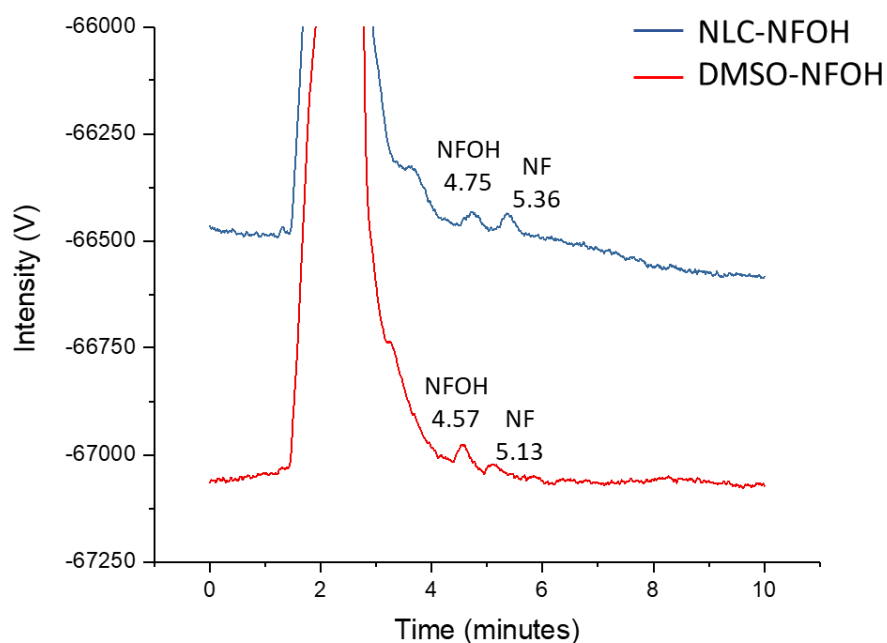
4.3.1. Cytotoxicity

Cytotoxicity indicated low toxicity on uninfected macrophages. The CC₅₀ was 1128.0 μ M for DMSO-NFOH, and for NLC-NFOH and blank-NLC showed more than 90% of viable cells at the maximum concentration used (2560 μ M).

4.3.2. Analysis of NFOH presence in serum

The presence of NFOH and NF in serum was evaluated with and without the injection of cycloheximide. Figure 4-1 shows the chromatograms of NFOH and NF peaks after oral administration of DMSO-NFOH or NLC-NFOH. NFOH and NF were detected only at the time of 1h after the gavage and without the cycloheximide pretreatment (Table 4-1). The concentration found for both solutions administered was similar, showing that the pathway of the absorption might be the same.

Figure 4-1. Chromatogram of rat serum for quantification of NFOH after oral administration of NLC-NFOH and DMSO-NFOH. Chromatographic conditions: Mobile Phase - acetonitrile:water (20:80); wavelength= 370nm; volume of injection= 20 μ L.



Source: The Author.

Table 4-1. The evaluation of NFOH and NF concentration in serum after the one-hour oral administration.

Oral administration*	Pre-treatment with cycloheximide	NFOH Concentration (μ g/mL)
DMSO-NFOH	No	0.0316 \pm 0.0043
NLC-NFOH	No	0.0291 \pm 0.0046
DMSO-NFOH	Yes	0
NLC-NFOH	Yes	0

* n=3 per group

4.4. Discussion

Understanding drug absorption is important to developing formulations. Lipid absorption occurs through the lymphatic system (YÁÑEZ et al., 2011), and substances with $\log P > 5$, long-chain lipids, and particle size can contribute to drug absorption preferentially to the lymphatic system (PORTER; TREVASKIS; CHARMAN, 2007). This knowledge has led to the development of nanostructured lipid systems intending to increase drug absorption and increase its effectiveness (KHAN et al., 2013).

Some studies have shown that formulations absorbed by the lymphatic system alter the pharmacokinetics and increase the maximum concentration (C_{max}) in the blood. Moreover, they have demonstrated this by blocking chylomicron flows using cycloheximide (FAN et al., 2013; XU et al., 2019). Table 4-1 shows NFOH was not found in the serum after 1h of oral administration when blocking the chylomicron flows. This is supported by studies that demonstrate a decrease in drug C_{max} after chylomicron flows are blocked (FAN et al., 2013; FU et al., 2013). Some pharmacokinetic studies have also proposed that changes in drug concentrations in blood after oral administration of nanostructured lipid systems are related to absorption through the lymphatic route (MANAGULI et al., 2018).

The pharmacokinetics of NFOH solved in DMSO (dose 200 mg/kg) showed a C_{max} of 0.99 $\mu\text{g/mL}$ and t_{max} of 1h (SERAFIM et al., 2013). This work showed NFOH at the concentration at the serum of approximately 0.025 $\mu\text{g/mL}$ for NLC-NFOH and DMSO-NFOH (both doses 2.8 mg/kg). Thus, to improve the NFOH concentration in rat serum, it is necessary to enhance the dose administered. Comparing the DMSO-NFOH and NLC-NFOH formulations, there was no significant difference in the concentration found in serum after oral administration. It is showing that NLC-NFOH with only 10% oil phase has the same absorption as DMSO solution. DMSO has been used *in vivo* experiments due to the facility to solubilize hydrophilic and hydrophobic substances (RABOW et al., 2021). Despite this, studies have shown that there may be complications associated with its use even at low doses. In this work, DMSO-NFOH showed more significant cytotoxicity when compared to NLC-NFO. Rabow et al. (2021) demonstrate in their animal study that even a low dose and short-term exposure, DMSO showed chronic alterations in glial cells and

regulatory brain metabolites, and it can change social behavior. In addition, the author is concerned about the neurotoxicity of DMSO and, consequently, its safety for human use. In their review, Madruga et al. (2017) describe some of the adverse effects of DMSO described in the literature, including nausea, vomiting, diarrhea, and severe hemolysis.

Despite DMSO being used in biological assays, humans' use as medicine might not be well accepted. On the other hand, NLC's are formulations well-established; the scale-up is feasible and has the potential to improve the availability of medicines for the population (DE SOUZA et al., 2018). NLC is commercialized and has several patents with the potential to be on the market (MÜLLER et al., 2007; SARTAJ; BABOOTA; ALI, 2021).

4.5. Conclusion

NLC-NFOH showed lower toxicity when compared to DMSO-NFOH. The NLC presented the NFOH absorption by the lymphatic system, demonstrated by blocking chylomicrons flow. NLC-NFOH showed potential to be used for treating leishmaniasis due to similar absorption of DMSO-NFOH.

4.6. References

- CHAUDHARY, S. et al. Recent approaches of lipid-based delivery system for lymphatic targeting via oral route. **Journal of Drug Targeting**, v. 22, n. 10, p. 871–882, 22 dez. 2014.
- DE SOUZA, A. et al. Promising nanotherapy in treating leishmaniasis. **International Journal of Pharmaceutics**, v. 547, n. 1–2, p. 421–431, 25 ago. 2018.
- DE SOUZA, A. et al. A new medium-throughput screening design approach for the development of hydroxymethylnitrofurazone (NFOH) nanostructured lipid carrier for treating leishmaniasis. **Colloids and Surfaces B: Biointerfaces**, v. 193, 2020.
- FAN, Z. et al. A new function of Vitamin E-TPGS in the intestinal lymphatic transport of lipophilic drugs: Enhancing the secretion of chylomicrons. **International Journal of Pharmaceutics**, v. 445, n. 1–2, p. 141–147, 10 mar. 2013.

FU, Q. et al. Nimodipine nanocrystals for oral bioavailability improvement: Role of mesenteric lymph transport in the oral absorption. **International Journal of Pharmaceutics**, v. 448, n. 1, p. 290–297, 1 maio 2013.

GALVÃO, J. G. et al. Carvacrol loaded nanostructured lipid carriers as a promising parenteral formulation for leishmaniasis treatment. **European Journal of Pharmaceutical Sciences**, v. 150, p. 105335, 1 jul. 2020.

HARSHITA et al. Lipid-Based Nanosystem As Intelligent Carriers for Versatile Drug Delivery Applications. **Current Pharmaceutical Design**, v. 26, n. 11, p. 1167–1180, 6 fev. 2020.

KHAN, A. A. et al. Advanced drug delivery to the lymphatic system: lipid-based nanoformulations. **International journal of nanomedicine**, v. 8, p. 2733–2744, 2013.

MADRUGA, G. M. et al. Comparative use of dimethyl sulphoxide (DMSO) in different animal species. **Veterinarni Medicina**, v. 62, n. 4, p. 179–185, 2017.

MANAGULI, R. S. et al. Targeting the intestinal lymphatic system: a versatile path for enhanced oral bioavailability of drugs. **Expert Opinion on Drug Delivery**, v. 15, n. 8, p. 787–804, 2018.

MENNINI, N. et al. Comparison of liposomal and NLC (nanostructured lipid carrier) formulations for improving the transdermal delivery of oxaprozin: Effect of cyclodextrin complexation. **International Journal of Pharmaceutics**, v. 515, n. 1–2, p. 684–691, 2016.

MONTEIRO, L. M. et al. Targeting *Leishmania amazonensis* amastigotes through macrophage internalisation of a hydroxymethylnitrofurazone nanostructured polymeric system. **International Journal of Antimicrobial Agents**, v. 50, n. 1, p. 88–92, 2017.

MOORE JR., J. E.; BERTRAM, C. D. Lymphatic System Flows. **Annu. Rev. Fluid Mech**, v. 50, p. 459–82, 2018.

MÜLLER, R. H. et al. Nanostructured lipid carriers (NLC) in cosmetic dermal products. **Advanced Drug Delivery Reviews**, v. 59, n. 6, p. 522–530, 10 jul. 2007.

PATEL, V. et al. Lipid-Based Oral Formulation Strategies for Lipophilic Drugs. **AAPS PharmSciTech**, v. 19, n. 8, p. 3609–3630, 1 nov. 2018.

PINDIPROLU, S. K. S. S. et al. Pulmonary delivery of nanostructured lipid carriers for effective repurposing of salinomycin as an antiviral agent. **Medical Hypotheses**, v. 143, p. 109858, 1 out. 2020.

POONIA, N. et al. Nanostructured lipid carriers: versatile oral delivery vehicle. **Future Science OA**, v. 2, n. 3, p. FSO135, 2016.

PORTER, C. J. H.; TREVASKIS, N. L.; CHARMAN, W. N. Lipids and lipid-based formulations : optimizing the oral delivery of lipophilic drugs. **Nature Reviews Drug Discovery**, v. 6, n. March, p. 231–248, 2007.

RABOW, Z. et al. Exposure to DMSO during infancy alters neurochemistry, social interactions, and brain morphology in long-evans rats. **Brain and Behavior**, v. 11, n. 5, p. e02146, 1 maio 2021.

SAHU, P. K. et al. An overview of experimental designs in HPLC method development and validation. **Journal of Pharmaceutical and Biomedical Analysis**, v. 147, p. 590–611, 5 jan. 2018.

SARTAJ, A.; BABOOTA, S.; ALI, J. Exploring the therapeutic potential of nanostructured lipid carrier approaches to tackling the inherent lacuna of chemotherapeutics and herbal drugs against breast cancer. **Journal of Drug Delivery Science and Technology**, v. 63, p. 102451, 1 jun. 2021.

SERAFIM, E. O. P. et al. Pharmacokinetics of hydroxymethylnitrofurazone, a promising new prodrug for chagas' disease treatment. **Antimicrobial Agents and Chemotherapy**, v. 57, n. 12, p. 6106–6109, 2013.

TREVASKIS, N. L.; KAMINSKAS, L. M.; PORTER, C. J. H. From sewer to saviour — targeting the lymphatic system to promote drug exposure and activity. **Nature Reviews Drug Discovery**, v. 14, n. 11, p. 781–803, 16 nov. 2015.

XU, Q. et al. Development and *in vivo* evaluation of baicalin-loaded W/O nanoemulsion for lymphatic absorption. **Pharmaceutical Development and Technology**, v. 24, n. 9, p. 1155–1163, 2019.

YÁÑEZ, J. A. et al. Intestinal lymphatic transport for drug delivery. **Advanced Drug Delivery Reviews**, v. 63, n. 10–11, p. 923–942, 10 set. 2011.

ZHUANG, C. Y. et al. Preparation and characterization of vinpocetine loaded nanostructured lipid carriers (NLC) for improved oral bioavailability. **International Journal of Pharmaceutics**, v. 394, n. 1–2, p. 179–185, 15 jul. 2010.

Chapter 5 : Final Conclusion

This present study proposed to advance understanding of the importance of nanotechnology for treating leishmaniasis; developing a novel NLC-NFOH using a D-optimal mixture statistical design and high-pressure homogenization for oral administration to treat leishmaniasis; to comprehend the absorption of the lipid nanoparticle to the lymphatic system using a suitable bioanalytical method. These goals were successfully achieved through the statistical and directed use of all these project activities. This project provided one review article and one research article highlighting the importance of nanotechnology to treat leishmaniasis and the prospect of a new nanostructured lipid carrier with NFOH.

In the review article, we discussed the recent advances in treating leishmaniasis using nanotechnology. The research field of nano-drug delivery systems has increased in the last decade for different nanosystems as metallic, polymeric, lipid nanoparticles, liposomes, and nanocrystals. Nanosystems can play an essential role in treating leishmaniasis due to reducing the duration of the treatment and frequency of administration by improving the adherence of patients to the therapy.

Chapter 2 present the selection of liquid and solid lipids for the development of the NLC-NFOH. The use of different tools for selecting lipids provided relevant scientific knowledge for the development of the NLC. The use of Crystal 16TM helped screen a large number of liquid lipids in a short time, low amount, without the use of organic solvent. Moreover, the association of DSC and microscopy helped in saving time, material, and labor. The liquid lipid selected was Miglyol® 840, and Precirol® ATO 5 and Gelucire® 50/13 were selected as solid lipids. To develop NLC-NFOH, we used an extreme vertex experiment with a five-factor, grade 3, two-level D-optimal mixture statistical design. This statistic method made it possible to understand the attributes that influence the z-average of the formulation. Furthermore, a preliminary assay for quantification of NFOH in rat plasma after oral administration of NLC-NFOH showed similar results compared with the literature.

In chapter 3, we developed and evaluated some figures of merit to validate a sensitive bioanalytical method using HPLC to quantify NFOH and NF in serum. The method showed to be linear, precise, and accurate. Moreover, in chapter 4, we evaluated the cytotoxicity of NLC-NFOH and DMSO-NFOH. DMSO-NFOH showed to be more cytotoxicity than NLC-NFOH. We also evaluated the absorption of NFOH to the lymphatic system after oral administration of NLC-NFOH. The lymphatic absorption was demonstrated by blocking chylomicrons flow. NLC-NFOH showed similar absorption of DMSO-NFOH.

This project developed a novel NLC with NFOH that might be the future for treating leishmaniasis and help the population to have affordable medicine.